A RECONNAISSANCE STUDY OF JASPEROID IN THE KELLY LIMESTONE, KELLY MINING DISTRICT, NEW MEXICO

Part I: GEOLOGY, PETROGRAPHY, AND ORIGIN

Part II: DIFFERENTIATION OF CHERT FROM JASPEROID BY X-RAY DIFFRACTION LINE RESOLUTION

by

Joe Iovenitti

OPEN FILE REPORT 85

Submitted in Partial Fulfillment
of the Requirements for the Degree of
Master of Science in Geology

New Mexico Institute of Mining and Technology

Socorro, New Mexico

May, 1977

ACKNOWLEDGEMENTS

My sincerest appreciation is expressed to my thesis advisor, Dr. Charles E. Chapin, for his guidance, understanding, supervision, encouragement and stimulating discussions during the research and writing of this thesis. The author cannot begin to express his gratitude to Dr. Jacques Renault for his stimulating discussions which at times extended for many long hours, his willingness to listen and respond, his understanding and patience during my stay at New Mexico Institute of Mining and Technology, and for suggesting the X-ray diffraction study discussed in Part II of this thesis. A sincere thanks is also extended to my other committee member, Dr. Richard E. Beane, for the excellent lectures, discussions and education provided, and for suggesting the thesis topic.

Special thanks are extended to Dr. Gary Landis of the University of New Mexico who generously permitted the use of his fluid inclusion equipment, to Dr. G. Bryon Bailey for the copies of the photographs in his dissertation which facilitated the petrographic analysis, and to Dr. James Robertson of the New Mexico Bureau of Mines and Mineral Resources who graciously allowed the use of his microscope and photographic equipment.

The author is indebted to the New Mexico Bureau of Mines and Mineral Resources for their financial support, field transportation, preparation of thin sections, and

use of analytical equipment. Appreciation is extended to Thea Davidson who slabed all my rock samples, prepared all thin sections and aided in the preparation of the doubly-polished sections used in the fluid inclusion analysis. The New Mexico Geological Society is also thanked for the grant-in-aid to cover expenses incurred in the preparation of this thesis.

Last, but certainly not least, I wish to express my appreciation to my wife, Linda, whose love and encouragement allowed me to reach this goal.

ABSTRACT

Part I: The Kelly mining district is situated in the northern Magdalena Mountains, Socorro County, New Mexico. The Range is a westward-tilted fault block consisting of an uplifted core of Precambrian igneous and metasedimentary rocks overlain by Carboniferous sedimentary rocks. Tertiary intrusive and extrusive rocks are also present, and the principal structure of the district is that of cauldron-margin faulting at the intersection of two overlapping cauldrons.

Silicic alteration (jasperoid) related to a late Oligocene - early Miocene mineralizing event occurs mainly in the Kelly Limestone (Mississippian) and is most conspicuous in the eastern portion of the mining district where this formation crops out along the crest of the range and along its western slopes. Both structural and stratigraphic controls were found to influence the distribution of jasperoid. Its preferential occurrence in the upper Kelly Limestone is thought to have been caused by lateral migration of silica-rich solutions beneath an impermeable cap formed by the overlying Sandia Formation (Pennsylvanian).

Detailed megascopic and petrographic studies suggest that jasperoid formation occurred by replacement of limestone by silica gel which converted to fine-grained quartz exhibiting a variety of microtextures during

the early stages of silicification. Precipitation of coarse-grained quartz in open spaces occurred during the later stages of silicification. Homogenization temperatures (uncorrected for pressure) from fluid inclusions in barite, fluorite, and coarse-grained quartz indicate that jasperoid was deposited in the temperature range of 145°-285°C. Microcrystalline quartz formed in the temperature range of 235°-285°C; coarse-grained quartz formed between 145°-235°C. The combination of decreasing temperature and increasing P_{CO_2} of the solutions is the mechanism postulated for silica deposition.

Part II: The Kelly Limestone contains two types of microcrystalline silica: nodular (and lenticular) chert and jasperoid. Field observations suggest that some of the "nodular chert" may be jasperoid. If jasperoid and chert originate as amorphous silica, then jasperoid being hydrothermal should display a coarser crystallite size than chert which is diagenetic in origin. To test this hypothesis, the resolutions of the 212 and 203 Cu K-alpha$_1$ X-ray diffraction lines of quartz were determined. As a qualitative measure of percent resolution, the relationship

$$R = 100(P - V)/P$$

was used, where R is the percent resolution, P and V are the net intensity of the peak and of its adjacent valley, respectively. Forty-one samples were analyzed: 13 cherts

and 12 jasperoids from the Kelly Limestone, 13 normal cherts (cherts which have not been subjected to hydrothermal activity) and 3 cherts from a known hydrothermal area. Samples were crushed to particles approximately 3 mm in size and hand picked to exclude any coarsely crystalline quartz.

The results are: (1) R(Kelly district jasperoid) > R(normal chert), (2) R(Kelly district chert) overlaps both the normal chert and Kelly district jasperoid fields, and (3) R(cherts from a known hydrothermal area) >> R(normal chert). These findings, though based on a limited sample population, suggest that X-ray diffraction line resolution can be used to differentiate between jasperoid and normal chert, but cannot differentiate between jasperoid and chert which has experienced a hydrothermal event. This type of analysis may be useful in exploration for Mississippi-Valley-type ore deposits in indicating whether chert has experienced a hydrothermal event.

An attempt was made to correlate R with petrographic textures exhibited by the samples analyzed. No correlation was discernible.

LIST OF CONTENTS

	Page
ACKNOWLEDGEMENTS	i
ABSTRACT	iii
LIST OF CONTENTS	vi
LIST OF FIGURES	x
LIST OF TABLES	xix
LIST OF PLATES	xx
PART I: GEOLOGY, PETROGRAPHY, AND ORIGIN	xxi
Chapter I: INTRODUCTION	1
Area of Study	1
Statement of Purpose	1
Previous Investigations	1
Definition of Jasperoid	3
Method of Investigation	3
Chapter II: GEOLOGIC SETTING OF THE KELLY MINING DISTRICT	8
Stratigraphy	8
Precambrian Rocks	8
Argillite and Schist	10
Early Gabbro or Diabase	11
Felsite	11
Granite	12
Late Diabase	12
Paleozoic Rocks	12
Mississippian System	13
Caloso Formation	16
Kelly Limestone	16
Pennsylvanian System	19
Sandia Formation	20
Madera Limestone	21
Permian System	23

Abo Formation 23
Yeso Formation 23
Glorieta Sandstone 24
San Andres Limestone 24
Tertiary Extrusive Rocks 24
Tertiary Intrusive Rocks 25
Latite Porphyry of Mistletoe Gulch. 25
Quartz Monzonite of the Linchburg Mine 27
Mafic Dikes 29
White Rhyolite Dikes 30
Structure 32

Chapter III: DISTRIBUTION AND CONTROLS OF SILICIFICATION 37
Geographic Distribution 37
Silicification of Rocks other than Kelly Limestone 37
Precambrian Rocks 39
Sandia Formation 39
Madera Limestone 40
White Rhyolite Dikes 40
Volcanic Rocks 40
Silicification of the Kelly Limestone 41
Primary Controls 41
Features of Unknown Importance 50

Chapter IV: PHYSICAL PROPERTIES OF JASPEROID 59
Megascopic Features 59
Color 59
Structures within Jasperoid 60
Associated Mineralogy 70
Microscopic Features 73
Major Microcrystalline Quartz Textures 73
Jigsaw-puzzle Texture 74
Jigsaw-puzzle-Xenomorphic Texture . 77
Xenomorphic-Granular Texture 82
Xenomorphic Texture 82

Subidiomorphic Texture 85
Minor Microcrystalline Quartz Textures 85
Vuggy Texture 90
Brecciated Texture 90
Spherulitic Texture 90
Coarse-grained Quartz Features 101
Jasperoid-Limestone Contact 106
Associated Mineralogy in Jasperoid 116

Chapter V: FLUID INCLUSION INVESTIGATION 118

Chapter VI: ORIGIN OF KELLY DISTRICT JASPEROID ... 124
Introduction 124
Genesis of Petrographic Textures 124
Genesis of Megascopic Features 133
Interpretation of Fluid Inclusion Data 136
Proposed Origin of the Jasperoid 138
Source of the Silica 138
Nature of Solutions that Dissolve and Transport Silica 140
Deposition of Silica 142
Mechanism of Limestone Replacement. 147

Chapter VII: SUMMARY AND CONCLUSIONS 152

PART II: DIFFERENTIATION OF CHERT FROM JASPEROID BY X-RAY DIFFRACTION LINE RESOLUTION 156

Introduction 157
Statement of the Problem 157
Method of Investigation 159
Previous Works 163
Experimental Procedure 164
Results 167
Interpretation of the Results 172
Correlation of Petrographic Textures with X-Ray Results 180
Summary and Conclusions 180

APPENDIX I 191
Sample Preparation Method for X-ray Diffraction Line Resolution 191

LIST OF REFERENCES 192

LIST OF FIGURES

Figure		Page
1	Index map showing the location of the Magdalena mining district and the area studied by Loughlin and Koschmann (1942) which is outlined (after Lasky, 1932). Thesis area is also shown	2
2	Stratigraphic column of Precambrian and Paleozoic rocks in the Magdalena area (from Chapin et al., 1975)	9
3	Generalized geologic map of the Kelly mining district (after Loughlin and Koschmann, 1942; Blakestad, 1976)	15
4	Typical stratigraphic section of the rocks in the Linchburg mine, from Titley (1958). Footwall beds in the figure are equivalent to the Caloso Formation, see text	18
5	Generalized map of the major structural features in the Magdalena area (modified after Chapin and Chamberlin, 1976)	34
6	Remnant of silicified upper Kelly Limestone on a dip slope with underlying unaltered limestone. On several dip slopes, the silicified upper Kelly has been eroded. The presence of numerous pieces of silicified float and scattered remnants of jasperoid which stand topographically and stratigraphically higher than the surrounding limestone, attest to the probability that at one time the entire dip slope was covered by a veneer of jasperoid	38
7	Silicified Kelly Limestone and Precambrian granite along an east-trending fault. Very minor and localized silicification of the Sandia Formation occurs along fracture zones ..	42
8a	Idealized cross-section of faulted Kelly Limestone portraying the deflection of silica-rich solutions laterally into the upper Kelly. Dashed lines represent banding in jasperoid. Outlined area represents Figure 8b below	44
8b	Vertically banded jasperoid within fault zone illustrated above, see text.	44

Figure		Page
9a	Shows extensive silicification of the Kelly Limestone along the intersection of two faults which becomes localized in three horizons at some distance (approximately 30 feet) away from the faults. Outlined area represents Figure 9b	46
9b	Jasperoid locallized along two favorable horizons in the Kelly Limestone. Contacts between jasperoid & limestone are sharp on a gross scale	46
10a	Silicified fissure in Kelly Limestone trending approximately N 10°W. Dashed lines indicate banding in jasperoid	49
10b	Close-up of area immediately to the right of the silicified fissure in Figure 10a. Note the intense fracturing and silicification in limestones above the 'silver pipe'. The nature of some silica lenses is discussed in Part II of this thesis	49
11	Swell in jasperoid horizon transgressing bedding in Kelly Limestone. Note the curvature of ribbon-rock in the swell and the maintainance of parallism between the vugs in ribbon-rock and the jasperoid-limestone contact	52
12	Arm-like extensions of jasperoid (b) in limestone (a)	53
13	Silicified pod in essentially unaltered limestone far removed from any jasperoid zone .	54
14a	A 'sheeted' silicified fault zone (outlined) cutting Kelly Limestone. Note: (1) density of fracturing and degree of silicification decreased to the right of the fault, (2) unaltered limestone pod within jasperoid mass and (3) the vertical banding of jasperoid in the foreground	56
14b	Close-up of the area immediately to the right of the fault zone in Figure 15a. The unaltered limestone contains silicified fractures and pods. The nature of these pods is discussed in Part II of this thesis ...	56

Figure		Page
15	Anastomosing fractures in Kelly Limestone	57
16	Silicified fractures which bear no direct relationship to either faults or fissures	58
17	Close-up of the jasperoid-limestone contact. Note the transition zone between microcrystalline quartz and unaltered limestone	62
18	Unaltered limestone remnant in Kelly district jasperoid. Lens cap in photograph is 2 inches in diameter	64
19	Unsilicified bed of dolomicrite (called the 'silver pipe' by miners, see Chapter III) in a jasperoid horizon. When present in the vicinity of jasperoid, the 'silver pipe' characteristically shows no signs of silica replacement	64
20	An example of ideal ribbon-rock structure displaying excellent parallelism between the layers of microcrystalline quartz (dark layers) and layers of coarse-grained quartz (light layers). Note: (1) this is a planar feature, and (2) vugs in this type of structure are lenticular and parallel to the ribbon-rock fabric. The degree of coarse-grained quartz development in the vicinity of the hammer is almost complete. Contrast this to the left-hand portion of the figure where coarse-grained quartz forms drusy masses lining platy vugs. Vugginess is inversely proportional to coarse-grained quartz development	67
21	The middle layer in this jasperoid mass is an example of irregular ribbon-rock. The degree of coarse-grained quartz development is complete but the microcrystalline layers are warped, discontinuous and less parallel relative to the microcrystalline layers in ideal ribbon-rock	67
22	Brecciated - vuggy ribbon-rock structure. Note, the contortion of microcrystalline and coarse-grained quartz layers	69
23	Close-up of the jasperoid-limestone contact showing the parallelism of both the layers of microcrystalline quartz and the vugs in ribbon-rock with this contact	69

Figure		Page
24	Close-up of cockade-structured quartz in irregular ribbon rock	72
25	Brecciated microcrystalline quartz cemented by a second generation of microcrystalline quartz	72
26	Photomicrograph of jigsaw-puzzle textured quartz in Kelly district jasperoid (crossed-nicols, 160x magnification)	76
27	Photomicrograph of fossil fragments replaced by jigsaw-puzzle quartz (crossed-nicols, 25x magnification)	76
28	Photomicrograph of jigsaw-puzzle textured quartz illustrating its 'dirtiness' (plane-polarized light, 160x magnification)	79
29	Photomicrograph of jigsaw-puzzle texture displaying desiccation-like fracturing. Note the clear spherical areas (s) which are interpreted as "ghosts" of Type II, spherulitic texture (see discussion p.90-101 and Chapter VI). The fact that jasperoid is a result of hydrothermal alteration in the Kelly district precludes the possibility that these spherical areas may be the result of biological activity (p.125;plane-polarized light, 160x magnification)	79
30a	Photomicrograph of jigsaw-puzzle-xenomorphic texture (crossed-nicols, 160x magnification) ..	81
30b	Photomicrograph of the above figure under plane-polarized light. The coarser-grained quartz areas are relatively cleaner than the jigsaw-puzzle regions (160x magnification)	81
31a	Photomicrograph of xenomorphic-granular texture (crossed-nicols, 160x magnification) ..	84
31b	Photomicrograph of the above figure in plane-polarized light. Note the cleanliness of the quartz relative to jigsaw-puzzle or jigsaw-puzzle-xenomorphic quartz (160x magnification).	84
32	Photomicrograph of xenomorphic textured quartz (crossed-nicols, 160x magnification)	87
33	Photomicrograph of subidiomorphic texture (crossed-nicols, 25x magnification)	87

Figure		Page
34	Photomicrograph of minute calcite (?) inclusions in elongate quartz grains of subidiomorphic texture (crossed-nicols, 160x magnification)	89
35a	Photomicrograph of an empty vug (crossed-nicols, 160x magnification)	89
35b	Photomicrograph of a vug in its initial stage of filling (crossed-nicols, 32x magnification)	92
35c	Photomicrograph of a completely filled vug; note that a xenomorphic-granular texture is exhibited (crossed-nicols, 40x magnification) .	92
36	Photomicrograph of brecciated texture cemented by a second generation of xenomorphic-granular quartz. Opaque material is Fe-oxide. Euhedral quartz crystals are present in vugs (crossed-nicols, 25x magnification)	94
37	Photomicrograph of Type I, spherulitic texture with a jigsaw-puzzle quartz core (crossed-nicols, 40x magnification)	94
38a	Photomicrograph of Type II, spherulitic quartz. Spherulites are partially recrystallized to jigsaw-puzzle texture (crossed-nicols, 100x magnification)	97
38b	Photomicrograph of the above figure in plane-light. Illustrated is the radiating fibrous structure of this texture. Also shown are "ghost" spherulites (Figure 29; 100x magnification)	97
39	Photomicrograph of Type II, spherulitic texture recrystallized to jigsaw-puzzle textured quartz. Figure 29 which is in the same field of view shows "ghost" spherulites as discussed in Figure 39b (crossed-nicols, 160x magnification)	99
40	Photomicrograph of Type II, spherulitic texture partially recrystallized to xenomorphic-granular quartz. A portion of the "polarization cross" typical of chalcedony is still evident (crossed-nicols, 125x magnification) ..	99

Figure		Page
41	Photomicrograph of Type I, spherulitic texture with a Type II core (crossed-nicols, 128x magnification)	100
42	Photomicrograph of coarse-grained quartz in a vug exhibiting patchy undulose extinction (crossed-nicols, 64x magnification)	102
43	Photomicrograph of coarse-grained quartz exhibiting splintery texture along its grain boundary (crossed-nicols, 32x magnification) ..	103
44	Photomicrograph of quartz grains showing inclusions and internal fractures that do not transect grain boundaries (crossed-nicols, 125x magnification)	105
45	Photomicrograph of inclusions along growth planes in coarse-grained, comb quartz (crossed-nicols, 100x magnification)	105
46	Photomicrograph of a silica patch (P) in a crinoid fragment. Note its 'dirty' appearance and the presence of calcite and other inclusions (plane-polarized light, 100x magnification)	108
47	Photomicrograph of a partial "ghost" quartz crystal (Q) in calcite cement (crossed-nicols, 160x magnification)	108
48a	Photomicrograph of a silica patch in a crinoid fragment displaying desiccation-like fracturing (plane-polarized light, 64x magnification)	111
48b	Photomicrograph of the above figure under crossed-nicols. Illustrated is Type II, spherulitic texture recrystallizing to xenomorphic quartz (64x magnification)	111
49	Photomicrograph representing Zone III in the jasperoid-limestone transition zone (see Figure 17 and p.106) (crossed-nicols, 25x magnification)	113
50	Photomicrograph of Zone IV in the jasperoid-limestone transition zone (crossed-nicols, 25x magnification)	113

Figure Page

51 Photomicrograph representing Zone V in the jasperoid-limestone transition zone (crossed-nicols, 25x magnification) 115

52 Paragenetic sequence for the dominant accessory minerals in Kelly district jasperoid. Lines in diagram represent only relative times of deposition, not amounts deposited. Dashed lines are indicative of uncertain temporal relationships 117

53 Paragenetic sequence of the minerals used in the fluid inclusion study. Lines only indicate the relative times of deposition, not amounts deposited. Dashed lines are indicative of uncertain temporal relationships 120

54 Frequency distribution diagram for primary and psuedosecondary homogenization temperatures in (a) fluorite, (b) calcite, (c) barite and (d) coarse-grained quartz. No pressure correction has been applied 123

55 Idealized illustration of the two processes by which Type II, spherulites recrystallize. One process, Steps (a) through (c) is by coalescence as described on p.129. The other, Steps (a) to (d), (a) to (f), (b) to (c) and (b) to (g) is by direct recrystallization. Lines (b) to (e), and (b) to (g) are dashed because the processes have not been observed in Kelly district jasperoid 134

56 Temperature v. time diagram for minerals in the Kelly district jasperoid amenable to fluid inclusion analysis 137

57 Quartz and amorphous silica solubility curves after Fournier and Rowe (1966). Superimposed on these curves is the temperature data discussed in p. 122-123. Zones A and B respectively represent the probable temperature range microcrystalline (silica gel) and coarse-grained quartz deposition. $\overline{CDEF}$ is a diagramatic representation of one possible path a solution which first precipitates microcrystalline quartz and then coarse-grained quartz may follow 145

58 "Chert" nodules occurring immediately below a jasperoid horizon 158

Figure		Page
59	Faulted section of Kelly Limestone with development of jasperoid in the hanging wall and chert in the footwall. Some "chert" nodules in footwall may be jasperoid	160
60	"Chert" lense (C) seems to grade into a jasperoid horizon	162
61	Another example of what appears to be a "chert" lense (C) grading into a jasperoid zone (J). Note the presence of vugs in the vicinity of the jasperoid	162
62	68° quintuplet profiles for the six mixtures of quartz from the Ottawa Sandstone and Brazilian agate	166
63	Typical 68° quintuplet for 100% quartz from the Ottawa Sandstone. Method for computing R_1 and R_2 is illustrated	168
64	Plot of R_1, R_2 and their standard deviations as a function of percent quartz from Ottawa Sandstone. The R_2 value for 100% quartz from Ottawa Sandstone has been slightly offset for the sake of clarity	170
65	Frequency distribution diagram of R_1 values for (a) normal chert and North Fork Canyon chert, (b) Kelly district chert, and (c) Kelly district jasperoid	173
66	Frequency distribution diagram of R_2 values for (a) normal chert and North Fork Canyon chert, (b) Kelly district chert, (c) Kelly district jasperoid	174
67	Covariance diagram of R_1 vs. R_2 for Kelly district chert and jasperoid, normal chert, and North Fork Canyon chert	175
68	Plot of R_1 vs distance from a silicified zone for four normal chert samples taken from c., NE¼, SE¼, NW¼, Sec. 2, T.2S., R.2W., New Mexico	177
69	Normality plot for Kelly district chert, Kelly district jasperoid, and normal chert.	179

Figure		Page
70	Photomicrograph of normal chert (C) sample 16. Predominant texture is jigsaw-puzzle, however, minute calcite grains produce the fuzzy image shown, R_1 = 5 (crossed-nicols, 160x magnification)	183
71	Photomicrograph of Kelly district jasperoid (KDJ) sample 216-1. Predominant texture is jigsaw-puzzle, opaque areas are Fe-oxides, R_1 = 34 (crossed-nicols, 160x magnification) ..	183
72	Photomicrograph of Kelly district jasperoid (KDJ) sample 193-1. Predominant texture is subidiomorphic, R_1 = 38 (crossed-nicols, 25x magnification)	185
73	Photomicrograph of Kelly district chert (KDC) sample 123-1. Predominant texture is jigsaw-puzzle-xenomorphic, R_1 = 39 (crossed-nicols, 160x magnification)	185
74	Photomicrograph of Kelly district jasperoid (KDJ) sample 225-4. Predominant texture is jigsaw-puzzle, R_1 = 45 (crossed-nicols, 100x magnification)	187
75	Photomicrograph of North Fork Canyon chert (NFC) sample 2. Predominant texture is jigsaw-puzzle-xenomorphic, calcite grains (C) are also present, R_1 = 49 (crossed-nicols, 100x magnification)	187
76	Photomicrograph of Kelly district chert (KDC) sample 11-1. Predominant texture is jigsaw-puzzle; xenomorphic-granular is also shown, R_1 = 52 (crossed-nicols, 128x magnification) ..	188

LIST OF TABLES

Table		Page
1	Location of normal chert (C) and North Fork Canyon chert (NFC). All samples are Pennsylvanian in age and from the Madera Limestone except for C -2, C -3, C -4, C -5 and C -6 (host formation not known) and NFC-2 which comes from the Sandia Formation (see Figure 2)	171
2	R_1 values and petrographic texture(s) (major, minor) for three Kelly district cherts (KDC), three normal cherts (C), one North Fork Canyon chert (NFC), and six Kelly district jasperoid (KDJ). Samples are listed in order of increasing R_1 within each group	181

LIST OF PLATES

Plate		Page
1	Geologic map of the eastern portion of the Kelly mining district Socorro County, New Mexico	in pocket

Part I: GEOLOGY, PETROGRAPHY, AND ORIGIN

Chapter I: INTRODUCTION

Area Of Study

The Kelly mining district situated in the northern Magdalena Mountains in west-central Socorro County, New Mexico constitutes a small portion of the larger Magdalena mining district. The study area encompasses approximately 2 square miles in the eastern portion of the Kelly district extending along the crest of the Range from North Baldy to Tip Top Mountain, and westward for approximately 1/2 mile (Figure 1).

Statement of Purpose

The objectives of this investigation were (1) to map the eastern portion of the Kelly mining district, (2) to determine the distribution and controls of jasperoid in the Kelly Limestone, and (3) to develop an hypothesis as to the origin of the jasperoid. This study was undertaken as part of the extensive geologic study of the Magdalena district by the New Mexico Bureau of Mines and Mineral Resources under the direction of Dr. Charles E. Chapin.

Previous Investigations

A general discussion of the Magdalena mining district is presented in Lindgren, Graton and Gordon (1910) and Lasky (1932). The earliest reference to the jasperoid of the Kelly mining district appears in the detailed study of the geology and ore deposits of the Magdalena mining

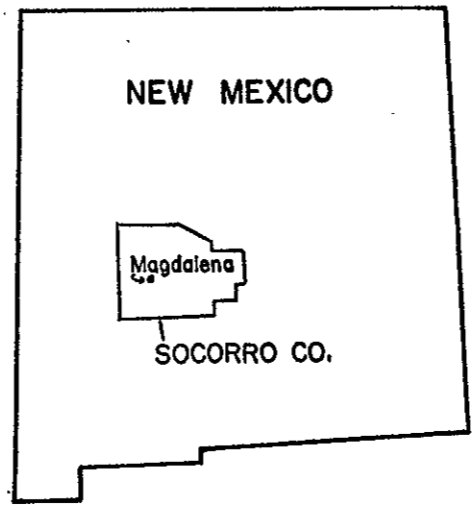

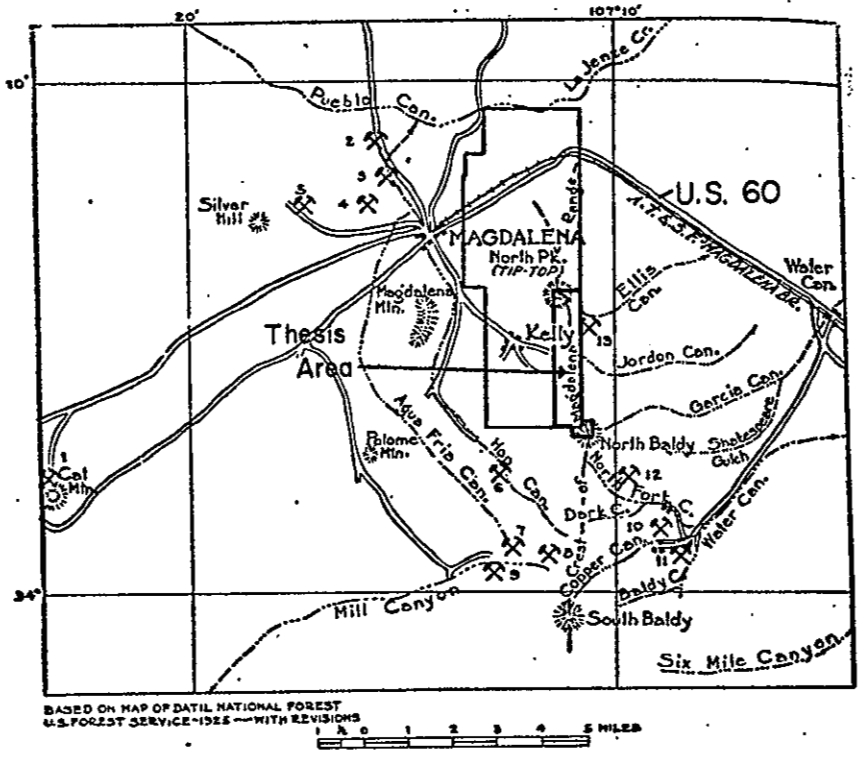

Figure 1. Index map showing the location of the Magdalena mining district and the area studied by Loughlin and Koschmann (1942) which is outlined (after Lasky, 1932). Thesis area is also shown.

district by Loughlin and Koschmann (1942). Blakestad (1976) who revised the geology of the Kelly mining district also makes reference to the occurrence of jasperoid. Other geologic studies in the Kelly district include Titley (1959, 1961) and Park (1971). Siemers (1973) described the stratigraphy and petrology of the Mississippian, Pennsylvanian and Permian rocks in the Magdalena area. A number of authors have studied the occurrence of jasperoid in other mining districts (Spurr, 1898; Lindgren and Loughlin, 1919; Gilluly, 1932; Butler and Singewald, 1940; Park and Cannon, 1943; Duke, 1959; Bailey, 1974; etc.). Lovering (1962, 1972) provides comprehensive reviews of the characteristics and possible origins of jasperoid; his 1972 study also includes a statistical method for distinguishing productive jasperoids (jasperoids related to an ore deposit) from non-productive jasperoids. These works have provided me with a large amount of background material on which the study of the Kelly district jasperoid could be based.

Definition of Jasperoid

Considerable confusion exists in the literature as to the precise definition of the term 'jasperoid' relative to two points: (1) the megascopic textural characteristics of jasperoid, that is whether jasperoid should only refer to aphanitic quartz or to both aphanitic and coarse-grained quartz, and (2) the application of the terms chert and jasperoid.

The AGI - Glossary of Geology (1972) defines jasperoid as:

> "A dense, usually gray, chert-like, siliceous rock in which chalcedony or cryptocrystalline quartz has replaced the carbonate minerals of limestone or dolomite; a silicified limestone. It typically develops as the gangue of metasomatic sulfide deposits of the lead-zinc type (as those of Missouri, Oklahoma and Kansas)."

Spurr (1898) who originally introduced the term while working in the Aspen mining district defined jasperoid as:

> " ... a rock consisting essentially of cryptocrystalline, chalcedonic, or phenocrystalline silica, which has formed by the replacement of some material, ordinarily calcite or dolomite. This jasperoid may be white or various shades of red, gray, brown or black, the colors resulting from different forms of iron in varying proportions."

In an excellent study of the characteristics, origin and economic significance of jasperoids, Lovering (1972) elected to return to Spurr's original definition and he uses the term to indicate:

> " ... an epigenetic siliceous replacement of a previously lithified host rock. Jasperoid, thus defined, excludes syngenetic or diagenetic forms of silica, such as primary chert and novaculite."

Lovering fails, however, to address himself to the megascopic textures exhibited by jasperoid which is one of the main discrepencies between the definitions given by Spurr (1898) and the AGI (1972). Lovering (1962) reported that jasperoids form by both replacement and silica deposition in voids. Replacement dominates in the early stages of jasperoid while direct precipitation dominates in the later stages; this

generally produces aphanitic and coarse-grained quartz, respectively.

Howd and Barnes (1975) experimentally produced both aphanitic and coarse-grained quartz in a closed system while trying to replace carbonates with sulfides. Similar results were obtained by Oehler (1976) who studied the hydrothermal crystallization of a silica gel.

The second point of confusion stems from the usage of terms like chert, replacement chert, jasperoid chert, etc. (e.g., McKnight, 1935) in reference to the fine-grained siliceous gangue commonly found in many ore deposits. This usage is misleading because chert is a diagenetic siliceous replacement deposit while jasperoid is an epigenetic siliceous replacement deposit. Therefore, siliceous gangue found in mineral deposits should be referred to as jasperoid. It should also be noted that jasperoid can be either hypogene or supergene in origin (Lovering, 1972, p. 6).

Thus, based on the evidence and data presented in this thesis, the term jasperoid is applied to both aphanitic and coarse-grained quartz formed during the 'epigenetic siliceous replacement of a previously lithified host rock'. It is used in the text synonymously with hydrothermal silicification.

Method of Investigation

In order to examine the distribution and controls of jasperoid in the Kelly Limestone and to develop a possible genetic model the following methods of study were employed

(1) field mapping, (2) petrographic analysis, (3) fluid inclusion analysis, and (4) X-ray diffraction analysis. The X-ray diffraction study was primarily used to differentiate between Kelly district chert and jasperoid, details are presented in Part II of this thesis.

Field work was conducted during the summer of 1975 and spring of 1976, ninety days were spent in the field. This aspect of the study was devoted to remapping the study area (where necessary), noting the distribution and controls of jasperoid, and collecting representative rock and mineral samples for laboratory analysis. The revised geology of the study area along with the distribution of jasperoid and the occurrence of mines, prospects and shafts were plotted on the Magdalena District, New Mexico special topographic map (1:12,000), in order to facilitate correlation with other maps of the district (Loughlin and Koschmann, 1942; Blakestad, 1976).

Detailed petrographic analysis was performed on fifty thin sections consisting of unsilicified and slightly silicified Kelly Limestone, chert and jasperoid from the Kelly district. An additional twenty thin sections of Kelly district jasperoid and fifteen thin sections of other rocks in the study area were scanned. Petrographic analysis was conducted on a Zeiss research microscope.

Homogenization temperatures were determined for fluid inclusions from barite, fluorite, calcite and quartz within the jasperoid. Temperatures were determined with a

chromel-alumel thermocouple in conjunction with a Doric (DS 350) digital temperature indicator. Filling temperatures were reproducable to within ±0.1°C. Doubly-polished thick sections were prepared for barite, calcite and quartz samples.

Chapter II: GEOLOGIC SETTING OF THE KELLY MINING DISTRICT

The geology and ore deposits of the Magdalena mining district have been described in some detail by Loughlin and Koschmann (1942). Titley (1958, 1961, 1963) provides an excellent study of the Linchburg mine, a pyrometasomatic ore deposit, in the southern part of the district. In recent years much of Loughlin and Koschmann's work has been revised (Park, 1971; Siemers, 1973; Blakestad, 1976). The description of the geology that follows is largely a condensation and integration of these works plus my own field data for the eastern portion of the Kelly mining district. The purpose of this section is to provide the reader with the geologic setting of the silicified Kelly Limestone.

Stratigraphy

Formations and rock types in the Magdalena area are only briefly described except for those rocks exposed in the study area (Plate 1). Figure 2 provides a stratigraphic column for the Precambrian and Paleozoic rocks in the Magdalena area.

Precambrian Rocks

Rocks of inferred Precambrian age crop out along two zones in the Kelly district. One zone lies along the crest of the northern Magdalena Mountains where Precambrian rocks are unconformably overlain by Carboniferous rocks

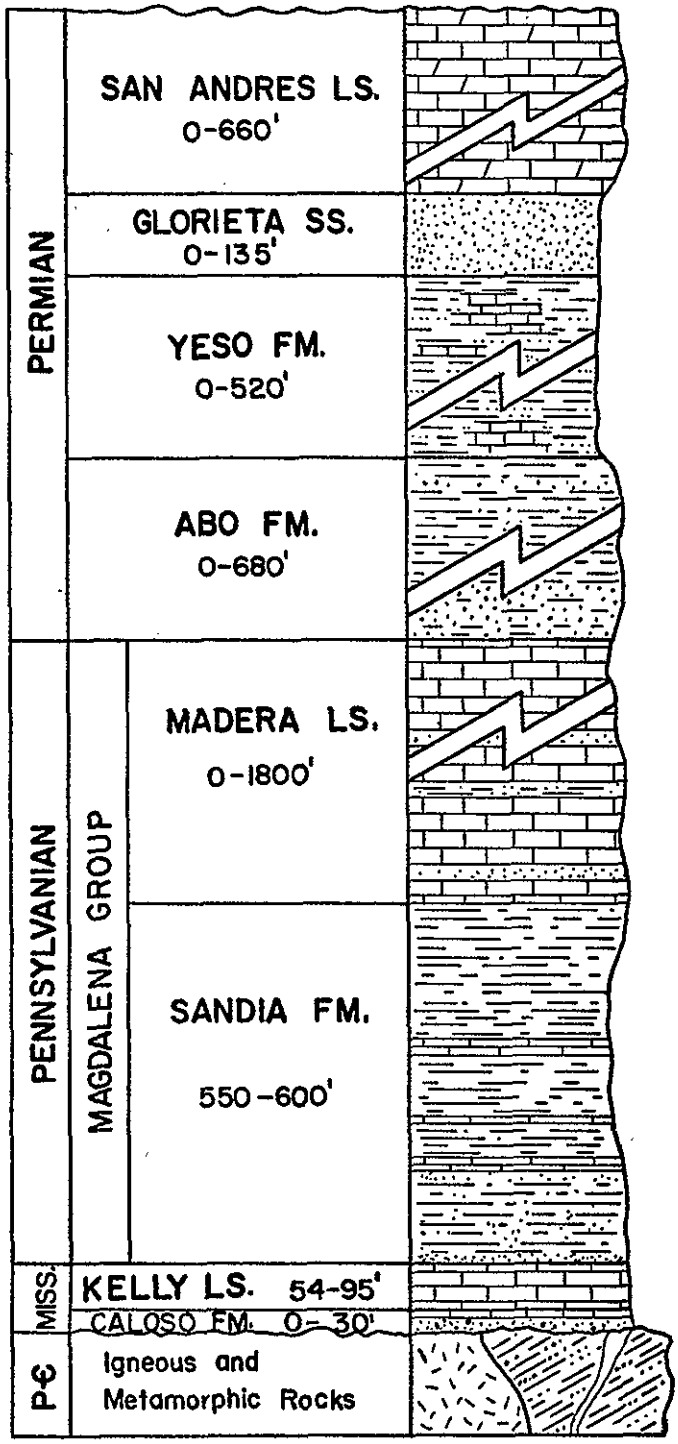

LIMESTONES: blk., fetid, v.-thk.-bdd., homogeneous, sparsely fossil., dolomicrites; weathers to rough, hackly surface; mapped as Madera Limestone by Loughlin and Koschmann.

SANDSTONES: lt. to med.-gry., v. thk. bdd., med.-gnd. v. well srt. calc., qtz. arenites and minor limestones; mapped as upper quartzite member of Sandia by Loughlin and Koschmann.

LIMESTONES, SANDSTONES, and SHALES: faulted, incomplete, poorly exposed section near Magdalena; dk.-gry., unfossil., dol. micrites, only exposed lithology; mapped as upper limestone member of Sandia Fm. by Loughlin and Koschmann.

SANDSTONES, SILTSTONES, and SHALES: rd.-brn., fn.-gnd., thn.-bdd., qtz. arenites and siltstones; abun. thn. lam. and ripple xlam.; bleached to lt.-rd.-brn. and grn.-gry. near Magdalena and Tres Montosas plutons; mapped as Sandia shales by Loughlin and Koschmann (1942)

LIMESTONES: Thick, homogeneous sequence of lime muds (micrites) with a few thn. bds. of grn.-gry. to gry., med. to crs.-gnd. quartzite; upper 200-300 ft. consists of rd., grn., and gry. micrites grading upward into arkosic strata of Abo Fm.; nodular micrites common throughout; micrites generally gry.

SHALES, QUARTZITES, and LIMESTONES: gry. to blk., sdy., carb., shales and siltstones with thn. bds. of gry., med.-gnd., crinoidal limestones and grn.-gry. to brn., med.-crs.-gnd quartzites. Loughlin and Koschmann (1942) divided the Sandia into six members but lenticular bedding and rapid facies changes make this subdivision of limited value.

LIMESTONES: lt. gry., med.-crs. gnd., thk.-bdd., crinoidal sparrites, thn. bd. of dol. micrite near middle (Silver Pipe)
LIMESTONES and CONGLOMERATES: gry., pbly., sdy., mas., qtz. micrites and basal ark. cgls.

ARGILLITES, QUARTZITES, and GRANITES: thick sequence of metasedimentary rocks intruded by granites, gabbros, felsites, and diabase dikes.

Figure 2. Stratigraphic column of Precambrian and Paleozoic rocks in the Magdalena area (from Chapin et al., 1975).

which form the west side of the range. The second zone consists of three irregular, largely fault bounded outcrops aligned north-northwest through the center of the district (Plate 1). The age of these rocks is based on their lithologic similarity to other Precambrian rocks in the state (Loughlin and Koschmann, 1942) and to their stratigraphic position beneath the Mississippian Kelly Limestone.

The Precambrian rocks in the district can be subdivided into five mappable units which are, from oldest to youngest: (1) argillite and schist, (2) early gabbro or diabase, (3) felsite, (4) granite and (5) late diabase. For the purposes of this study, the Precambrian rocks were not subdivided in mapping. Detailed descriptions have been given by Loughlin and Koschmann (1942) and Blakestad (1976) for all five units, and by Titley (1958) and Krewedl (1974) for the argillite and granite in the Linchburg mine and the central portion of the Magdalena Mountains, respectively. A brief description of the five units taken from the above authors follows.

Argillite and Schist. The argillite is generally light-greenish gray, fine-grained to microgranular, thin-bedded with a distinct siliceous appearance. Weathered surfaces are tan or gray and characteristically show banding of relatively light and dark layers. The principal mineral constituents determined microscopically are quartz and sericite, smaller amounts of orthoclase, green biotite and chlorite are also present.

The schist, which is reportedly not present in the Kelly area, ranges from a banded siliceous rock to a very schistose sericitic rock. The siliceous variety composed of alternating light-gray layers about one-fourth inch thick and thinner brown and green layers, consists of quartz, orthoclase, chlorite and muscovite with subordinate amounts of rutile, zircon and magnetite. The sericitic variety is silvery gray and finely foliated with quartz grains visible on surfaces across the foliation. In thin section, interlocking quartz grains with oriented muscovite, minor amounts of biotite, magnetite, chlorite, apatite and rutile are present.

Early gabbro or diabase. The gabbro, or coarse-grained diabase, is found to be intrusive into the argillite. It is dark-green to black, weathering gray consisting predominantly of plagioclase and uralitic hornblende. Plagioclase constitutes about 70 percent of the rock. Accessory minerals are leucoxene, magnetite, green biotite, apatite, chlorite, epidote and calcite.

Felsite. The felsite, which intrudes the argillite, is dark-purplish gray to black, weathering light gray to pale pink, dense to extremely fine-grained and finely porphyritic. It looks like the argillite but can be differentiated by its porphyritic texture and lack of bedding. Phenocrysts of quartz, oligoclase and perthitic orthoclase embedded in a microgranular groundmass of feldspar and quartz were identified petrographically.

Granite. The granite intrudes all older Precambrian rocks. It is fine- to medium-grained, pink to tan, weathering to a pinkish-gray and occasionally being stained yellow and buff. It consists chiefly of quartz and microperthitic orthoclase, with minor amounts of green biotite.

Late diabase. The late diabase consists of coarse-grained and fine-grained varities, occurring primarily as dikes in the Magdalena area. The coarse-grained variety is dark-greenish gray; on weathered surfaces, the bleaching of altered feldspar brings out the diabasic texture provided that the alteration is not too intense. The fine-grained variety is grayish-black to greenish-gray with darker facies showing minute glistening cleavage surfaces of biotite. The dikes appear to be extensively altered in thin section and consist of masses of green hornblende with minor amounts of chlorite, epidote, zoisite, granular aggregates of albite, and leucoxene.

Paleozoic Rocks

Paleozoic rocks of Mississippian to Permian age are exposed in the Kelly mining district; no record of early to middle Paleozoic rocks have been found. Only the Caloso Formation and Kelly Limestone of Mississippian age, and the Sandia Formation and Madera Limestone of Pennsylvanian age are present in the study area. The Kelly Limestone not only caps the range but also forms the western dip slope along with the younger units (Plate 1). Paleozoic rocks also occur as a large down-faulted block on the

eastern slope of the Magdalena range directly east of the town of Kelly. Permian rocks crop out immediately to the west of the study area (Abo Formation, Figure 3) and to the north in the Granite Mountain-Stendel Ridge area (Abo Formation, Glorieta Sandstone and San Andres Formation, see Siemers and Blakestad, 1976). The Yeso Formation (Figure 2) appears to have been faulted out (Siemers, personal commun., 1976). These Permian rocks were thought to be a Mississippian-Pennsylvanian (Kelly-Sandia-Madera) complex by Loughlin and Koschmann (1942).

Mississippian System

Herrick (1904) named the Mississippian strata in the Magdalena area the Graphic-Kelly Limestone after the two leading mines in the district. Gordon (1907) renamed the strata the Kelly Limestone after the town of Kelly. Armstrong (1958) divided the Mississippian strata into a lower clastic unit and an upper crystalline unit, called the Caloso and Kelly Formations, respectively; the former occupies channels and troughs on the Precambrian surface. The total thickness of these rocks ranges from 60 to 125 feet. Siemers (1973) reported that these units are of variable thickness, ranging from 0 to 35 feet for the Caloso Formation and 54 to 95 feet for the Kelly Limestone. The units were not differentiated while mapping because of the cliff-like outcrops and thinness of the Caloso Formation. They are described separately, however,

Figure 3. Generalized geologic map of the Kelly mining district (after Loughlin and Koschmann, 1942; Blakestad, 1976).

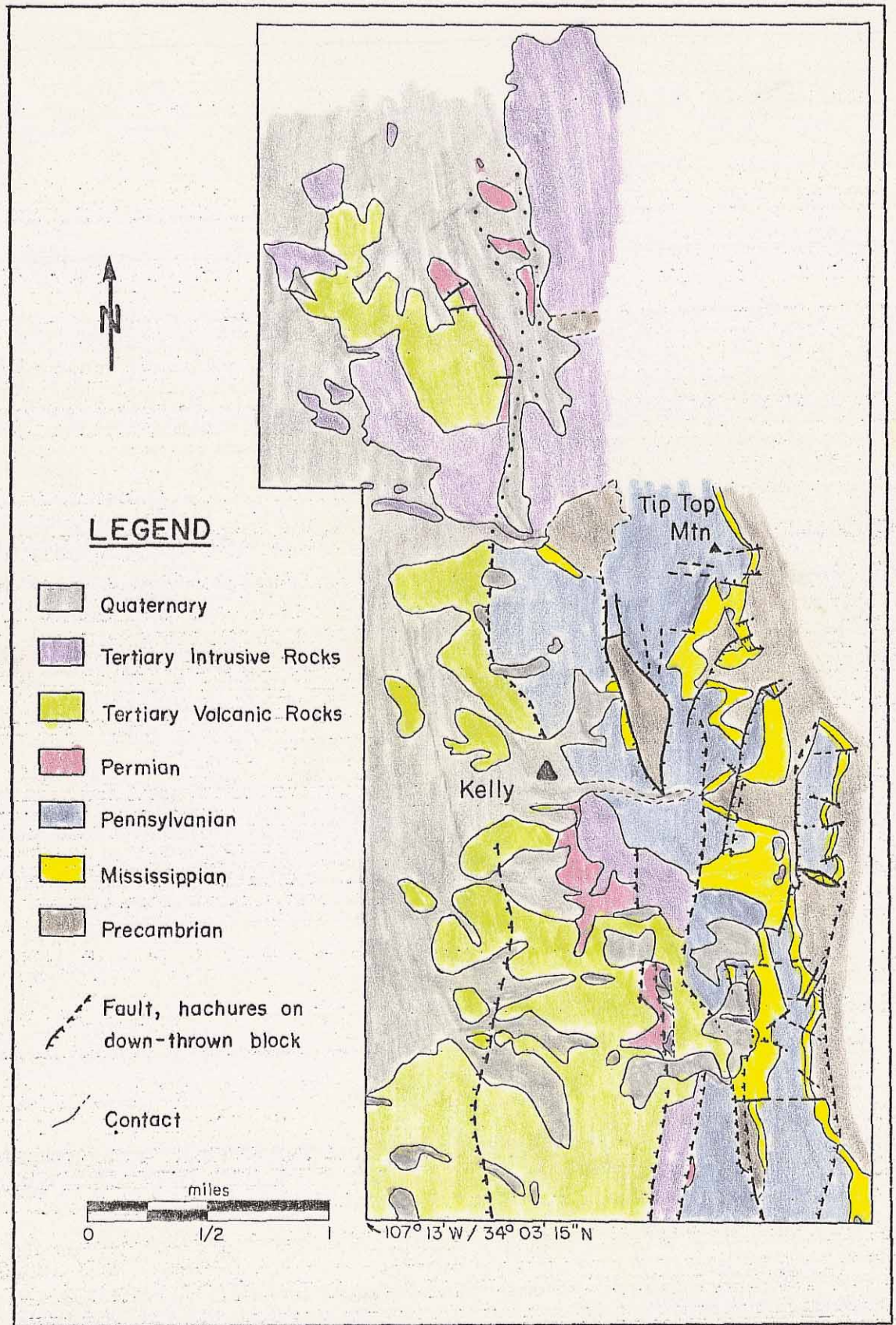
N
LEGEND
Quaternary
Tertiary Intrusive Rocks
Tertiary Volcanic Rocks
Permian
Pennsylvanian
Mississippian
Precambrian
Fault, hachures on down-thrown block
Contact
miles
0
1/2
1
Tip Top Mtn
Kelly
107° 13' W / 34° 03' 15" N

because of their relationship to hydrothermal mineralization and alteration.

Caloso Formation. The Caloso Formation, unconformably overlying the Precambrian basement, consists of a sequence of basal sands, arkoses and shales overlain by a fine-grained, cherty, algal, massive gray limestone (Armstrong, 1958).

The basal terrigenous unit exhibits rapid facies changes and varies in thickness from 2 to 8 feet. It is characterized by poorly sorted, rounded to angular fragments of Precambrian quartz, granite, greenschist and epidote. The grains range in size from coarse sand to small pebbles and are cemented by a carbonate matrix. An arenaceous to arkosic, medium-crystalline, gray-to-green fossiliferous limestone is locally present.

Approximately 25 feet of massive, thick-bedded, light- to medium-gray limestone overlies the basal unit. The limestone contains abundant rounded to angular, medium- to coarse-grained, quartz sand with occasional Precambrian lithic fragments. The fossil content of this unit is very limited.

The Caloso Formation is generally not silicified. The only significant exception is the North Baldy area where extensive alteration has completely silicified the Caloso Formation and the overlying Kelly Limestone.

Kelly Limestone. Conformably overlying the Caloso Formation is 54 to 95 feet of thin to thick-bedded,

fine- to coarse-grained, bluish-gray crinoidal limestone. Abundant nodules and lenses of chert are present in the upper portions of the formation. Siemers (1973) reported that the limestones in this formation are predominantly biomicrudites but the lithologies are quite varied and biosparites, biomicrites, and micrites are also present. This author has found that biosparrudites are particularly common in the uppermost portion of this unit.

Loughlin and Koschmann (1942), Titley (1958) and Armstrong (1958) subdivided the Kelly Limestone into lower and upper crystalline units separated by 4 to 8 feet of lithographic to finely crystalline argillaceous dark-gray to light-gray dolomitic limestone called the 'silver pipe' (see Figure 4). This unit was reported to be a conspicuous horizon which was frequently used by miners as a marker bed because of its relationship to the ore deposits in the district. However, Siemers (1973) could not identify this unit in any of the Paleozoic sections he measured in the Magdalena area. I found the 'silver pipe' to be lenticular in nature and to crop out only locally. When present at the surface, it occurs as a dense, extremely fine-grained dolomitic limestone which is pale-yellowish-brown to grayish-orange on fresh surfaces and medium-orange-pink to light-gray on weathered surfaces. The 'silver pipe' occurs too erratically to be a reliable marker horizon at the surface.

The uppermost beds in the Kelly Limestone are very

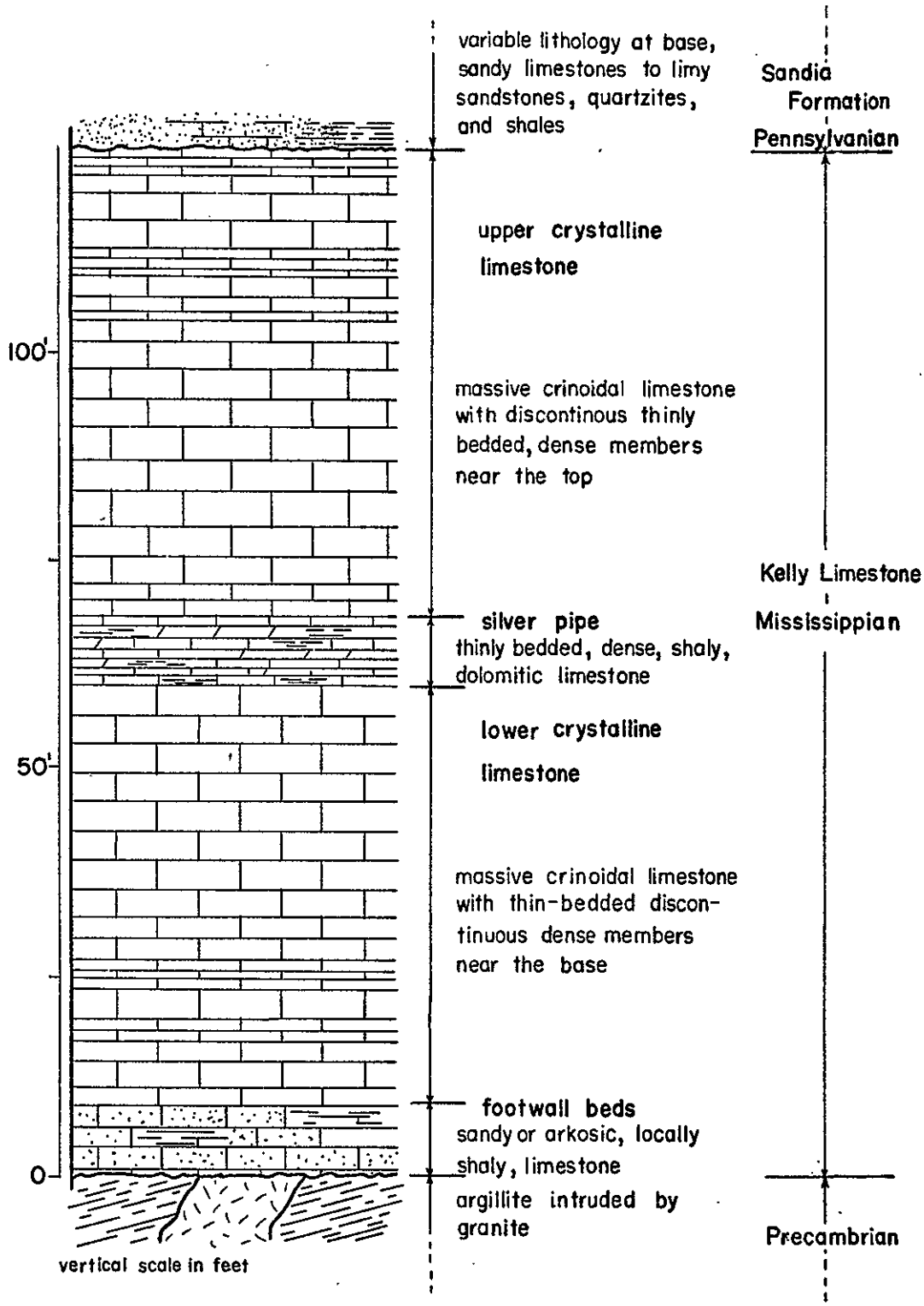

Figure 4. Typical stratigraphic section of the rocks in the Linchburg mine, from Titley (1958). Footwall beds in the figure are equivalent to the Caloso Formation, see text.

coarsely crystalline due to abundant crinoid stems and other fossiliferous material. The upper 5 to 10 feet are remarkably thin-bedded and weather to platy outcrops. The combination of coarse grain size and thin bedding apparently enhanced the lateral permeability of these limestones thus rendering them highly susceptible to hydrothermal alteration relative to other limestone horizons in the formation. Jasperoidization of the Kelly Limestone is persistent over much of the district (Plate 1) being primarily concentrated in the uppermost Kelly just below the Kelly Limestone-Sandia Formation contact; in a few places (e.g., North Baldy), the entire thickness of the formation is silicified. Details of the silicification process are described in the following chapters. At least two types of silicification are present in the upper Kelly Limestone: jasperoid and chert (see p. 3). In a number of areas scattered throughout the district, I had difficulty distinguishing between the two. Part II of this thesis discusses the attempt made to differentiate chert from jasperoid by X-ray diffraction line profile analysis.

Pennsylvanian System

Gordon (1907) named the Pennsylvanian rocks in New Mexico the Magdalena Group after the type section in the Magdalena Mountains; he divided the section into a lower terrigenous unit, the Sandia Formation, and an upper carbonate unit, the Madera Limestone. Detailed descriptions

of these formations are given by Loughlin and Koschmann (1942) and Siemers (1973).

Sandia Formation. A paraconformity exists between the Sandia Formation and the underlying Mississippian Kelly Limestone. Loughlin and Koschmann (1942) subdivided the Sandia Formation into six members; from oldest to youngest they are: (1) lower quartzite member, (2) lower limestone member, (3) middle limestone member, (4) shale member, (5) upper crystalline member and (6) upper quartzite member. Siemers (1973) found that this subdivision was impractical for field use because these members are lenticular and vary considerably in thickness. In this study, the Sandia Formation was mapped as a single unit.

The Sandia Formation is approximately 600 feet thick. It consists predominantly of shale and wacke (constituting greater than 75 percent of the unit) with minor interbedded medium- to coarse-grained quartzite and dark-gray to black fossiliferous micritic limestone (Siemers, 1973). Bedding varies from thin- to thick-bedded. The quartzites are cross-bedded on a small to medium scale and the limestones show planar and small-scale laminations.

Loughlin and Koschmann's lower quartzite member was found to consistently overlie the Kelly Limestone. This member is about 90 feet thick and consists of gray, greenish-gray and reddish-brown quartzites with subordinate amounts of interbedded shale and limestone. The quartzite layers are composed of coarse-grained quartz sand that

occasionally becomes conglomeratic with quartz pebbles as much as 1-1/2 inches in diameter. The limestones are generally light to dark-gray, thin- to medium-bedded micrites. The shale crops out poorly, generally being covered by an immature soil.

The quartzite or shale units of this member typically overlie the Kelly Limestone, rarely does the limestone unit occupy this position. In the Linchburg mine, Titley (1958, 1961) states that:

> "An intensely folded and slickensided black, carbonaceous shale is the most common basal Sandia rock type. Less commonly the Kelly formation lies in contact with a dirty, impure limestone bed whose relation in time to the Sandia or Kelly formations is not known. Rarely, a bed of quartzite is present as the basal unit in the Sandia formation."

This appears to be in marked contrast to the surface geology just described.

Madera Limestone. A gradational contact exists between the Madera Limestone and the underlying Sandia Formation. Loughlin and Koschmann (1942) divided the Madera Limestone into a lower and upper member totalling 600 feet in thickness. The lower 300 feet consists of thin-bedded, bluish-black limestone with thin beds of bluish-gray fissile shale and gray medium-grained quartzite, somewhat similar to the Sandia Formation. The upper member was reported to be at least 300 feet thick, characterized by bluish-gray, fine- to coarse-grained, massive limestone containing

abundant black chert nodules. Interbedded with the limestones are thin-bedded, mottled, shaley limestones, lenses of gray shale, gray to brown quartzite and limestone conglomerate. Prominent lenses of conglomerate, consisting of pebbles of quartzite and Madera Limestone and grading into thin, fine- to medium-grained quartzite beds at their tops, have been found locally (Blakestad, 1976). Siemers (1973) reports that the Madera is predominantly a dark-gray to black, medium- to very thick-bedded, fossiliferous micritic limestone with subordinate amounts of coarse-grained, poorly- to moderately-sorted, calcareous quartzites and black carbonaceous shales; nodules of black chert are common near the top.

The contact between the Sandia Formation and the Madera Limestone was arbitrarily placed by Loughlin and Koschmann at the upper quartzite of the Sandia Formation, above which limestone beds are dominant and below which shale predominates. Siemers agreed with this definition and it was subsequently used in this study.

Loughlin and Koschmann were not able to determine the true thickness of the Madera Limestone because of faulting and erosion but noted that it may be close to 1000 feet. Siemers found the maximum thickness to be 800 feet in the sections he measured but they were all bounded by faults. Blakestad reports that in the southernmost areas of the Kelly district a probable thickness of 1800 feet should be considered.

Permian System

No Permian rocks crop out in the eastern portion of the Kelly district (Plate 1), however, they are exposed in the Magdalena area (Figure 3). Detailed descriptions of some of these rocks are given by Siemers (1973), Blakestad (1976), Siemers and Blakestad (1976) and Siemers (in preparation). The following is a very brief description of these rocks taken from the above authors and from Figure 2.

Abo Formation. Conformably overlying the Madera Limestone is the Abo Formation which in the Kelly district typically consists of dark-red to reddish-gray, fine-grained, thin-bedded sandstones which are occasionally shaly. Locally, interbedded lenses and layers of green to gray, generally argillaceous sandstones are present. Fine- and cross-laminations are abundant. A maximum thickness of about 700 feet is reported for this formation in the Magdalena area (Blakestad, 1976; Chapin et al., 1975).

Bleaching of the Abo Formation from red to greenish-gray by propylitic alteration caused Loughlin and Koschmann (1942) to misidentify these rocks in the northern part of the district as shales of the Sandia Formation (see Blakestad, 1976 for details).

Yeso Formation. Only an unfossiliferous dolomitic micrite of the Yeso Formation is exposed in the Magdalena area. Siemers (personal commun., 1976) reports that the rest of the formation appears to have been faulted out.

Maximum thickness is approximately 520 feet (Chapin et al., 1975).

Glorieta Sandstone. The Glorieta Sandstone consists of light- to medium-gray, very thick-bedded, medium-grained, well-sorted quartz sandstone and minor limestones. Maximum thickness is about 135 feet (Chapin et al., 1975).

San Andres Limestone. The San Andres Limestone conformably overlies the Glorieta Sandstone. It consists of black, fetid, very thin-bedded, poorly fossiliferous dolomicrites in the Magdalena area and has a reported thickness of 660 feet (Chapin et al., 1975).

Tertiary Extrusive Rocks

No Tertiary volcanic rocks have been found in the eastern portion of the Kelly mining district (Plate 1); however, these rocks occupy a large area to the west (Figure 3). A discussion of the volcanic stratigraphy in this area is beyond the scope of the present investigation. For a comprehensive review of the volcanic section in the Kelly district the reader is referred to Blakestad (1976). At the time of hydrothermal alteration and mineralization in late Oligocene or early Miocene, the Kelly district could have been covered by as much as 5000 feet of volcanic rocks; however, in the light of recent structural interpretations a probable thickness of 2000 feet can be considered (Chapin, personal commun., 1976).

Tertiary Intrusive Rocks

No Tertiary intrusive rocks have been found at the surface in the eastern portion of the Kelly mining district, except for a few dikes and sills (Plate 1). In marked contrast, several large intrusive bodies are present in the western and northern portions of the district (Loughlin and Koschmann, 1942; Park, 1971; Blakestad, 1976) and in North Fork Canyon (Krewedl, 1974).

Four major intrusives and several varieties of dikes and sills have been reported in the Kelly district. The Anchor Canyon Granite and the Nitt Monzonite (facies of the larger Magdalena composite pluton) appear to be relatively fresh, barren intrusives (Chapin, personal commun., 1976); whereas, the latite porphyry of Mistletoe Gulch and quartz monzonite of the Linchburg mine are altered and appear to have played an important role in the hydrothermal mineralization and alteration episode. A Brief discussion of the Mistletoe Gulch and Linchburg mine intrusives and of the dikes and sills which crop out in the study area follows. The reader is referred to the authors cited above for an extensive treatment of these intrusive rocks.

Latite Porphyry of Mistletoe Gulch. The latite porphyry of Mistletoe Gulch crops out immediately to the west of the study area (Figure 3), as a discontinuous mass that extends from the town of Kelly to the southern

edge of the district. Loughlin and Koschmann (1942) interpreted this body as a sill but recent studies by Blakestad (1976) have found it to be the dike-like top of a larger intrusive of unknown dimensions which occupies a major north-trending cauldron-margin fault (Figure 3, p. 33).

The intrusive is generally greenish-gray on a fresh surface and greenish-yellow or yellow-brown on a weathered surface. It has a dense groundmass with phenocrysts of hornblende, biotite (?) and plagioclase, and ranges in composition from hornblende latite to quartz latite. The latter usually occurs as dikes in the hornblende facies.

In thin section, the latite porphyry shows a uniform texture with phenocrysts of hornblende, plagioclase and biotite (?) in a groundmass of altered plagioclase microlites. Alteration ranges from moderate to intense with plagioclase going to calcite and sericite and ferromagnesium minerals altering to chlorite and pyrite (or magnetite). Blakestad (1976) reports that the rock becomes noticably bleached and more sericitic near faults and veins with pyrite generally becoming more abundant as the intensity of alteration increases.

This intrusive apparently acted as a barrier to the circulation of hydrothermal fluids as rocks east of this body are highly altered and mineralized in the central and southern portions of the Kelly district while rocks to the

west show little or no alteration. An excellent example of this is evident near the Patterson adit where the Spears Formation west of the dike is relatively fresh whereas, east of the dike it is highly altered (Chapin, personal commun., 1976).

Quartz Monzonite of the Linchburg Mine. No surface exposures of this stock exist in the Kelly mining district. Nevertheless, its existence in the Linchburg mine area has been postulated by Loughlin and Koschmann (1942) on the basis of the occurrence of metamorphic minerals in the Kelly Limestone and extensive silicification of the Precambrian argillite along a major north-trending fault in the area (Figure 3), by Titley (1958, 1961) during his study of the pyrometasomatic replacement deposits in the Linchburg mine, and by Austin (1960) who inferred the presence of the stock from the occurrence of schellite along a major north-trending fault.

Blakestad (1976) reports that during recent mining, an irregular mass of porphyritic quartz monzonite was encountered in the southern end of the Linchburg workings. Dikes of the same material have also been found in a short adit north of the Grand Ledge tunnel and in drill holes collared in the ravine just east of the Patterson adit. The exact geometry and extent of this stock are not known at the present time. The following description of the intrusive is taken from Blakestad's work.

In hand specimen, the rock appears to be fairly fresh

exhibiting a distinct porphyritic texture defined by rounded quartz "eyes" and by rounded to subhedral phenocrysts of plagioclase in an aphanitic matrix. The color varies as a function of the amount of epidote, chlorite, and potash feldspar from light-greenish-gray to pinkish-gray. Although fresh in hand specimen, Blakestad (1976) reports that in thin section it is one of the most highly altered intrusive rocks in the district. Plagioclase crystals have been extensively altered to sericite and the large quartz "eyes" are thoroughly embayed and corroded.

In drill holes, approximately 500 feet south of the southernmost Linchburg workings, the quartz monzonite porphyry was found to pass into an equigranular quartz monzonite. Blakestad states that:

> "This associated (?) intrusive is generally hypidiomorphic equigranular in character and is light buff to orange in color. Scattered clots of chlorite and veinlets of quartz and sericite are common. Sericite also replaces some of the plagioclase. Quartz and pyrite occur in thin veinlets and with some chlorite in ragged patches that may represent former biotite. Microscopic examination reveals that the rock is less altered than the porphyritic facies, with the grade of alteration corresponding to mild to moderate propylitization."

There is some discrepency in the age relationships of these two intrusives but Blakestad believes that the porphyritic facies is a later intrusive phase into the equigranular quartz monzonite facies.

The quartz monzonite of the Linchburg Mine is thought to extend to the North Baldy area because of the development

of a small mineralized skarn in the Kelly Limestone analogous to the mineralized skarn in the Linchburg mine. The occurrence of this intrusive in proximity to the major pyrometasomatic ore deposits of the Linchburg mine may be significant to the origin of the mineralization and to the hydrothermal silicification of the Kelly Limestone.

Mafic Dikes. Several aphanitic to porphyritic mafic dikes were mapped in the area north of Chihuahua Gulch; one sill-like body was found along the crest of the range immediately south of the gulch (Plate 1). These dikes are equivalent to the lamprophyre dikes described by Loughlin and Koschmann (1942) and to the mafic dikes described by Brown (1972) and Blakestad (1976). Detailed work on these rocks was beyond the scope of this study; the following is a brief summary of the descriptions provided by Loughlin and Koschmann and Brown.

The mafic dikes vary considerably in appearance, color and degree or propylitic alteration. The least altered rocks are dark gray and basaltic-looking while the most altered are green owing to the abundance of chlorite. Most are stained a rusty brown on weathered surfaces. Some mafic dikes are porphyritic with a fine-grained groundmass, some are only slightly porphyritic with a fine, equigranular groundmass and others are nonporphyritic with a very fine-grained texture. Phenocrysts of pyroxene, hornblende, biotite and plagioclase

are present in some; xenocrysts of quartz and plagioclase are common. Calcite grains and clusters are also found in some mafic dikes. Brown states that:

> "Most varieties are too fine-grained and altered to be identified petrographically and they are best described as lamprophyres in the sense that they are dark, fine-grained rocks in which ferromagnesium minerals usually occur as phenocrysts."

Microscopically, felty plagioclase microlites, pyroxene and Fe-oxides with accessory biotite and apatite were identified in the aphanitic ground mass. Generally, the dikes are altered to calcite, chlorite, epidote and sericite.

The wall rocks surrounding some of the mafic dikes are silicified in the eastern portion of the Kelly district. A similar situation is reported by Brown (1972) who states that the alteration of the wall rocks is later than the intrusion of the dikes. This appears to be also true in the area of this investigation.

White Rhyolite Dikes. The white rhyolite dikes (and sills) are younger than the mafic dikes. In the southeastern portion of the Kelly district, numerous dike swarms are found in the North Fork Canyon area, along a north-trending fault zone WNW of North Baldy Peak and one has been mapped by Blakestad (1976) east of the Cavern tunnel. Several white rhyolite sills have also been mapped in the region south of Chihuahua Gulch along the crest of the range (Plate 1). Loughlin and Koschmann (1942) and Titley (1958, 1961) report the occurrence of

a white rhyolite dike in the Grand Ledge tunnel and Linchburg mine, respectively. Titley postulated the existence of more white rhyolite dikes in the Linchburg mine but owing to their highly altered nature positive identification was extremely difficult.

In general, the dikes occupy a north-northwest trending fault zone which is about 1-1/2 miles wide extending south of the study area into the central Magdalena Mountains (Krewedl, 1974) and north into the southern Bear Mountains (Brown, 1972). These dikes are found to generally occupy the roof zones of exposed stocks (Chapin, personal commun., 1976).

The white rhyolite dikes average between 5 to 10 feet in width and range in length from a few feet to more than a thousand feet. They dip steeply to the east or west and some are nearly vertical. In the field, their light color makes them quite conspicuous. They are grayish-white to white on a weathered surface, white to pinkish-gray when fresh, and fine-grained with phenocrysts of quartz and feldspar. The dikes are often flow-banded, which results in a platy grus upon weathering; limonite psuedomorphs after pyrite are common. The white rhyolite sills are similar to the dikes except that they are locally highly vesicular with lineated vesicles.

Petrographically, these rocks display a porphyritic texture with a dense, microgranular groundmass of irregular quartz and feldspar. The orthoclase phenocrysts

are subhedral to euhedral exhibiting moderate to strong alteration to sericite and carbonate. Quartz phenocrysts, anhedral to euhedral in shape, occasionally show minor resorption along their edges. Hair-like veinlets of quartz and sericite are also common.

The dikes (and sills) are characteristically highly silicified. They generally occupy major north-trending fault zones that were often used as channel-ways for mineralizing solutions.

Structure

The conspicuous structural features of the eastern portion of the Kelly mining district as shown in Plate 1 are:

1. faulted, westward-dipping homoclinal blocks of Mississippian and Pennsylvanian sedimentary rocks;
2. a belt of elongate fault blocks of Precambrian rocks;
3. steepening of the dips exhibited by Mississippian and Pennsylvanian rocks in the area between Chihuahua Gulch and Tip Top Mountain relative to the area south of the gulch;
4. a major transverse fault (the North Fork Canyon fault of Krewedl, 1974, which is part of the Capitan lineament) just south of North Baldy that juxtaposes Paleozoic and Tertiary volcanic rocks (Krewedl, 1974); and
5. gravity slide blocks of Mississippian and Pennsylvanian rocks on the eastern slope of the Magdalena Range directly east of the town of Kelly (Chapin, personal commun., 1977).

The structure of the Kelly mining district, initially described by Loughlin and Koschmann (1942), is being extensively revised by C. E. Chapin and R. B. Blakestad in light of recently recognized overlapping cauldrons. A brief summary of the structural features exhibited by the district which is based primarily on discussion with C. E. Chapin is attempted here.

The Kelly mining district is located at the intersection of the Magdalena cauldron (to the east) and the North Baldy cauldron (to the south), Figure 5. K-Ar dating of the flow-banded member of the A-L Peak Tuff (see Blakestad, 1976 for description) extruded from the Magdalena cauldron and of the stocks which intrude it indicate an age of 29 million years. The major north-trending, down-to-the-west, longitudinal faults in the Kelly district (Figures 3 and 5) are cauldron-margin faults. The latite porphyry of Mistletoe Gulch (p. 25-27) occupies one of these faults and may be considered a ring dike. The northern margin of the North Baldy cauldron is well exposed along the southern flank of North Baldy (Figure 5) and along North Fork Canyon to the southeast (Figure 1). Cauldron-margin faults stepped down-to-the-south juxtapose Paleozoic and Tertiary volcanic rocks (Plate 1 Blakestad, 1976). The age of this cauldron is approximately 32 million years as indicated by several K-Ar dates on the Hells Mesa Tuff (see Blakestad, 1976 for description). The quartz monzonite of the Linchburg mine is located near the intersection

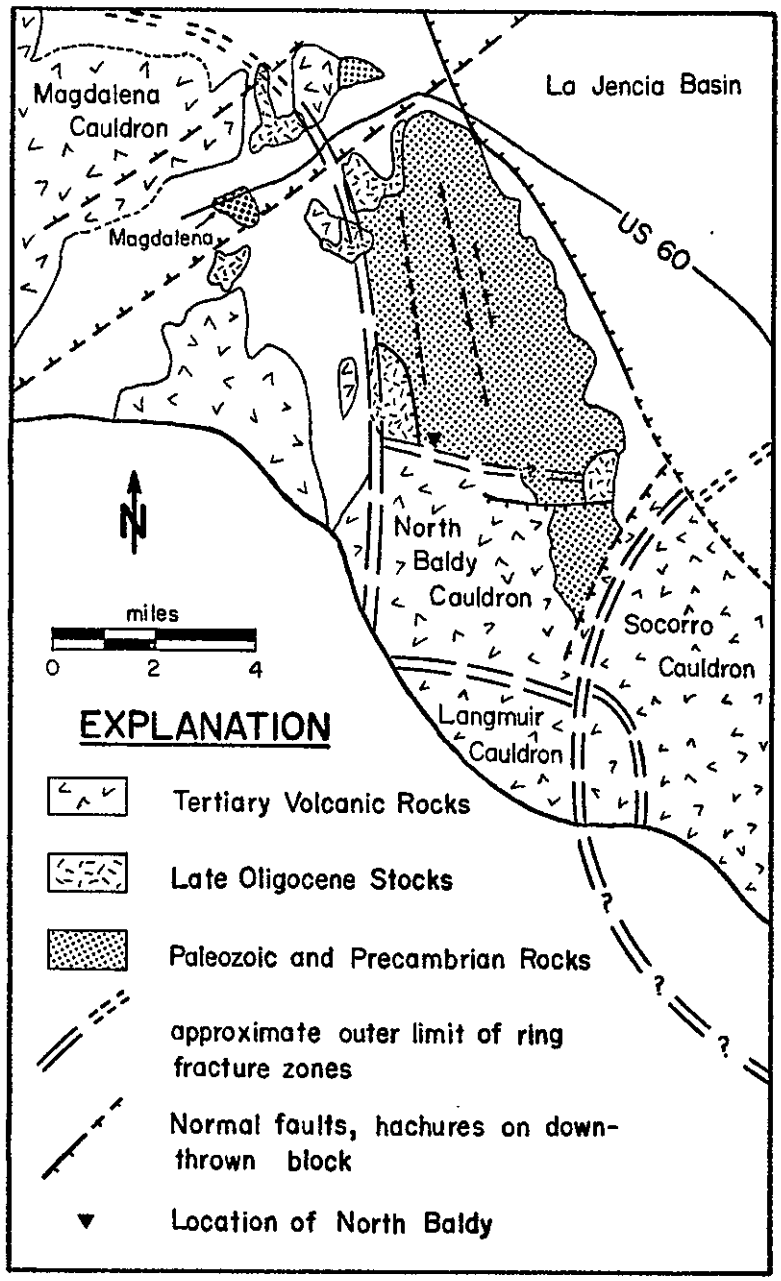

Figure 5. Generalized map of the major structural features in the Magdalena area (modified after Chapin and Chamberlin, 1976).

of the Magdalena and North Baldy cauldrons. Chapin believes that this stock is probably younger than both cauldrons as evidenced by the alteration of the Lemitar Tuff (Blakestad's, 1976 Tuff of Allen Well) on the ridge west of North Baldy. The Lemitar Tuff which erupted from the Socorro cauldron has been dated at 26 million years.

Thus, the structure of the district is one of cauldron-margin faulting near the intersection of two overlapping cauldrons. The dominant fault trend is about N 10°W with down-to-the-west displacements towards the Magdalena cauldron; many east-trending faults are also present and are radial to the cauldron margin. In the south end of the district, near North Baldy, several WNW-trending faults are stepped down-to-the-south towards the older cauldron.

Late Cenozoic block faults related to the Rio Grande rift are superimposed upon the Oligocene cauldron-margin faults. The Magdalena Range was uplifted along major north-trending rift faults and rotated to the west in Miocene and Pliocene time. The movement continues today as indicated by a prominent Holocene fault scarp along the northeast side of the Range. Several large blocks of Paleozoic rocks just east of the crest of the Magdalena Range may have been isolated from the main Paleozoic outcrop by gravity sliding on the east-facing enscarpment; alternatively, these blocks may overlie low-angle normal faults which represent rotated early-rift faults similar to those described by Chamberlin (1976) in the Lemitar Range of New Mexico.

The north end of the Magdalena Range was truncated by a major northeast trending border fault of the San Augustin arm of the Rio Grande rift which parallels the Morenci-Magdalena lineament that has been recurrently active since at least Laramide time. The downfaulting and preservation of Yeso, Glorieta, and San Andres Formations of Permian age (Chapter II) at the north end of the Magdalena Range was probably related to Laramide faulting along the Morenci-Magdalena lineament. Elsewhere in the Kelly district, the late Eocene erosion surface beveled the Laramide uplift down to the level of the Abo Formation. The WNW-trending Capitan lineament also crosses the Magdalena area and the North Baldy cauldron margin along North Fork Canyon which may have been localized by this lineament.

In summary, the Kelly district is located on the north flank of a Laramide uplift that was transected by major northeast and WNW crustal lineaments and truncated by the late Eocene erosion surface. Two overlapping cauldron margins bounded the district on the west and south in middle to late Oligocene time. The cauldron margin faults controlled the emplacement of stock and dike-like intrusions and provided the main channel-ways for hydrothermal solutions. In late Cenozoic time, the district was uplifted and rotated westward to form a fault-block mountain range. Concurrent erosion has dissected the range and exposed silicified Kelly Limestone along the crest and dip slopes.

Chapter III: DISTRIBUTION AND CONTROLS OF SILICIFICATION

Geographic Distribution

The eastern portion of the Kelly mining district displays the most intensive silicic alteration of any area in the Magdalena region. This is because Kelly Limestone, main host formation for hydrothermal alteration and mineralization, is exposed almost continuously along the crest of the range and part of its western dip slope (Figure 3). Jasperoid crops out along the crest of the Magdalena range southward from Tip Top Mountain to North Baldy and westward from the crest to the major north-trending faults which drop Kelly Limestone to the west (Plate 1). In this study, the distribution of silicification has been somewhat modified relative to the work done by Loughlin and Koschmann (1942) to include several dip slopes where jasperoid remnants were encountered in place and as float (see Figure 6). Other occurrences of silicified Kelly are found due east of Tip Top Mountain (Plate 1) and in the Ambrosia mine area (Loughlin and Koschmann, 1942).

Silicification of Rocks Other than Kelly Limestone

Although the Kelly Limestone is the most extensively silicified formation in the district, other rock types and formations have been affected. A discussion of these occurrences is presented because it contributes information regarding some of the geologic parameters governing the silicification process.

Figure 6. Remnant of silicified upper Kelly Limestone on a dip slope with underlying unaltered limestone. On several dip slopes, the silicified upper Kelly has been eroded. The presence of numerous pieces of silicified float and scattered remnants of jasperoid which stand topographically and stratigraphically higher than the surrounding limestone, attest to the probability that at one time the entire dip slope was covered by a veneer of jasperoid.

Precambrian Rocks

Minor occurrences of silicified Precambrian argillite and granite have been found along several fault and fracture zones which acted as conduits for hydrothermal solutions. Figure 7 is an example of silicified Precambrian rocks along a fault zone. A large area of Precambrian argillite has been intensely silicified (along with Kelly Limestone and portions of Madera Limestone) just southeast of the Grand Ledge tunnel. This led Loughlin and Koschmann (1942) to conclude that the Grand Ledge fault was a main channelway for the migration of silica-rich solutions. Blakestad (1976) reports that this area directly overlies the Linchburg stock.

Sandia Formation

As previously mentioned (p. 21), the lower quartzite member of the Sandia Formation consistently overlies the Kelly Limestone. Shale and limestone beds of this member are locally silicified in several places where they lie in depositional contact with jasperoidized Kelly Limestone and along a few silicified fault and/or fracture zones. The quartzite beds of this member generally remain unaffected except for a few sporadic areas along silicified fracture zones. Isolated patches of silicified siltstones also occur in the district. In general, however, the Sandia Formation was not susceptible to silica replacement.

Madera Limestone

Jasperoidized Madera Limestone is found in only two places in the eastern portion of the Kelly district. One area is along the Grand Ledge fault and the other is near the intersection of two major faults at the southwest corner of North Baldy Peak (Plate 1). Blakestad (1976) reports the finding of silicified Madera in a drill hole approximately 500 feet south of the Vindicator shaft in the northern part of the district.

White Rhyolite Dikes

All white rhyolite dikes (and sills) in the Magdalena region are silicified to some degree (Loughlin and Koschmann, 1942; Brown, 1972; Krewedl, 1974; Blakestad, 1976). When completely jasperoidized, white rhyolite dikes are almost indistinguishable from other silicified rocks. The dikes (and sills) are often spatially related to silicified and/or silicated Kelly Limestone, an excellent example being the North Baldy skarn. The dikes (and sills) generally occupy faults and/or fracture zones which were later utilized by the hydrothermal solutions responsible for mineralization and alteration (Chapin, personal commun., 1976).

Volcanic Rocks

Silicification of volcanic rocks occur throughout the Magdalena region. Blakestad (1976) reports some locally intense silicification of volcanic rocks northwest of the Smith tunnel along late Oligocene faults. Silicified

volcanic formations have been also reported in the central Magdalena Mountains and southern Bear Mountains by Krewedl (1974) and Brown (1972), respectively.

Silicification of the Kelly Limestone

The band of Kelly Limestone that crops out along the crest of the range provided this investigator with excellent lateral and vertical exposures; thus allowing for a detailed study of the jasperoid masses. The controls on silicification are of two types, stratigraphical and structural. The importance of the latter is evident from the preceding discussion. For the sake of clarity, the parameters influencing the distribution of jasperoid are divided into primary controls, and features of unknown importance.

Primary Controls

The interplay between primary stratigraphic and structural controls is considerable. Structural features provided conduits for ascent of hydrothermal fluids while stratigraphic variables provided an impermeable cap rock and controlled the permeability and reactivity of individual beds to alteration and mineralization. To facilitate the discussion of these parameters, a series of illustrations are presented to demonstrate their effects.

Figure 7 shows silicified Kelly Limestone and Precambrian granite along an east-trending fault. The

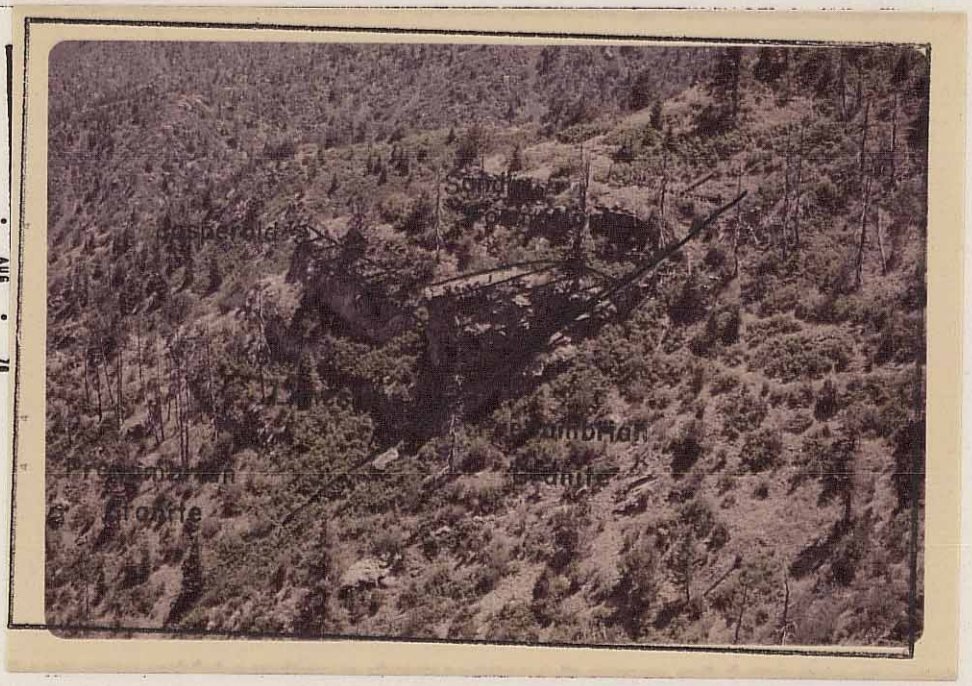

Figure 7. Silicified Kelly Limestone and Precambrian granite along an east-trending fault. Very minor and localized silicification of the Sandia Formation occurs along fracture zones.

Sandia Formation is only locally silicified along fractures. This figure provides the following data:

1. the Kelly Limestone is silicified to varying degrees away from the fault;
2. the uppermost Kelly shows the greatest development of jasperoid;
3. the Sandia Formation is essentially unaltered and in sharp contact with silicified limestone;
4. a sharp but irregular contact exists between jasperoid and unaltered limestone on a macroscopic scale (in hand specimen, the contact is gradational, see Chapter IV);
5. Precambrian granite was replaced by silica for a distance of less than one foot away from the fault where jasperoid was forming in the Kelly Limestone; elsewhere along the fault Precambrian rocks were not extensively silicified.

The large mass of jasperoid in the Kelly Limestone along the fault is interpreted as being the result of solutions being dammed by the impermeable Sandia Formation which also caused the solutions to migrate laterally into the upper Kelly Limestone.

Figure 8a is an idealized diagram illustrating the occurrence of jasperoid in a fault zone and in the upper Kelly Limestone immediately below the Sandia Formation. Figure 8b shows vertically banded jasperoid within the fault zone. The following observations can be made from these figures:

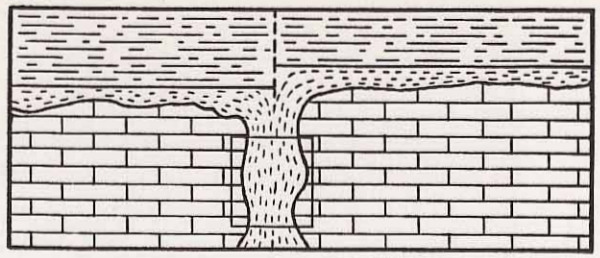

Sandia Formation

Jasperoid

Kelly Limestone

Fault

Figure 8a. Idealized cross-section of faulted Kelly Limestone portraying the deflection of silica-rich solutions laterally into the upper Kelly. Dashed lines represent banding in jasperoid. Outlined area represents Figure 8b below.

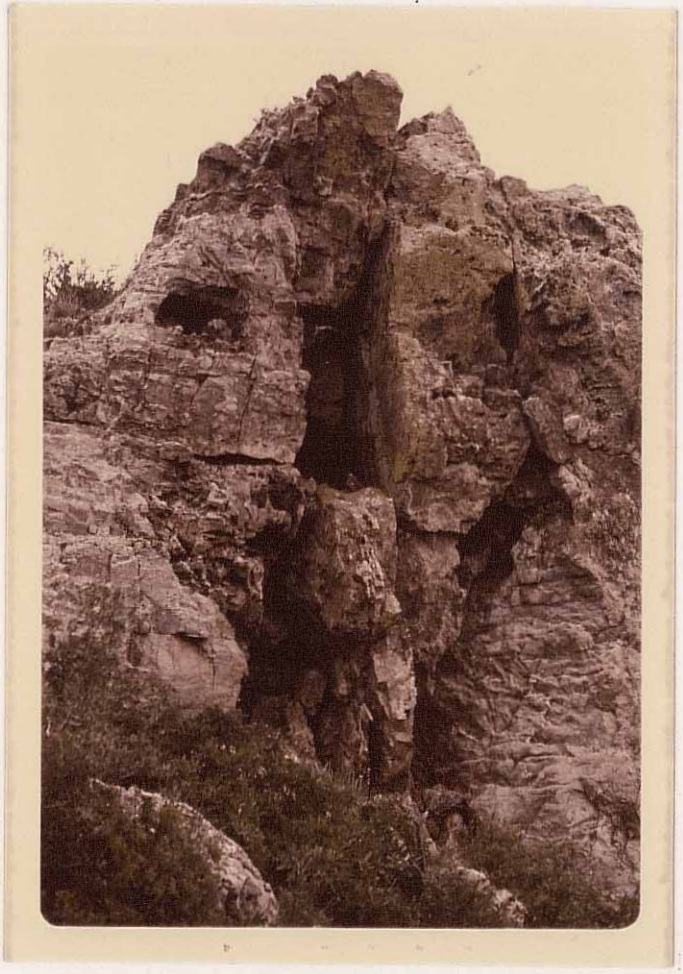

Figure 8b. Vertically banded jasperoid within fault zone illustrated above, see text.

1. jasperoid is concentrated in the upper Kelly Limestone immediately below the Sandia Formation;
2. the Sandia Formation is essentially unaltered and in sharp contact with the underlying jasperoid;
3. banding in jasperoid changes from approximately normal to bedding in the fault zone to parallel to bedding away from it; and
4. a sharp but irregular contact exists between jasperoid and unaltered limestone on a macroscopic scale.

The mushroom-like distribution of jasperoid shown in Figure 8a is interpreted as being the result of deflection of silica-rich solutions rising along a fault as the fluids encountered the impermeable Sandia Formation and were forced to migrate laterally into the Kelly Limestone.

Figure 9a is a generalized diagram portraying the pervasive development of jasperoid in Kelly Limestone at the intersection of two faults. Beyond approximately 20 feet from the fault, jasperoid becomes concentrated along three different stratigraphic horizons and persists for hundreds of feet in two of them. Figure 9b represents the area outlined in Figure 9a where silicification exists in two different stratigraphic horizons. From these figures, the following observations can be made;

1. extensive silicification of the entire Kelly Limestone has occurred for about 20 feet from the intersection of the faults;

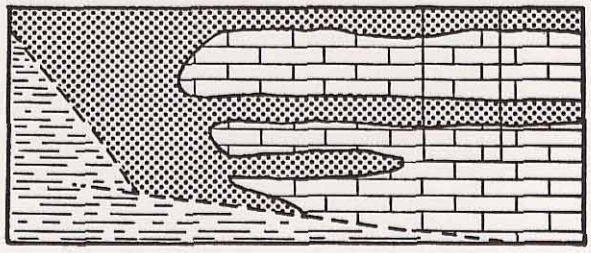

Sandia Formation

Kelly Limestone

Jasperoid

Fault

Figure 9a. Shows extensive silicification of the Kelly Limestone along the intersection of two faults which becomes localized in three horizons at some distance (approximately 30 feet) away from the faults. Outlined area represents Figure 9b.

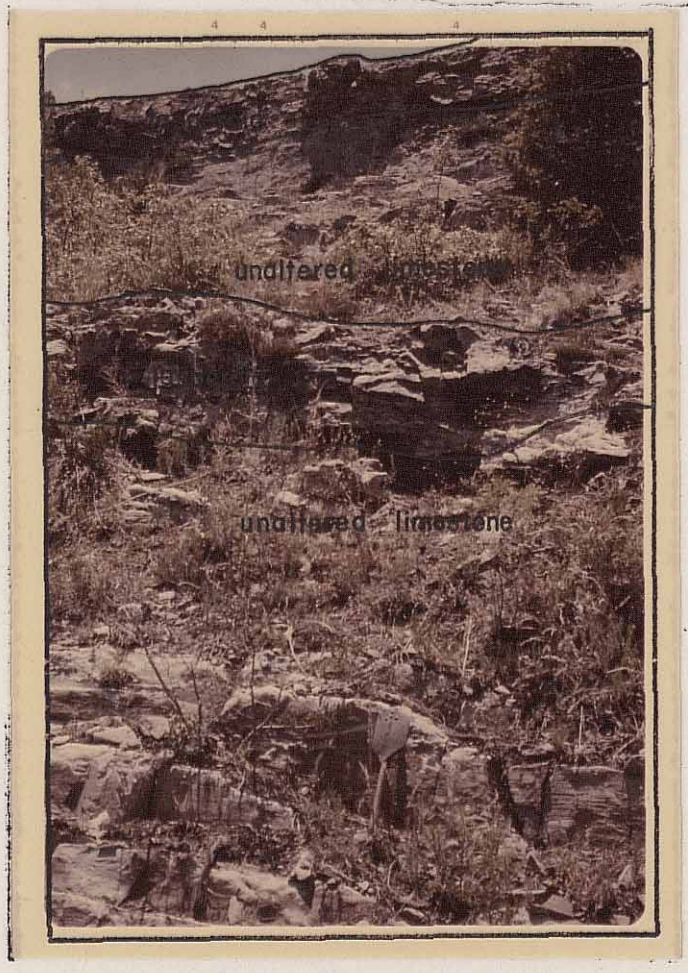

Figure 9b. Jasperoid locallized along two favorable horizons in the Kelly Limestone. Contacts between jasperoid & limestone are sharp on a gross scale.

2. three distinct silicified stratigraphic horizons are present in the Kelly Limestone beyond the zone of pervasive replacement;
3. silicification in the Sandia Formation was restricted to very minor development along several fractures;
4. on a macroscopic scale, the contact between jasperoid and limestone is sharp but irregular;
5. banding in jasperoid is generally parallel to the limestone-jasperoid contact; and
6. unaltered limestones between jasperoid horizons are generally biomicrites and micrites (locally, the silver pipe has been found capping a jasperoid horizon; outcrops of silver pipe are too erratic on the surface to be considered a control, however, in the subsurface the silver pipe is known to cap and underlie ore).

Figure 10a shows a silicified fissure in Kelly Limestone. A number of silicified fissures occur in the study area all trending about N 10°W. This appears to be a major structural alignment of middle to late-Tertiary age in the Magdalena region. Figure 10b is a close-up of the highly fractured and silicified limestone to the right of the fissure in Figure 10a. The following observations can be made from these figures:

1. jasperoid is banded generally parallel to the walls of the fissure;

Figure 10a. Silicified fissure in Kelly Limestone trending approximately N 10°W. Dashed lines indicate banding in jasperoid.

Figure 10b. Close-up of area immediately to the right of the silicified fissure in Figure 10a. Note the intense fracturing and silicification in limestones above the 'silver pipe'. The nature of some silica lenses is discussed in Part II of this thesis.

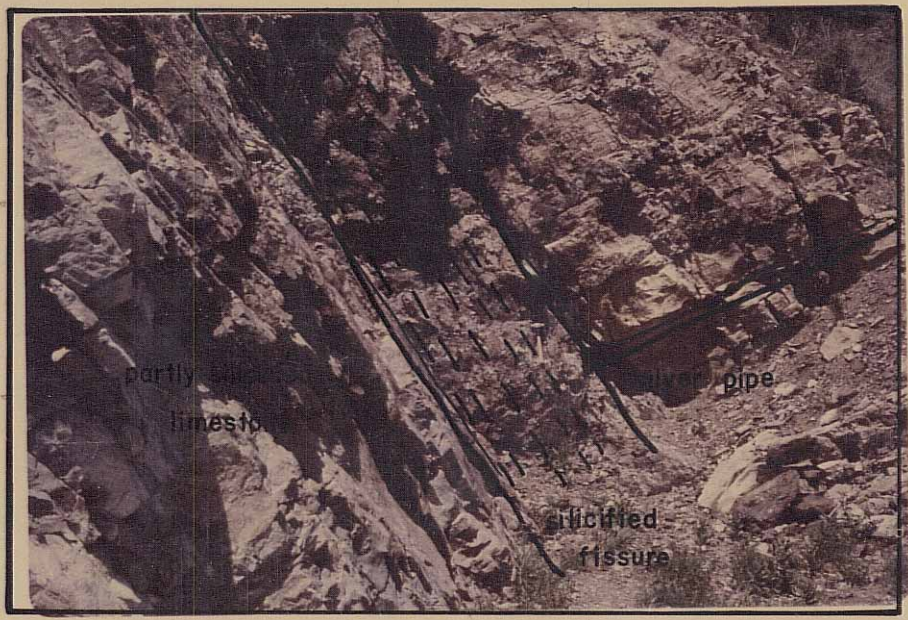
partly
limesto
pipe
silicified
fissure


silver pipe

2. the limestone is only partially silicified in the immediate area of the photograph, however, silicification related to the fissure increases markedly in the upper Kelly Limestone;
3. intensive fracturing and silicification occurred in the limestones above the silver pipe (a dolomicrite) while little of both developed in the silver pipe itself; and
4. several lenses of microcrystalline silica are cut by silicified fractures.

Based on these observations, several conclusions can be drawn with respect to the dominant controls of silicification. Primary stratigraphic controls are: (1) the impermeable nature of the Sandia Formation which deflected the silicifying solutions into the upper Kelly Limestone, and (2) permeable and reactive limestone horizons (biosparrudites) which were highly susceptible to silica replacement. It is this authors contention that the major factor responsible for the extensive silicification of the upper Kelly is the impermeability of the Sandia Formation. The primary structural controls were faults and fissures which allowed the introduction of the silica-bearing fluids into the Kelly Limestone.

Features of Unknown Importance

A number of features which appear to be related to the silicification process have been noted in the Kelly Limestone. Their significance, however, could not be

evaluated adequately because the replacement process has obscured them. These features can be divided (as Primary Controls were) into stratigraphic and structural categories.

The only stratigraphic feature of unknown importance still preserved locally is the thin-bedded nature of the uppermost Kelly Limestone. To what extent the thin-bedded limestones aided in the silicification process cannot be determined but it is inferred that they significantly increased the lateral permeability of this horizon.

Features suggestive of possible stratigraphic control are: a) swells (Figures 7, 8a, 11) and pinches (Figure 8a) in the jasperoid horizon which transgress the bedding in the limestone strata, b) arm-like extensions of jasperoid into limestone (Figure 12), and c) silicified pods, far removed from silicified zones, in what is otherwise unaltered limestone (Figure 13). The structural features of unknown importance are of three types: a) fractures related to faults, of which two varieties exist — (1) parallel fractures (Figures 14a, 14b) and (2) anastomosing fractures (Figure 15), b) fractures related to fissures (Figures 10a, 10b), and c) fractures beneath the silicified horizon that bear no relationship to either faults or fissures (Figure 16). The extent to which the upper Kelly Limestone may have been fractured and its importance relative to the formation of jasperoid is not known.

Figure 11. Swell in jasperoid horizon transgressing bedding in Kelly Limestone. Note the curvature of ribbon-rock in the swell and the maintainance of parallism between the vugs in ribbon-rock and the jasperoid-limestone contact.

Figure 12. Arm-like extensions of jasperoid (b) in limestone (a).

Figure 13. Silicified pod in essentially unaltered limestone far removed from any jasperoid zone.

Figure 14a. A 'sheeted' silicified fault zone (outlined) cutting Kelly Limestone. Note: (1) density of fracturing and degree of silicification decreased to the right of the fault, (2) unaltered limestone pod within jasperoid mass and (3) the vertical banding of jasperoid in the foreground.

Figure 14b. Close-up of the area immediately to the right of the fault zone in Figure 15a. The unaltered limestone contains silicified fractures and pods. The nature of these pods is discussed in Part II of this thesis.

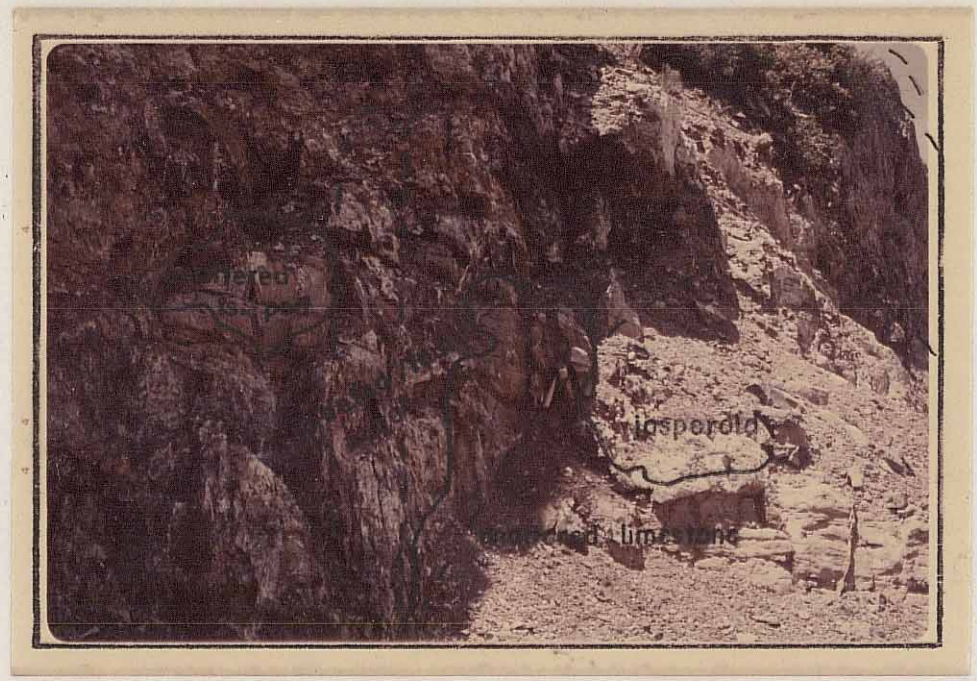
jasperoid


jasperoid

Figure 15. Anastomosing fractures in Kelly Limestone.

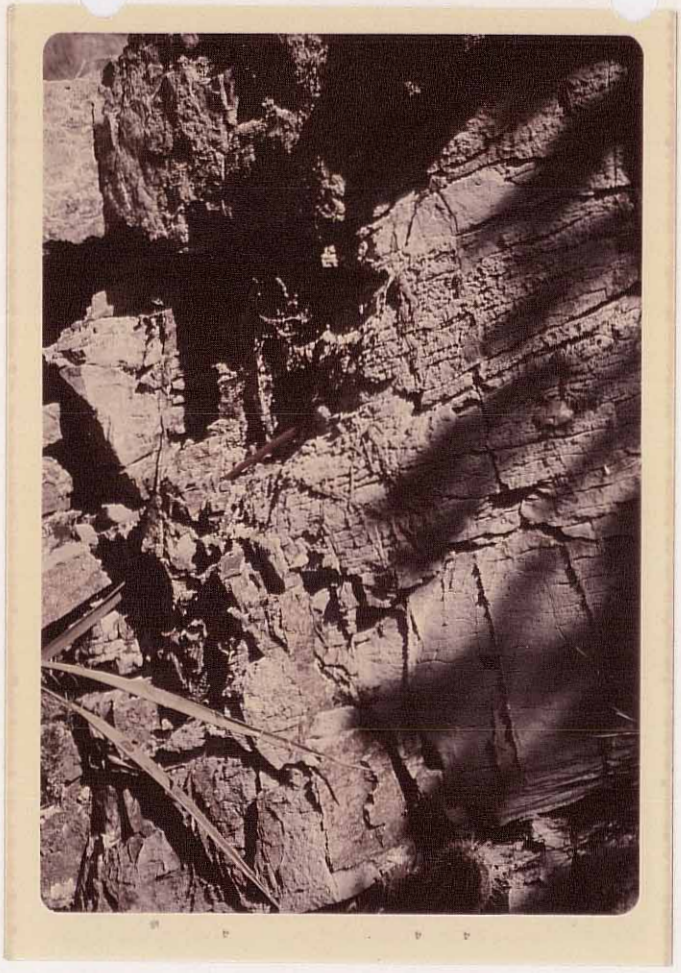

Figure 16. Silicified fractures which bear no direct relationship to either faults or fissures.

Chapter IV: PHYSICAL PROPERTIES OF JASPEROID

Megascopic Features

Jasperoid in the Kelly mining district crops out as tabular masses in the upper Kelly Limestone immediately below the Kelly-Sandia contact (see Chapter III). It is highly resistent to erosion and commonly caps the western dip slopes of the northern Magdalena Mountains (Plate I). Where the emplacement of jasperoid has been controlled by faults wall-like outcrops are commonly developed through differential erosion. These jasperoid walls have been used to infer fault traces where field relationships are not clear.

Silicified Kelly Limestone characteristically consists of both microcrystalline and coarse-grained quartz. The relative proportions of each change markedly from place to place and vary irregularly in the same outcrop. Color, internal structures and associated mineral assemblage of the jasperoid also vary significantly throughout the district.

Color. The color of the microcrystalline quartz phase is variable; it exhibits various shades of white, gray, black, yellow, orange, brown and red, and combinations of the above in mottled patterns. Liesegang color banding is locally present. The range in coloration is attributed to differences in iron concentration and/or differing stages of iron oxidation (Lovering, 1972). Coarse-grained

quartz is usually clear to white, but locally, may be tan or red.

Structures within Jasperoid. The following structures have been identified in Kelly district jasperoid: (1) fractures, (2) a sharp jasperoid-limestone contact (on a macroscopic scale), (3) limestone remnants, (4) ribbon-rock, (5) vugs, and (6) breccia.

Four types of fractures are present in silicified Kelly Limestone. Three of these are related to jasperoid formation; the other is thought to be post, jasperoid formation. The types of fractures contemporaneous with jasperoidization are as follows:

1. fractures subparallel or parallel to a fault trend;
2. fractures developed parallel to ribbon-rock structure (see discussion given below); and
3. randomly distributed fractures filled with coarse-grained quartz.

The fourth type of fracture, cross-cuts primary jasperoid structures and does not show any coarse-grained quartz development (see Figure 20). These fractures are thought to be the result of post-silicification tectonics.

The sharp contact which exists between jasperoid and unaltered limestone (Figures 7-9, 11 and 14) is one of the most conspicuous features of Kelly district jasperoid. Close examination of this contact however, reveals that it is gradational over the distance of approximately, less

than 1 inch (Figure 17). A detailed description of this contact begins on p. 106.

Limestone remnants are common in the silicified limestone. They range in size from a few inches to several tens of feet in their longest dimension, and are usually ellipitical to lenticular in shape (Figures 14a, 18 and 19).

Another distinctive feature of the jasperoid is the presence of ribbon-rock which consists of alternating layers of microcrystalline and coarse-grained quartz. The individual layers vary from 1/4 to 1-1/2 inches thick and the entire ribbon-rock mass may vary from less than one foot to greater than several feet in thickness. Several variations of this structure (ideal, irregular, and brecciated-vuggy) are defined on the basis of (1) parallelism of the layers, and (2) development of coarse-grained quartz between the microcrystalline layers which is categorized as either being complete (no vugs) or incomplete (vuggy), see sketch.

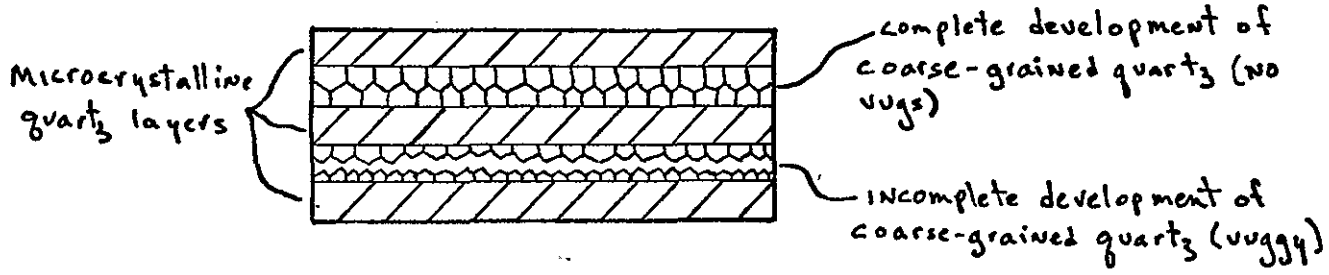

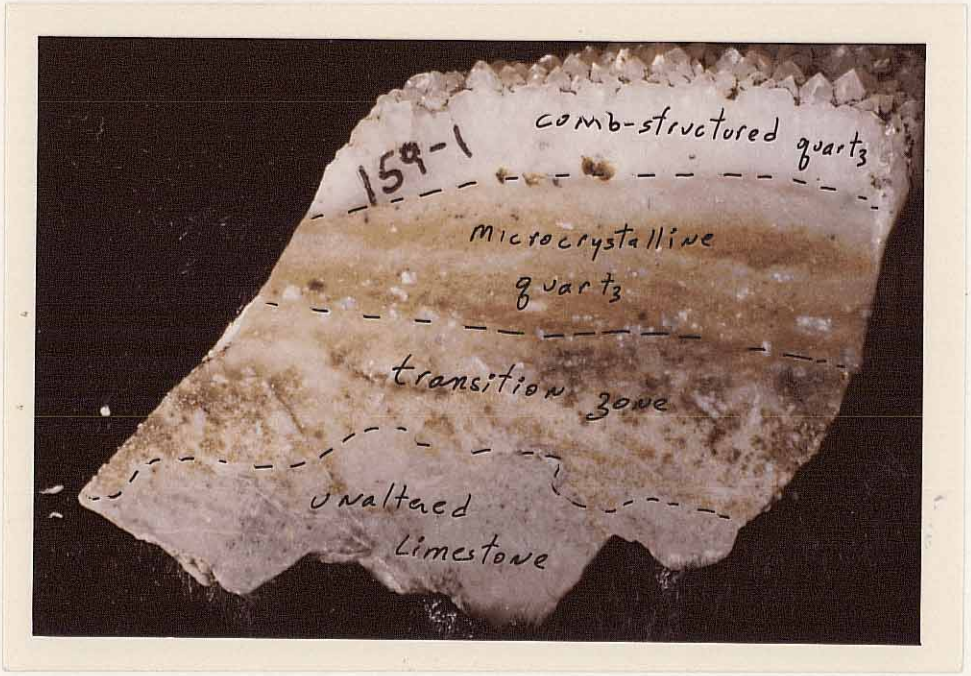

Figure 17. Close-up of the jasperoid-limestone contact. Note the transition zone between microcrystalline quartz and unaltered limestone.

Figure 18. Unaltered limestone remnant in Kelly district jasperoid. Lens cap in photograph is 2 inches in diameter.

Figure 19. Unsilicified bed of dolomicrite (called the 'silver pipe' by miners, see Chapter III) in a jasperoid horizon. When present in the vicinity of jasperoid, the 'silver pipe' characteristically shows no signs of silica replacement.


unaltered
Limestone


Jasperoid
Silver Tape
Jasperoid

The right-hand portion of Figure 20 is an example of ideal ribbon-rock structure; the layers are parallel, and the degree of coarse-grained quartz development is essentially complete. In irregular ribbon-rock (Figure 21) the microcrystalline layers are warped, discontinuous, and less parallel relative to the microcrystalline layers in ideal ribbon-rock, and the development of coarse-grained quartz is complete. Brecciated-vuggy ribbon-rock contains microcrystalline layers which can be either parallel or warped, and displays an incomplete development of coarse-grained quartz (Figure 22). The distinction between irregular ribbon-rock and brecciated-vuggy ribbon-rock is a function of coarse-grained quartz development. No systematic trends were observed in the overall distribution of ribbon-rock structure or its variants. The three types, described above, are exposed throughout the district and grade into each other in a random manner.

Vugs are abundant in Kelly district jasperoid. They range in size from microscopic opening (see discussion on p. 90) to greater than 2 x 4 feet (Figures 7, 8b, 11-13, and 20-22). Loughlin and Koschmann (1942) suggested that at least some of the larger vugs may have originally been limestone remnants which have been subsequently eroded away. Vugs in ribbon-rock, display a strong preferred orientation, generally forming lenticular voids parallel to the ribbon-rock fabric. Randomly oriented, irregularly shaped vugs are present in the rest of the jasperoid. Ideal

Figure 20. An example of ideal ribbon-rock structure displaying excellent parallelism between the layers of microcrystalline quartz (dark layers) and layers of coarse-grained quartz (light layers). Note: (1) this is a planar feature, and (2) vugs in this type of structure are lenticular and parallel to the ribbon-rock fabric. The degree of coarse-grained quartz development in the vicinity of the hammer is almost complete. Contrast this to the left-hand portion of the figure where coarse-grained quartz forms drusy masses lining platy vugs. Vugginess is inversely proportional to coarse-grained quartz development.

Figure 21. The middle layer in this jasperoid mass is an example of irregular ribbon-rock. The degree of coarse-grained quartz development is complete but the microcrystalline layers are warped, discontinuous and less parallel relative to the microcrystalline layers in ideal ribbon-rock.

Figure 22. Brecciated - vuggy ribbon-rock structure. Note, the contortion of microcrystalline and coarse-grained quartz layers.

Figure 23. Close-up of the jasperoid-limestone contact showing the parallelism of both the layers of microcrystalline quartz and the vugs in ribbon-rock with this contact.

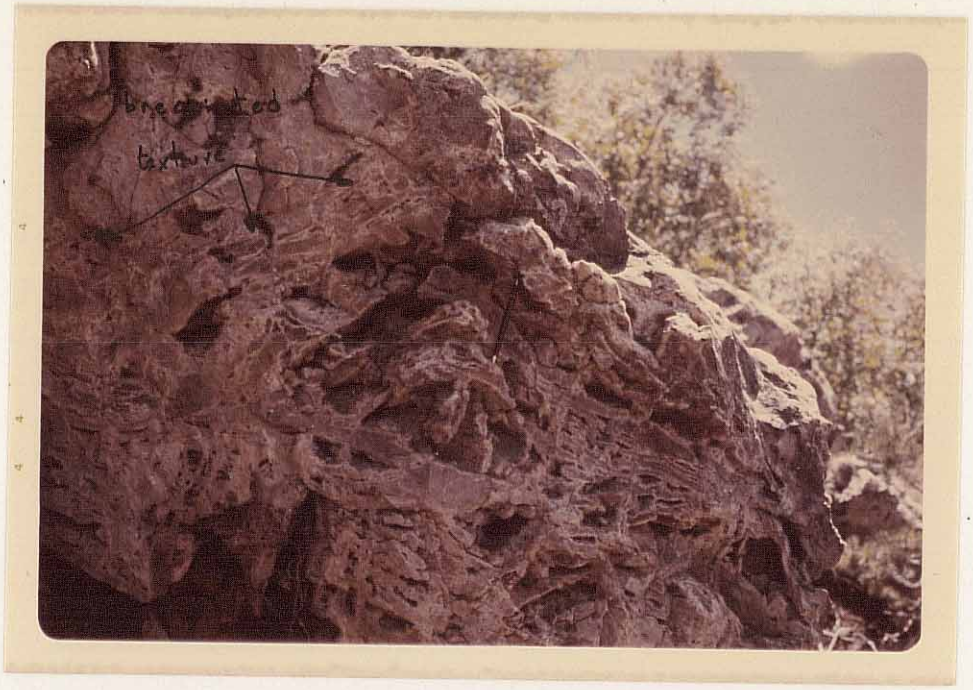
brecciated
texture

ribbon-rock (and the vugs contained therein) characteristically parallels the jasperoid-limestone contact (Figures 11 and 23). The significance of this tendency is discussed in Chapter VI. Vugs are characteristically lined with coarse-grained, comb-structured quartz and are frequently accompanied by several accessory minerals (see discussion given below).

Two types of breccia structure have been recognized in the jasperoid. One type consists of microcrystalline fragments cemented by coarse-grained, comb quartz (Figures 21, 22 and 24), and it is probably the result of solution movement rather than tectonically induced movement because ideal ribbon-rock often occurs in close proximity and commonly grades into this structure. Brecciated microcrystalline quartz cemented by a second generation of microcrystalline quartz is the other type of breccia (Figure 25). Each microcrystalline stage developed its own coarse-grained quartz in vugs. This has been established through detailed examination of slabs similar to that shown in Figure 25. This type of breccia is always found in fault zones, attesting to its tectonic origin.

Associated Mineralogy. Kelly district jasperoid typically consists of 90 to 95 percent quartz. Barite, fluorite and galena are the most common accessory minerals with barite being the most abundant and widespread. Minor amounts of pyrite, sphalerite, cerussite, hydrothermal calcite and gold are also present. Boxwork structures

Figure 24. Close-up of cockade-structured quartz in irregular ribbon rock.

Figure 25. Brecciated microcrystalline quartz cemented by a second generation of microcrystalline quartz.

1 inch

are locally abundant but their origin has not been determined. Supergene minerals such as Fe-oxides (some of which is after pyrite), malachite, azurite, and aurichalcite are common. The paragenetic relationships of the primary minerals in jasperoid is given in Figure 52.

Microscopic Features

Detailed petrographic analysis of Kelly district jasperoid reveals that the quartz exhibits a wide range of microtextures and variable grain size. Any one thin section will commonly display more than one microtexture indicating a complex crystallization history.

Microscopic features have been subdivided into several categories in order to facilitate their discussion. Each petrographic texture displayed by the jasperoid is described individually. Terminology used in the following descriptions follows that of Lovering (1972) and Bailey (1974), in addition, a new term is proposed. The data given below are discussed relative to the origin of jasperoid in Chapter VI.

Major Microcrystalline Quartz Textures

Five major microcrystalline quartz textures are present in Kelly district jasperoid. They are: (1) jigsaw-puzzle, (2) jigsaw-puzzle-xenomorphic, (3) xenomorphic-granular, (4) xenomorphic, and (5) subidiomorphic. Unless otherwise noted, grain size dimensions given by Bailey (1974) for

the above textures, were found to be consistent with measurements taken in this study.

Jigsaw-puzzle Texture. A highly irregular, tightly interlocking mosaic of quartz grains resembling a jigsaw-puzzle is defined by Lovering (1972) as jigsaw-puzzle texture. Bailey (1974) further describes this texture as a low porosity network of quartz grains exhibiting irregular to amoeboid shapes, ranging from less than 5 microns to greater than 20 microns in diameter, averaging between 10 and 15 microns. This texture is typical of fine-grained, relatively homogeneous varieties of jasperoid.

Figure 26 is an example of typical jigsaw-puzzle texture in Kelly district jasperoid. Occasionally, this texture preserves fossil structures as shown in Figure 27. Characteristics displayed by jigsaw-puzzle quartz in jasperoid are similar to those described in cherts by Folk and Weaver (1952). They are:

1. small quartz grains and aggregates (less than 5 microns) exhibit pin-point bireference; some grains are so small that they appear isotropic;
2. each grain or aggregate of grains show undulose extinction (this may be due, in part, to superimposition of grains and in part, to the property of each grain);
3. under plane-polarized light, jigsaw-puzzle quartz is very 'dirty' (Figure 28); this turbid appearance is attributed to the presence of

Figure 26. Photomicrograph of jigsaw-puzzle textured quartz in Kelly district jasperoid (crossed-nicols, 160x magnification).

Figure 27. Photomicrograph of fossil fragments replaced by jigsaw-puzzle quartz (crossed-nicols, 25x magnification).*

*Circular areas with bright centers are bubbles in the thin section.

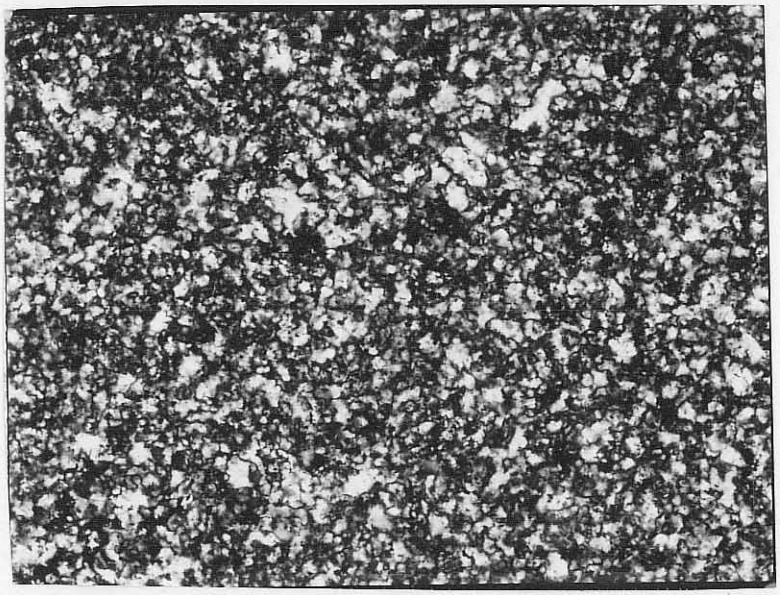

0.1 mm

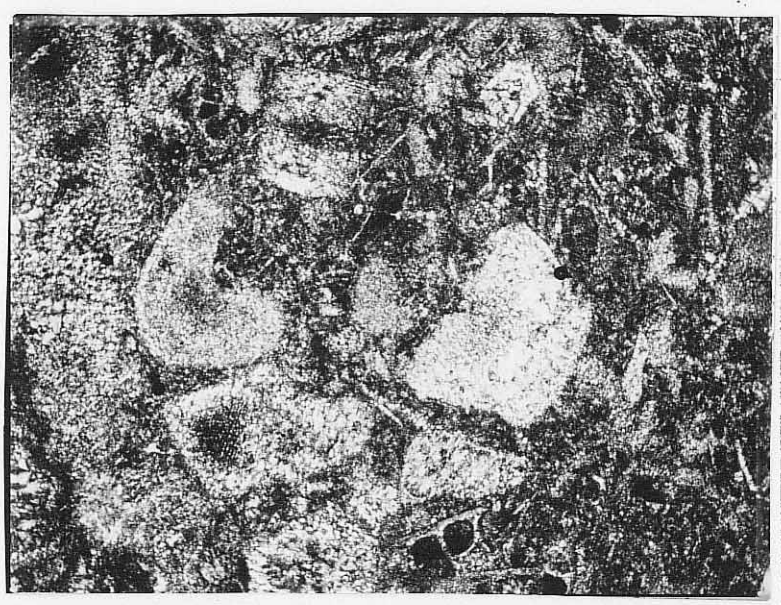

1mm

(a) opaques, such as pyrite and Fe-oxides; (b) water-filled cavities (see discussion Chapter VI); and (c) minute specks of calcite, epidote, sericite and other minerals too small to be resolved at 500x magnification; and

4. a very fine, curvilinear fracture pattern which resembles desiccation cracks (Figure 29).

Jasperoid exhibiting this texture is found throughout the study area with no preferred mode of occurrence. It is generally the only texture present in homogeneous varieties of Kelly district jasperoid; it is commonly associated with other microtextures in heterogeneous types.

Jigsaw-puzzle-Xenomorphic Texture. Jigsaw-puzzle-xenomorphic texture is defined by Bailey (1974) as consisting of:

> " ... varying amounts of very fine-grained, highly irregular, typical jigsaw-puzzle texture and somewhat coarser-grained (10 to 100 microns or greater), less irregular, though still anhedral to subhedral, grains of quartz."

Figure 30a is an example of jigsaw-puzzle-xenomorphic texture in Kelly district jasperoid. The coarser-grained quartz commonly displays undulose extinction, and is relatively cleaner than the finer-grained jigsaw-puzzle quartz (Figure 30b). This texture is the most common microtexture in the jasperoid, however, like jigsaw-puzzle,

Figure 28. Photomicrograph of jigsaw-puzzle textured quartz illustrating its 'dirtiness' (plane-polarized light, 160x magnification).

Figure 29. Photomicrograph of jigsaw-puzzle texture displaying desiccation-like fracturing. Note the clear spherical areas (s) which are interpreted as "ghosts" of Type II, spherulitic texture (see discussion p.90-101 and Chapter VI). The fact that jasperoid is a result of hydrothermal alteration in the Kelly district precludes the possibility that these spherical areas may be the result of biological activity (p.125; plane-polarized light, 160x magnification).

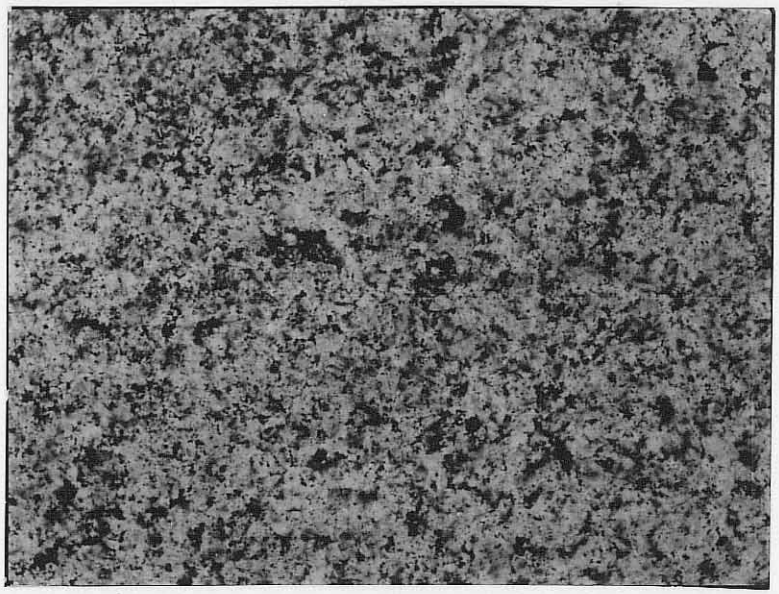

0.1 mm

0.1 mm

Figure 30a. Photomicrograph of jigsaw-puzzle-xenomorphic texture (crossed-nicols, 160x magnification).

Figure 30b. Photomicrograph of the above figure under plane-polarized light. The coarser-grained quartz areas are relatively cleaner than the jigsaw-puzzle regions (160x magnification).

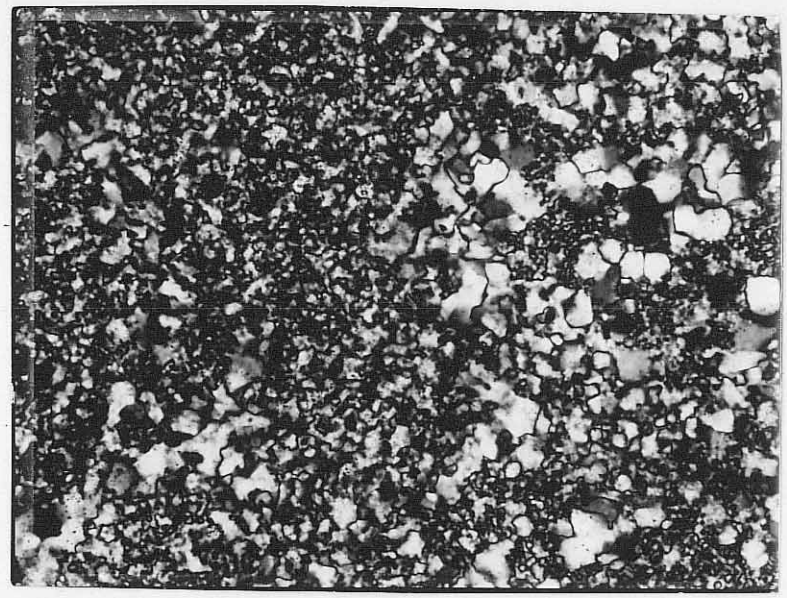

0.1 mm

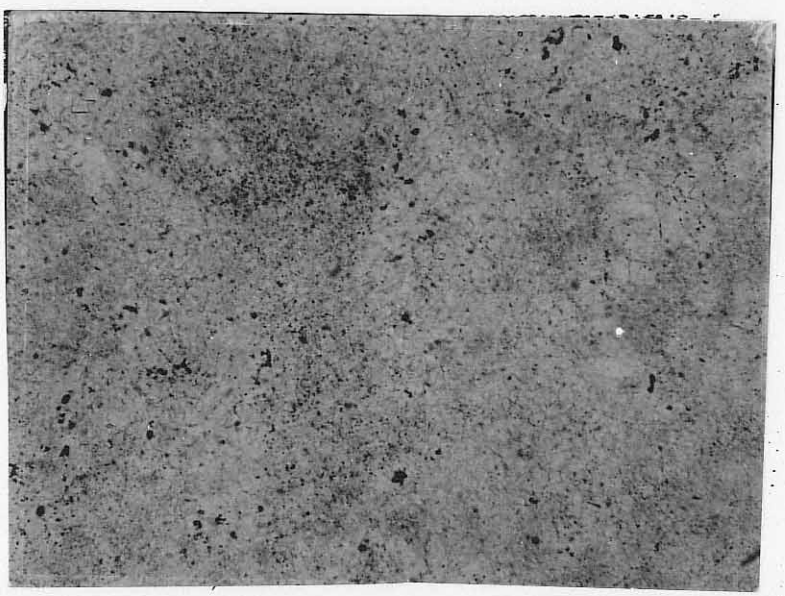

0.1 mm

there is no preferential mode of occurrence. Bailey (1974) states that jigsaw-puzzle-xenomorphic texture represents an early stage in jasperoid formation.

Xenomorphic-Granular Texture. Xenomorphic-granular textured quartz consists of approximately equidimensional, anhedral grains averaging between 50 to 100 microns (Bailey, 1974); in Kelly district jasperoid, the quartz grains range in size from less than 35 microns to approximately 200 microns, in diameter. A typical example of this texture is shown in Figure 31a. Quartz exhibiting this texture occurs as lenticular patches within areas displaying other microtextures. Individual quartz grains frequently show undulose extinction, and are cleaner than those in jigsaw-puzzle-xenomorphic or jigsaw-puzzle textures (compare Figure 31b with Figures 30b and 28). Xenomorphic-granular textured quartz is commonly found in heterogeneous varieties of Kelly district jasperoid, filling veins and vugs.

Xenomorphic Texture. Bailey (1974) describes an extremely common texture in Drum Mountain jasperoid as consisting of irregular, anhedral quartz grains, ranging in size from less than 10 microns to greater than 1 mm (averaging between 80 to 130 microns, in diameter), as xenomorphic. Quartz grains, in Kelly district jasperoid, range in size from 5 microns to greater than 200 microns. No grains larger than 235 microns were found. This texture is similar to textures exhibited by plutonic,

Figure 31a. Photomicrograph of xenomorphic-granular texture (crossed-nicols, 160x magnification).

Figure 31b. Photomicrograph of the above figure in plane-polarized light. Note the cleanliness of the quartz relative to jigsaw-puzzle or jigsaw-puzzle-xenomorphic quartz (160x magnification).

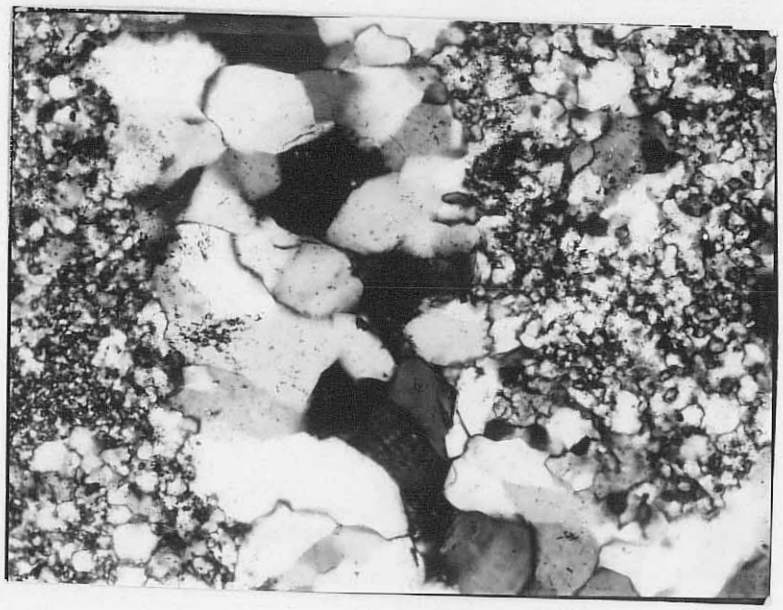

0.1 mm

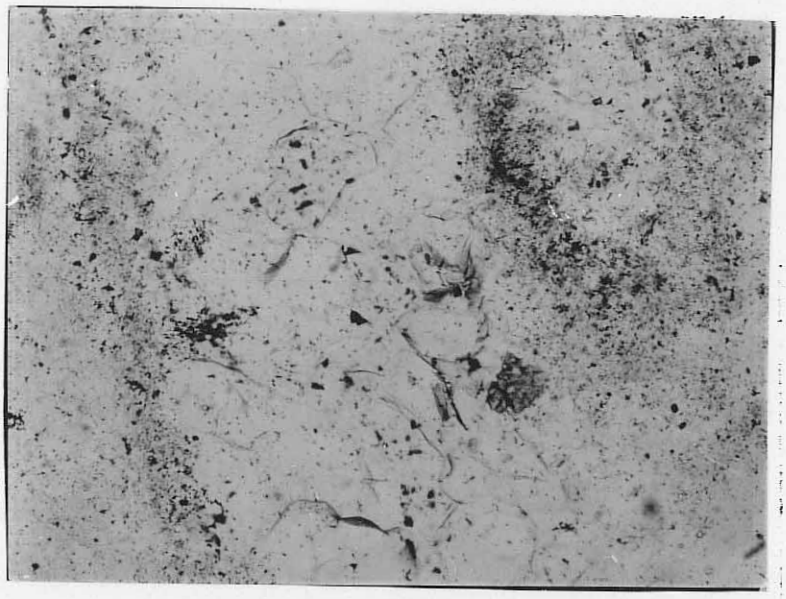

0.1 mm

igneous rocks and it is highly characteristic of jasperoids with a heterogeneous grain size distribution (Lovering, 1972). Xenomorphic-textured quartz occurs as lenticular to roughly spherical patches, filling in fractures and vugs, in heterogeneous varieties of Kelly district jasperoid. This texture is not common in the study area. Figure 32 is a typical example of xenomorphic texture in jasperoid in the Kelly district. Individual quartz grains rarely display undulose extinction.

Subidiomorphic Texture. Subidiomorphic texture as described by Bailey (1974) is similar to the reticulated texture of Lovering (1972). This texture consists of quartz grains elongated parallel to the c-axis, many showing euhedral outlines with a length-to-width ratio of 3:1 or greater. These grains are randomly distributed in a matrix of smaller, nearly equant, anhedral quartz grains giving the appearance of a crude mesh or network (Lovering, 1972). Subidiomorphic texture is considered by Lovering to be highly diagnostic of jasperoids, even though only a small percentage of them display it. This texture (Figure 33) is very common in heterogeneous types of Kelly district jasperoid. It also occurs in homogeneous types of jasperoid on a scale analogous to jigsaw-puzzle texture. The elongate quartz grains frequently contain minute calcite (?) inclusions (Figure 34).

Minor Microcrystalline Quartz Textures

Several minor microcrystalline quartz textures have

Figure 32. Photomicrograph of xenomorphic textured quartz (crossed-nicols, 160x magnification).

Figure 33. Photomicrograph of subidiomorphic texture (crossed-nicols, 25x magnification).*

-> *see p. 75

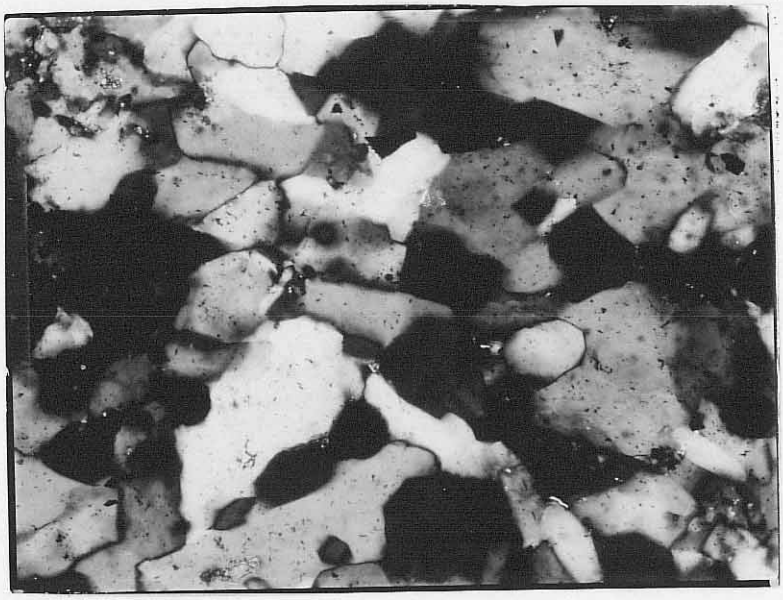

0.1 mm

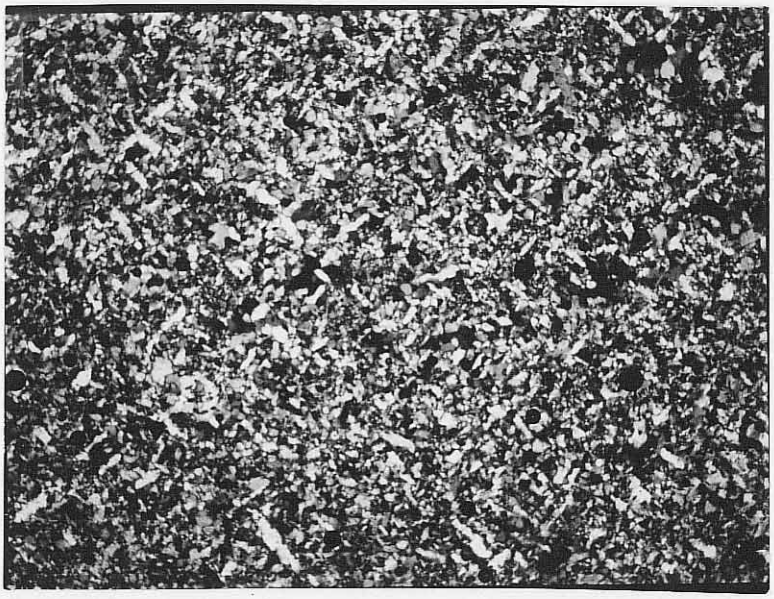

1 mm

Figure 34. Photomicrograph of minute calcite (?) inclusions in elongate quartz grains of subidiomorphic texture (crossed-nicols, 160x magnification).

Figure 35a. Photomicrograph of an empty vug (crossed-nicols, 160x magnification).

0.1 mm

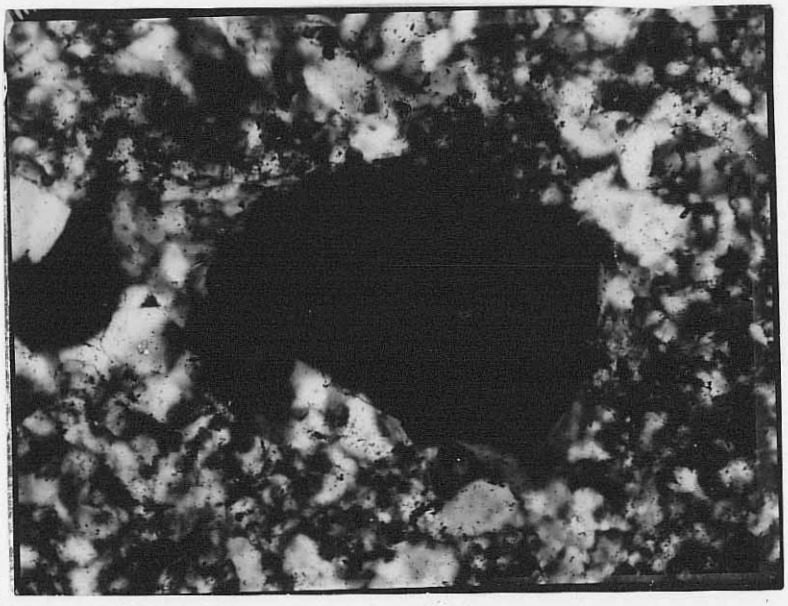

0.1 mm

Figure 35b. Photomicrograph of a vug in its initial stage of filling (crossed-nicols, 32x magnification).*

Figure 35c. Photomicrograph of a completely filled vug; note that a xenomorphic-granular texture is exhibited (crossed-nicols, 40x magnification).

*See p. 75

1mm

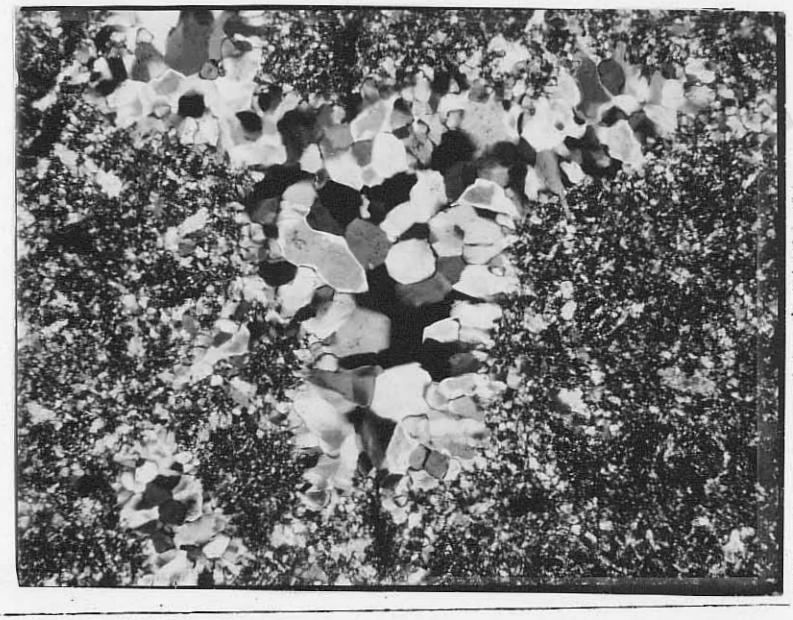

1mm

Figure 36. Photomicrograph of brecciated texture cemented by a second generation of xenomorphic-granular quartz. Opaque material is Fe-oxide. Euhedral quartz crystals are present in vugs (crossed-nicols, 25x magnification).*

Figure 37. Photomicrograph of Type I, spherulitic texture with a jigsaw-puzzle quartz core (crossed-nicols, 40x magnification).*

*See p. 75

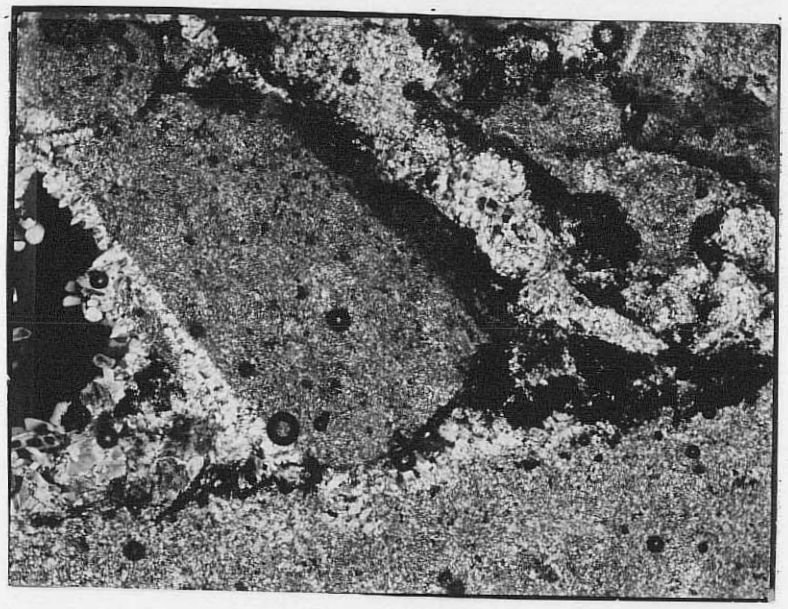

1mm

1mm

texture consists of radiating aggregates of anhedral to euhedral quartz grains, with a core of finer-grained quartz (Figure 37). Bailey (1974) describes this texture as consisting of individual aggregates, ranging from less than 0.2 mm to greater than 1 mm, generally containing:

> " ... a core of xenomorphic-textured quartz surrounded by the elongate subhedral, radiating quartz grains whose mutual boundaries are structurally incoherent. Quartz crystals are elongate in the shape optic direction and display a typical "polarization cross"."

A core of jigsaw-puzzle or jigsaw-puzzle-xenomorphic quartz is typical for Type I, spherulitic texture in Kelly district jasperoid. Spry (1969) states that this type of texture results from the reorganization of: 1) a finely-crystalline, random aggregate, or 2) a uniform crystal, by the rotation of small units and their addition to the nucleus.

Type II, spherulitic texture is composed of radiating chalcedonic quartz, ranging in size from less than 20 microns to greater than 200 microns, averaging between 50 and 100 microns, in diameter (Figures 38a, 38b). Oehler (1976) has shown that this type of texture is characteristic of quartz deposited from a silica gel. Type II, spherulitic quartz is commonly found recrystallizing to jigsaw-puzzle (Figures 38a and 39), xenomorphic (Figure 48b), or xenomorphic-granular (Figure 40). The reader is referred to Oehler (1976, Figures 9B through 9H). Figure 41 shows Type I, spherulitic quartz with a Type II

Figure 38a. Photomicrograph of Type II, spherulitic quartz. Spherulites are partially recrystallized to jigsaw-puzzle texture (crossed-nicols, 100x magnification).

Figure 38b. Photomicrograph of the above figure in plane-light. Illustrated is the radiating fibrous structure of this texture. Also shown are "ghost" spherulites (Figure 29; 100x magnification).

0.25 mm

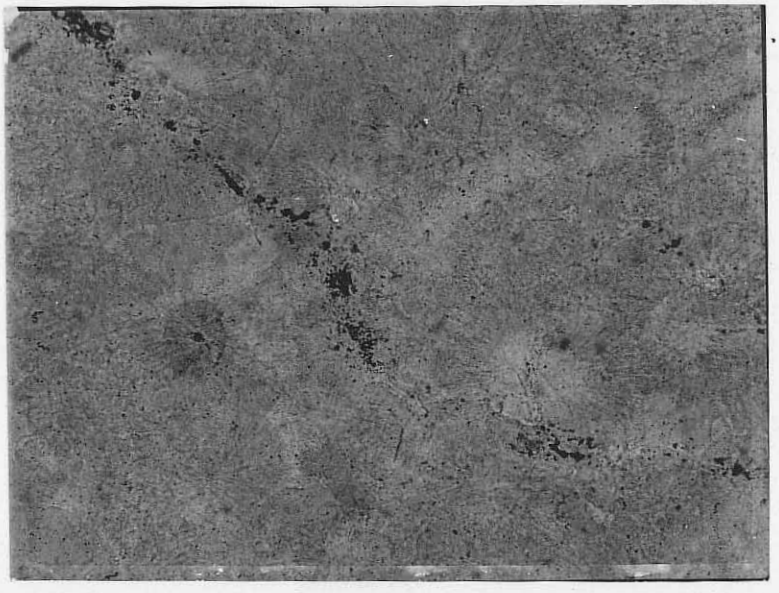

0.25 mm

Figure 39. Photomicrograph of Type II, spherulitic texture recrystallized to jigsaw-puzzle textured quartz. Figure 29 which is in the same field of view shows "ghost" spherulites as discussed in Figure 39b (crossed-nicols, 160x magnification).

Figure 40. Photomicrograph of Type II, spherulitic texture partially recrystallized to xenomorphic-granular quartz. A portion of the "polarization cross" typical of chalcedony is still evident (crossed-nicols, 125x magnification).

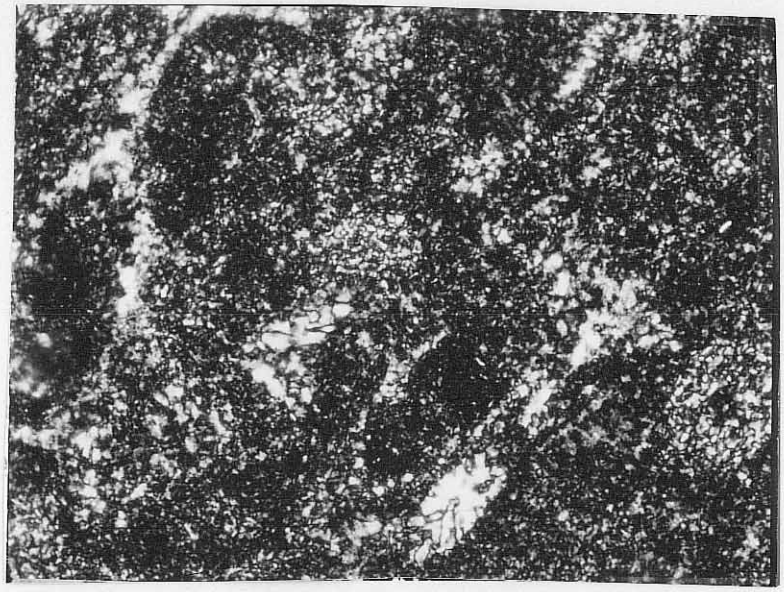

0.1 mm

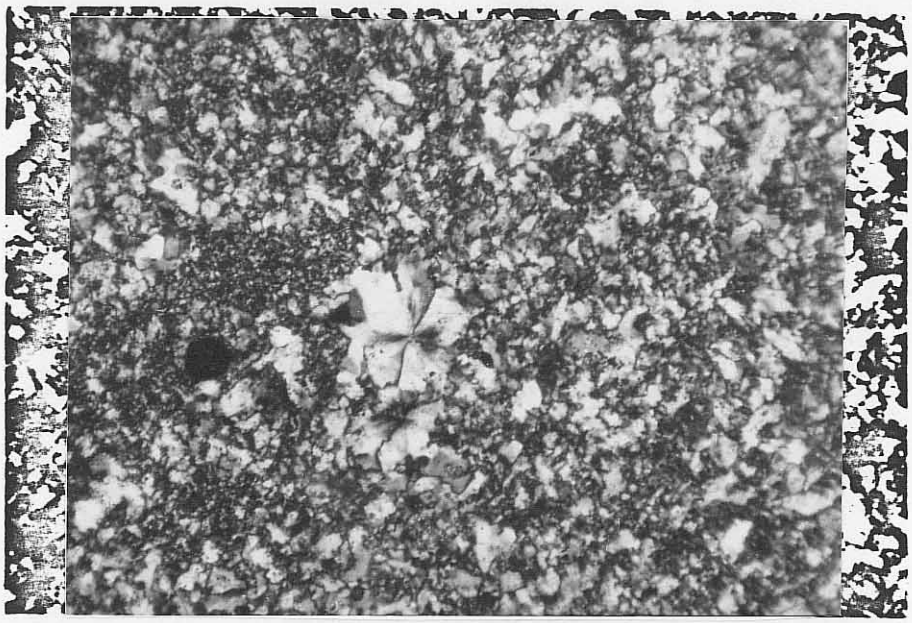

0.5 mm

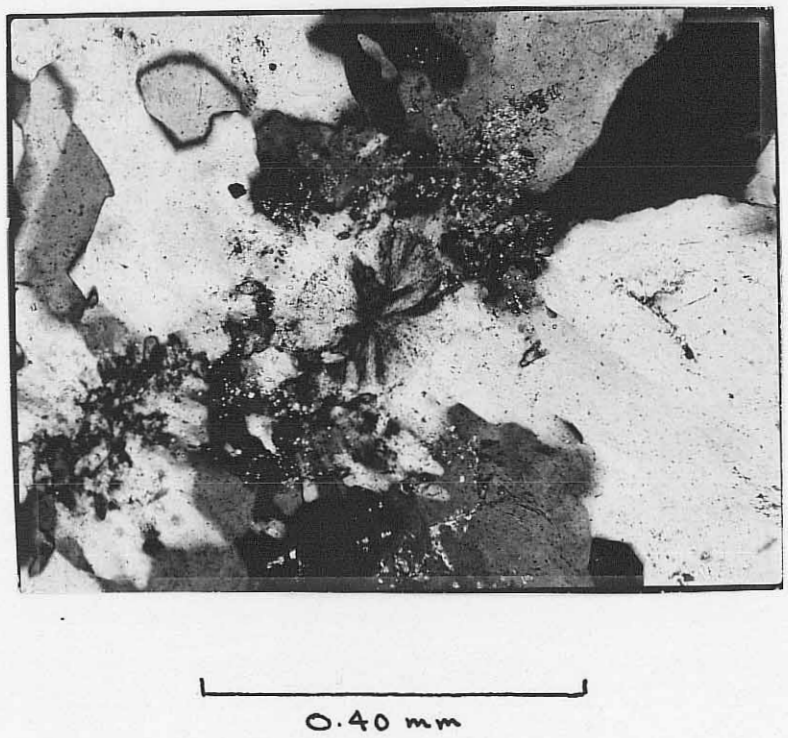

Figure 41. Photomicrograph of Type I, spherulitic texture with a Type II core (crossed-nicols, 128x magnification).

core. This figure suggests that at least some of the Type I spherulites are the result of the reorganization of material with an amorphous structure (silica gel).

Coarse-grained Quartz Features

A number of features have been identified in thin-sections of coarse-grained quartz exhibiting comb structure. This structure is restricted to subhedral-to-euhedral quartz which has precipitated in vugs, and in the areas between the microcrystalline layers in ribbon-rock (see Figures 20-23). The following features have been observed in the coarse-grained quartz:

1. straight to slightly undulose extinction;
2. patchy undulose extinction (extinction occurring in different domains within a single crystal as the petrographic stage is rotated, Figure 42);
3. feather or splintery quartz (Adams, 1920; Figure 43);
4. microfractures within quartz grains that do not transect grain boundaries (Figure 44); and
5. numerous inclusions (Figure 44) which consist of fluid-filled cavities, minute calcite (?) particles, opaque minerals and minerals too small to be resolved at 500x magnification. Inclusions are commonly present along growth planes (Figure 45).

Figure 42. Photomicrograph of coarse-grained quartz in a vug exhibiting patchy undulose extinction (crossed-nicols, 64x magnification).*

Figure 43. Photomicrograph of coarse-grained quartz exhibiting splintery texture along its grain boundary (crossed-nicols, 32x magnification).*

*See p. 75

0.5 mm

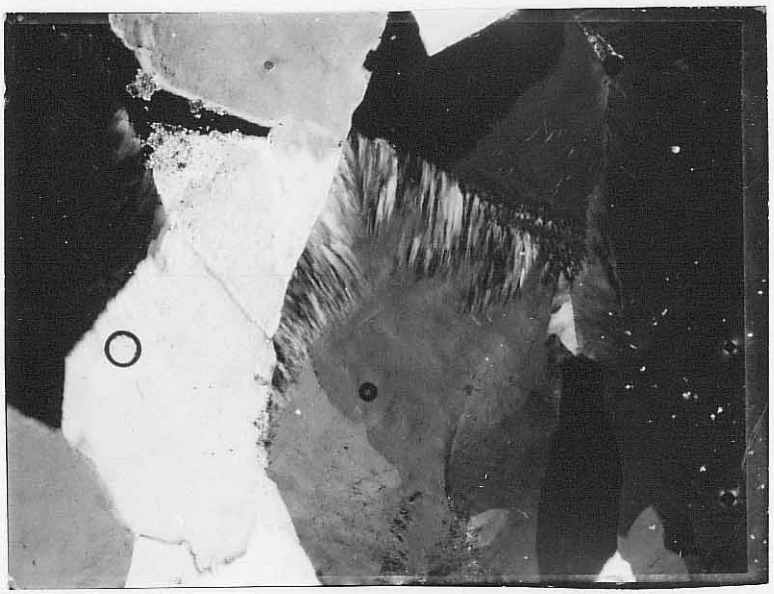

1 mm

Figure 44. Photomicrograph of quartz grains showing inclusions and internal fractures that do not transect grain boundaries (crossed-nicols, 125x magnification).

Figure 45. Photomicrograph of inclusions along growth planes in coarse-grained, comb quartz (crossed-nicols, 100x magnification).

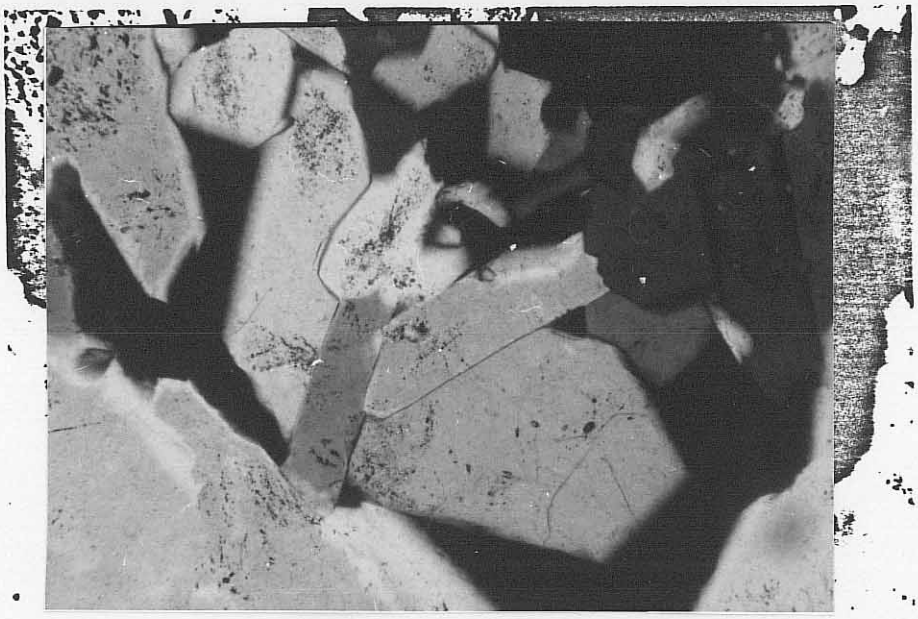

0.5 mm

0.25 mm

Jasperoid-Limestone Contact

Close examination of the jasperoid-limestone contact reveals that it is gradational over the distance of less than one inch (see Figure 17). Microscopic examination of this contact has established the presence of six zones. These zones range from unaltered limestone to limestone completely replaced by microcrystalline quartz to coarse-grained comb quartz in vugs. Zones II through IV are gradational and they represent the transitional zone shown in Figure 17. A detailed description of the six zones follows.

Zone I

Zone I consists of limestone (generally biosparite or biosparrudite) that has not been visibly affected by the silicifying event. For a detailed description of unaltered Kelly Limestone the reader is referred to Siemers (1973).

Zone II

Zone II demarks the incipient stages of silicification. This zone is characterized by the presence of:

1. fine-grained quartz in fossil fragments (predominantly crinoid fragments, Figure 46) or more rarely,
2. scattered occurrence of subhedral to euhedral quartz grains preferentially set in calcite cement (Figure 47).

Fine-grained quartz in fossil fragments displays the following textures: (a) jigsaw-puzzle, (b) Type II,

Figure 46. Photomicrograph of a silica patch (P) in a crinoid fragment. Note its 'dirty' appearance and the presence of calcite and other inclusions (plane-polarized light, 100x magnification).

Figure 47. Photomicrograph of a partial "ghost" quartz crystal (Q) in calcite cement (crossed-nicols, 160x magnification).

0.25 mm

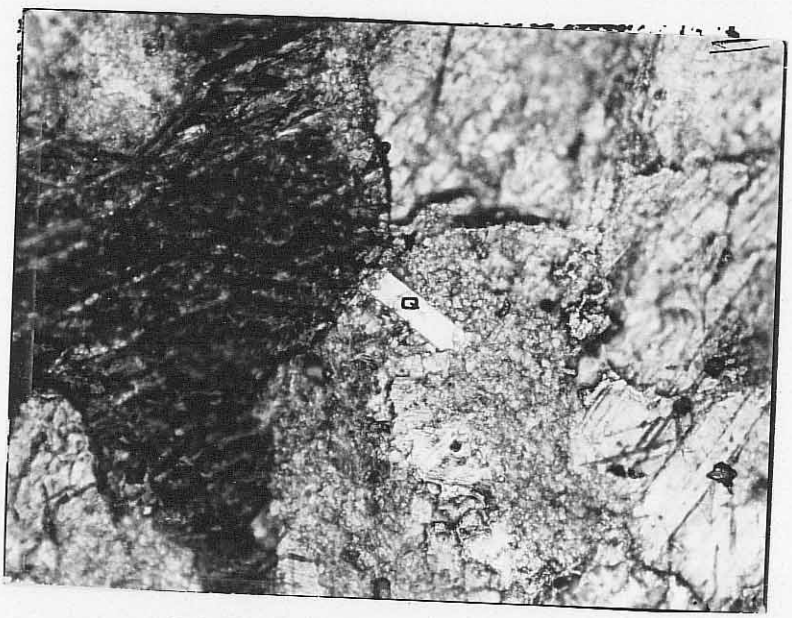

0.1 mm

spherulitic or (c) a texture which is transitional between Type II, spherulitic and xenomorphic (Figure 48b). This transitional texture consists of Type II, spherulitic quartz in the early stages of recrystallization to xenomorphic-granular or xenomorphic quartz (Bailey, 1974, p. 97 cites a similar occurrence). The characteristics exhibited by patches of fine-grained quartz in fossil fragments are identical to those described for jigsaw-puzzle quartz (p. 74). The patches:

1. occur as dirty brown areas under plane polarized light;
2. contain calcite and other unresolved inclusions;
3. commonly display desiccation-like fractures (Figure 48a); and
4. contain quartz which exhibits undulose extinction.

Zone III

The following features are characteristic of Zone III:

1. silicified patches within fossil fragments occur with greater frequency;
2. calcite cement shows signs of replacement by jigsaw-puzzle or, more commonly, xenomorphic-granular and xenomorphic textured quartz;
3. open spaces (vugs); and
4. silicified areas with numerous calcite (?) inclusions.

Figure 49 is a typical example of this zone.

Zone IV

Zone IV (Figure 50) displays the following characteristics:

Figure 48a. Photomicrograph of a silica patch in a crinoid fragment displaying desiccation-like fracturing (plane-polarized light, 64x magnification).*

Figure 48b. Photomicrograph of the above figure under crossed-nicols. Illustrated is Type II, spherulitic texture recrystallizing to xenomorphic quartz (64x magnification).*

*See p. 75

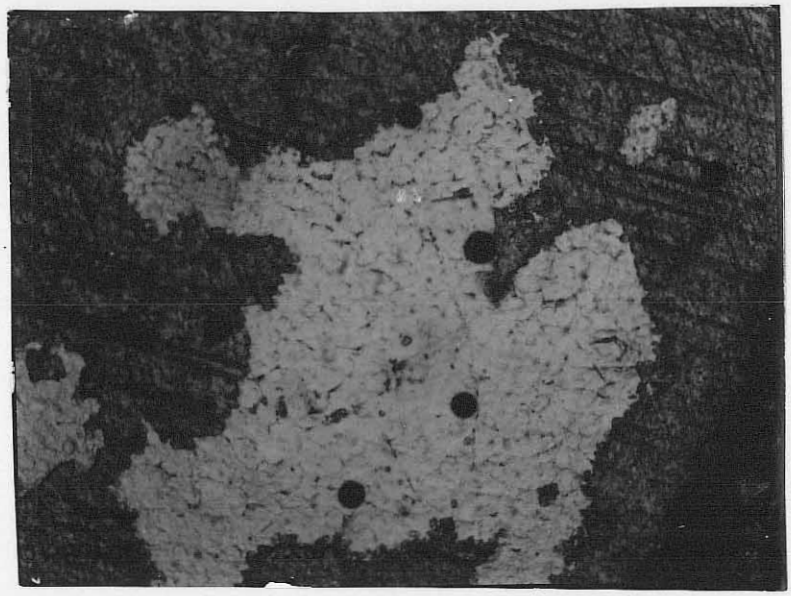

0.5 mm

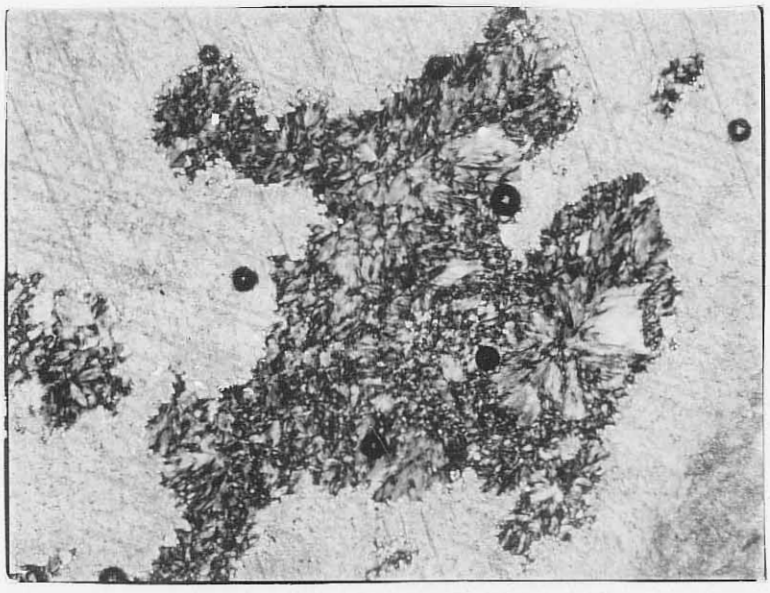

0.5 mm

Figure 49. Photomicrograph representing Zone III in the jasperoid-limestone transition zone (see Figure 17 and p. 106)(crossed-nicols, 25x magnification).

Figure 50. Photomicrograph of Zone IV in the jasperoid-limestone transition zone (crossed-nicols, 25x magnification).

1 mm

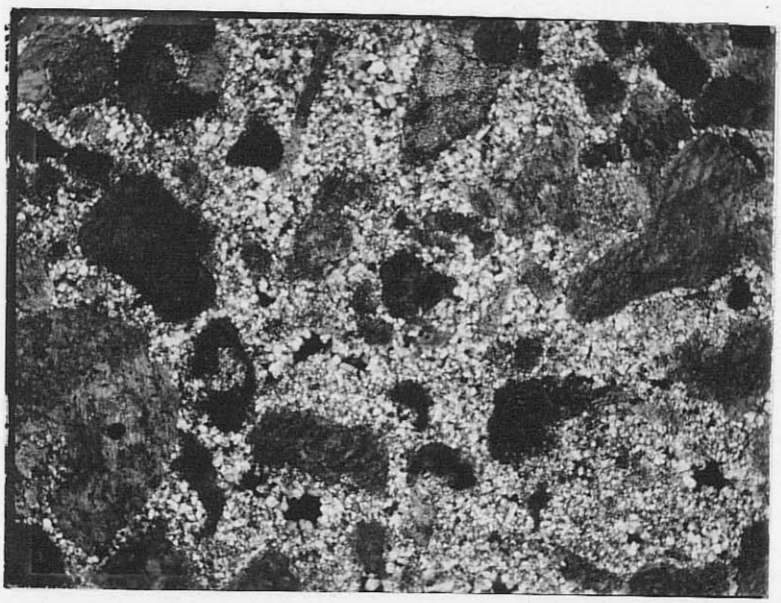

1 mm

1. calcite islands in a sea of quartz exhibiting jigsaw-puzzle or, more commonly, xenomorphic-granular or xenomorphic texture (giving the impression of jigsaw-puzzle-xenomorphic texture);
2. calcite islands in various stages of dissolution, producing vugs which display varying degrees of filling by xenomorphic-granular and xenomorphic textured quartz;
3. quartz exhibiting subidiomorphic texture; and
4. numerous calcite inclusions within quartz.

Zone V

Zone V (Figure 51) represents the microcrystalline zone in Figure 17. This zone is characterized by the presence of:

1. no calcite islands;
2. numerous vugs (resulting from the dissolution of calcite islands) in varying degrees of filling by xenomorphic or xenomorphic-granular quartz; and
3. quartz exhibiting any of the major microcrystalline textures previously described.

Zone VI

Zone VI consists of coarse-grained, comb quartz in vugs. The characteristics of this zone have been previously described (see p.101).

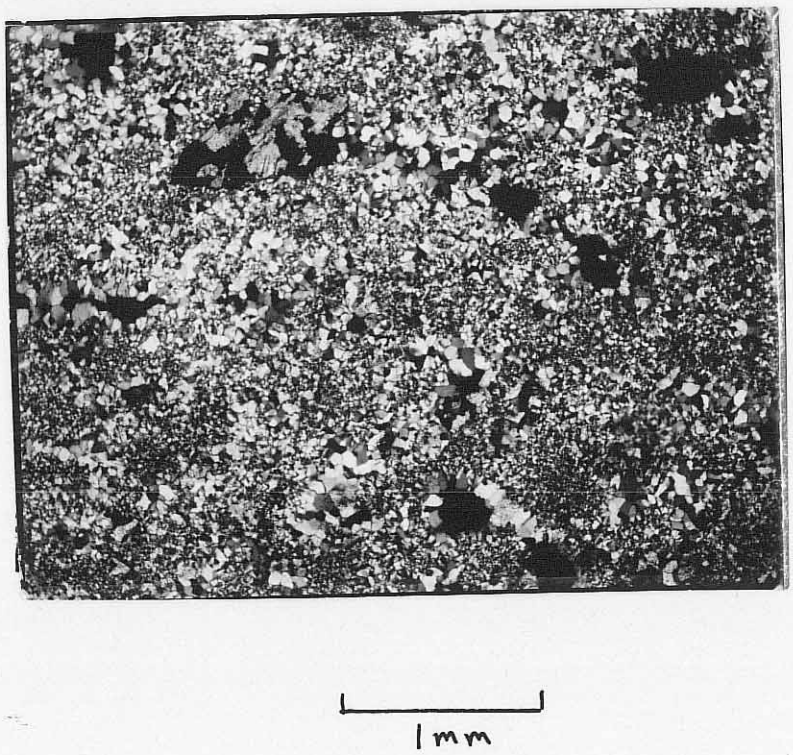

Figure 51. Photomicrograph representing Zone V in the jasperoid-limestone transition zone (crossed-nicols, 25x magnification).

Associated Mineralogy in Jasperoid

A number of minerals, in addition to quartz, occur in the jasperoid. Major accessory minerals are barite, fluorite, galena, pyrite, Fe-oxides (some clearly, the result of pyrite oxidation; some of questionable origin), relict and hydrothermal calcite. Minor amounts of sericite, biotite and muscovite are present. Cerussite of unknown origin also occurs; no gold was observed in thin section. Additional minerals may be present within quartz grains (Figures 28, 31b, 34, 44, 45 and 46), but they are too small to be resolved at 500x magnification. Figure 52 shows the paragenetic relationships for the dominant accessory minerals. The lines in the diagram represent only the relative time of deposition of the minerals, not the amounts deposited. The relationships among several of the accessory minerals shown in Figure 52 are uncertain because (1) they do not occur together and (2) when they do, there is a lack of mutual grain boundaries. The uncertain relationships are:

1. sphalerite relative to galena;
2. moderately late pyrite relative to late fluorite and late barite;
3. early pyrite relative to early fluorite;
4. early fluorite relative to early barite; and
5. late barite to calcite.

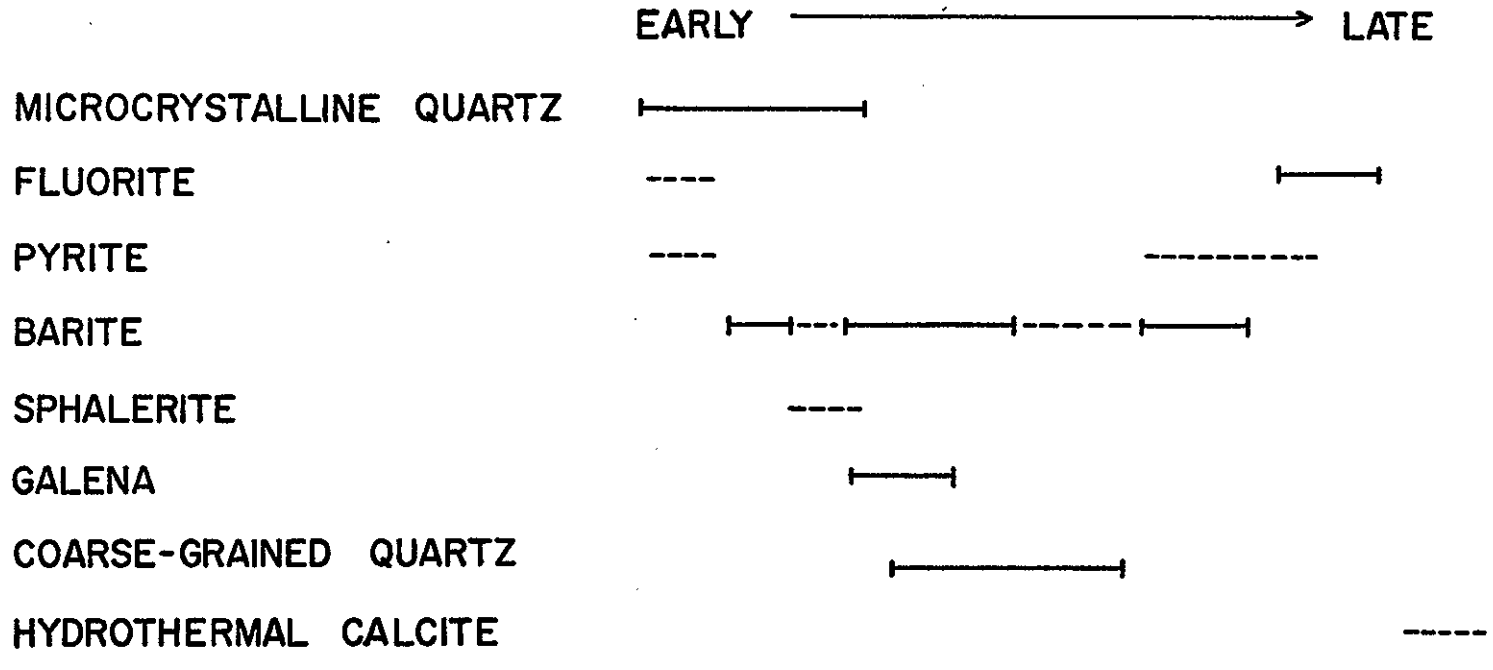

Figure 52. Paragenetic sequence for the dominant accessory minerals in Kelly district jasperoid. Lines in diagram represent only relative times of deposition, not amounts deposited. Dashed lines are indicative of uncertain temporal relationships.

Chapter V. FLUID INCLUSION INVESTIGATION

Homogenization temperatures were determined for barite, fluorite, coarse-grained quartz, and calcite in Kelly district jasperoid. The objectives of this investigation were:

1. to delineate the temperatures of jasperoid deposition, and
2. to determine if any areal temperature zonation existed in the study area which may be indicative of solution flow direction and, thus, provide data as to the source and origin of the fluids.

To assess the presence of any areal temperature zonation fluorite samples were collected from four widely spaced areas along the crest of the northern Magdalena Range. Fluorite was used because of its amenability to fluid inclusion analysis (i.e., its good cleavage allows small chips of sample to be easily obtained and, because these chips are generally transparent fluid inclusions are easily located).

The analytical procedure utilized in this study for determining homogenization temperatures is that used by Allmendinger (1975, p. 41) and is as follows:

> "Cleavage fragments or doubly-polished plates are placed in the heating stage adjacent to the thermocouple probe and an inclusion is located while the stage is heating. The first heating run is made at a high rate (~10°C/min.) to

> determine the approximate filling temperature. The stage and mineral plates are then allowed to cool until the vapor phase re-segregates from the liquid phase. A heating curve is then chosen which will allow temperatures to approach the approximated filling temperature at a slow rate (1°C/(5-10) min.). Several runs are made at the slow heating rate and the temperature noted when the vapor phase completely homogenizes with the liquid phase. If temperatures from successive runs are within 1°C of each other (temperatures are within 0.3°C in this study) the temperature is recorded as the filling temperature."

The minerals used for fluid inclusion studies were: three types of barite (vein barite, barite contemporaneous with microcrystalline quartz, and vug barite), fluorite (green and purple) and coarse-grained quartz from vugs, and calcite from a silicified fracture. Microcrystalline quartz was not analyzed because its fluid inclusions are too small to give reliable results with the available equipment and, because of the uncertainty of their origin. Figure 53 presents the paragenetic relationships among the minerals analyzed in the fluid inclusion study.

Homogenization temperatures represent the lowest possible temperature at which the inclusions were trapped. Two additional parameters are required to determine the actual temperature of entrapment; they are: the salinity of the solutions, and the pressure which existed on the system during the time of entrapment. The pressure can be estimated in two ways: (1) consideration of the physical

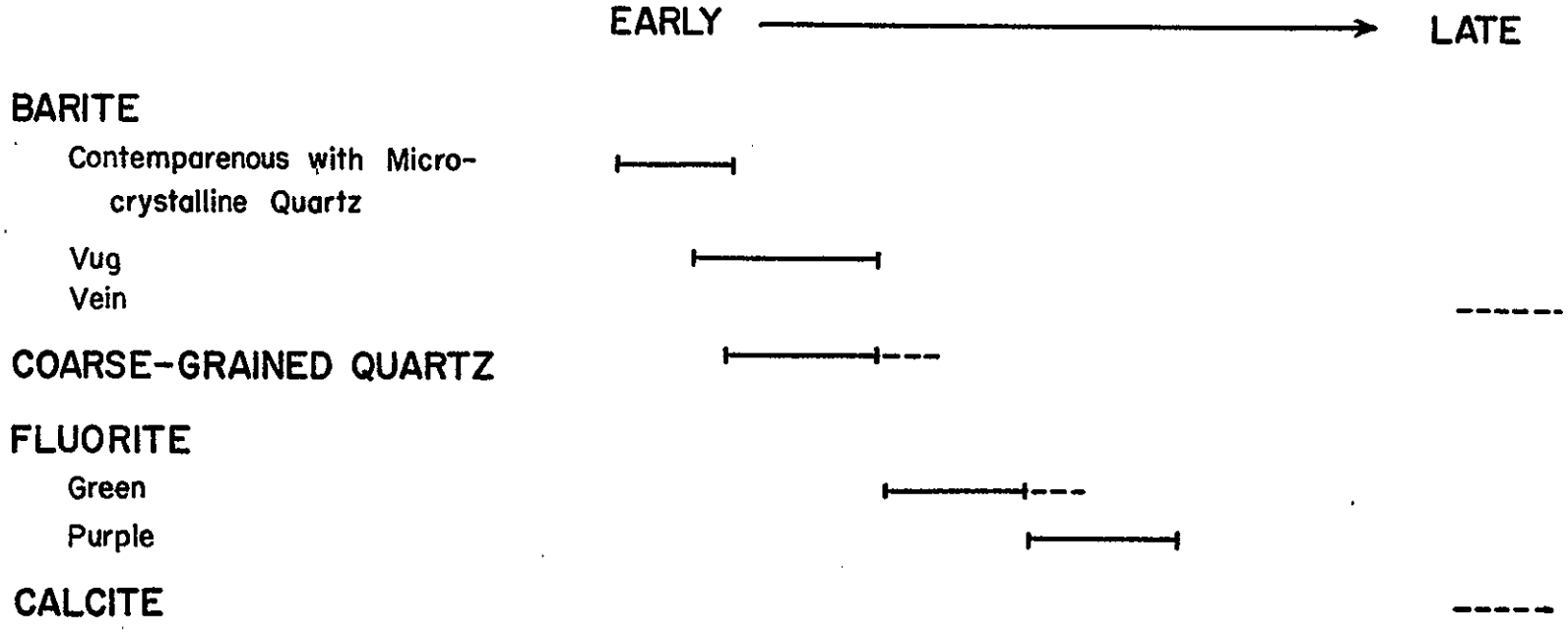

Figure 53. Paragenetic sequence of the minerals used in the fluid inclusion study. Lines only indicate the relative times of deposition, not amounts deposited. Dashed lines are indicative of uncertain temporal relationships.

appearance of the fluid inclusions, and (2) reconstruction of overburden at the time of mineralization. If fluid inclusions show evidence of boiling (inclusions will exhibit variable liquid/vapor ratios), then the data of Hass (1971) can be used in conjunction with salinity measurements to determine the hydrostatic pressure. All fluid inclusions studied were of the simple, two-phase liquid-vapor type which homogenized to a liquid. No evidence to indicate that the solutions were boiling at the time of mineralization were found (i.e., the total pressure on the system was above the liquid-vapor phase boundary). Reconstructing the overburden in the Kelly district during the time of mineralization is difficult because of the uncertainty of the age of the deposits. Chapin (personal commun., 1976) believes mineralization occurred during the late Oligocene or early Miocene. Recent work (Siemers, in preparation; Blakestad, 1976; and Chapin, personal commun., 1977) suggest a maximum overburden of 4000 feet (2000 feet of volcanic rocks and 2000 feet of sedimentary rocks, see Chapter II) can be considered to have existed over the Kelly Limestone at the time of mineralization. This gives a lithostatic pressure of about 370 atms. However, because of the relatively shallow depth of burial and the high degree of faulting in the area the pressure was certainly hydrostatic (Beane, personal commun., 1977). Since salinity determinations were not made the exact

hydrostatic pressure which existed during mineralization cannot be calculated.

Uncorrected homogenization temperatures for primary and psuedosecondary inclusions are summarized in Figure 54. Temperature measurements on secondary inclusions were not conducted. The data is reported in the form of frequency diagrams because of the limited number of inclusions studied. Each temperature reported represents a minimum of three determinations with a precision of ±0.3 C, an accuracy of ±5 C is assigned to each homogenization temperature reported because of sampling errors (Landis, personal commun., 1977).

Fluid inclusion data (Figure 54) indicate temperatures of deposition of (1) about 235° to 285°C for barite contemporaneous with microcrystalline quartz; (2) about 260° to 275°C for vug barite; (3) about 250°C for vein barite; (4) about 165° to 185°C for coarse-grained quartz; (5) about 185° to 200°C for calcite; (6) about 195° to 235°C for green fluorite (temperatures as low as 158°C and 173°C were also recorded); and (7) about 145°C to 190°C for purple fluorite.

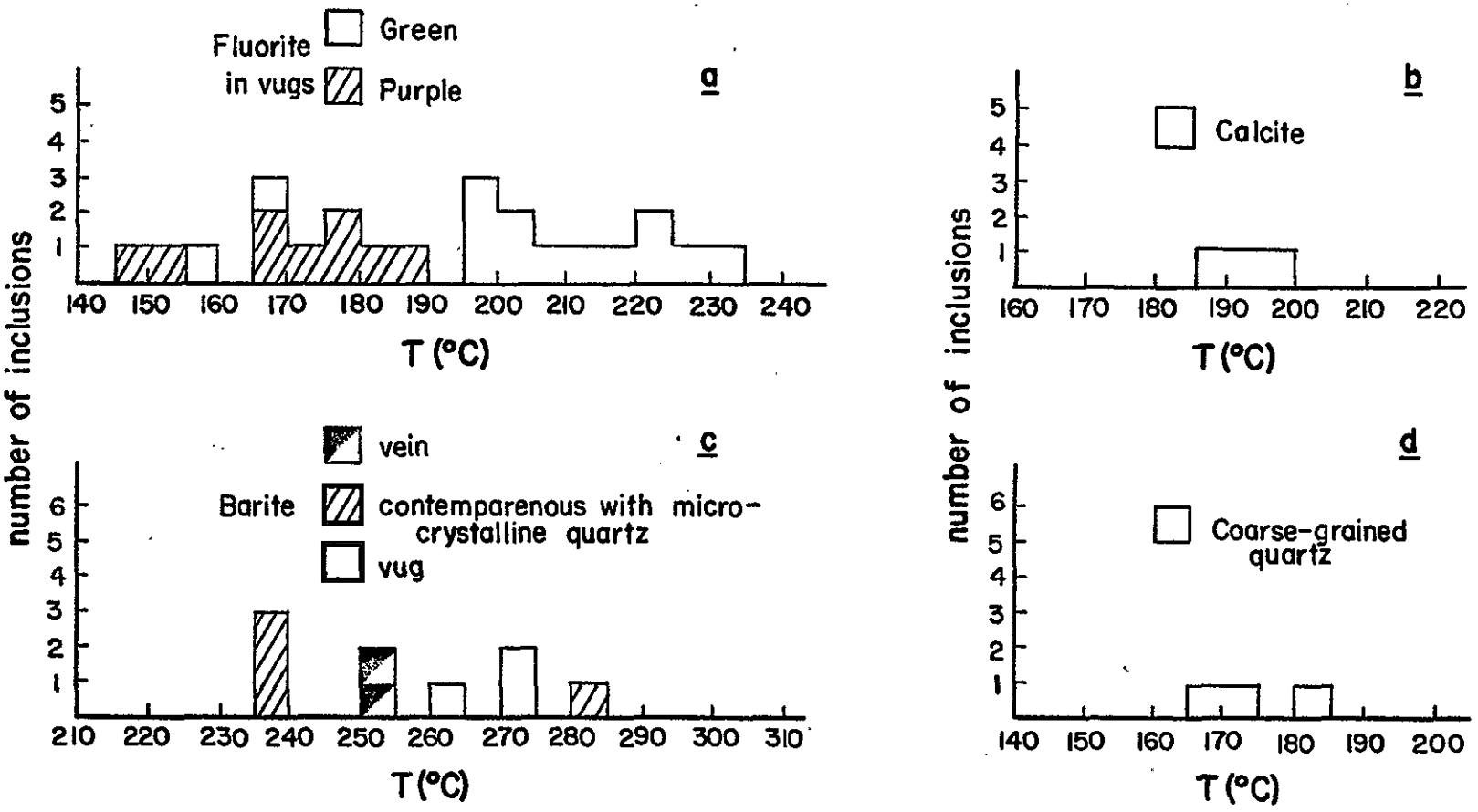

Figure 54. Frequency distribution diagram for primary and psuedosecondary homogenization temperatures in (a) fluorite, (b) calcite, (c) barite and (d) coarse-grained quartz. No pressure correction has been applied.

Chapter VI: ORIGIN OF KELLY DISTRICT JASPEROID

Introduction

Any discussion of the genesis of a jasperoid body should consider the following aspects: (1) the source of the silica, (2) the nature of the solutions that dissolve and transport silica, (3) the conditions at the site of deposition which cause silica to replace limestone, and (4) the mechanism of limestone replacement (Lovering, 1962, 1972). Clearly, a geochemical analysis of Kelly district jasperoid is needed to answer some of these. Certain constraints can be imposed however, and several answers obtained through a detailed field and petrographic study of a jasperoid body. On the basis of these types of analyses and temperature data (obtained from fluid inclusion studies), an interpretation is presented as to the origin of Kelly district jasperoid.

Genesis of Petrographic Textures

Spherulitic texture (especially Type II, p. 95) and desiccation-like fractures suggest that Kelly district jasperoid was deposited as a silica gel. Thus, a colloidal silica sol may have played a significant role in the formation of jasperoid. The presence of silica gels in the genesis of jasperoid has been proposed by many authors, notably Irving (1911), Cox et al. (1916), Lindgren and Loughlin (1919), Adams (1920), Gilluly (1932), Butler and

Singewald (1940), Park and Cannon (1943), Lovering (1962, 1972), and Bailey (1974). However, it was not until Oehler's (1976) work that both a theoretical and experimental base became available to support this hypothesis. He has shown that the formation of quartz spherulites (Type II, spherulitic quartz in this study) requires the former presence of a silica gel. Oehler uses the existence of these structures in cherts as indicative of a colloidal precursor. Biological activity can also account for some of these structures in cherts (Pettijohn, 1957). White and Corwin (1961) found that most chalcedony and chert are secondary products which require the former presence of a silica gel, silica glass, opal or cristobalite.

Many studies have been conducted on the transformation of amorphous silica to quartz (Corwin et al., 1953; Yalman and Corwin, 1957; Carr and Fyfe, 1960; White and Corwin, 1961; Mitsyuk, 1974; Oehler, 1976; etc.). All these studies, except for Oehler (1976), have shown the transformation of amorphous silica to quartz taking place in several stages, the generalized crystallization trend being amorphous silica to cristobalite to quartz, with or without any new intermediary silica phases at each step. This transformation is extremely sensitive to physico-chemical conditions (temperature, pressure, solution composition) and time. Many cherts of Tertiary age contain cristobalite, whereas, many cherts of Cretaceous age or older contain quartz (Hathaway, 1972, p. 773). In the

crystallization of silica gel to quartz, Oehler found no intermediary silica phases. This would suggest that under his experimental conditions (3kb, 100° to 300°C, 25 to 5200 hr) either: (1) quartz formed directly from a gel, or (2) any intermediary phases that did develop were short-lived.

The influence of previous phases (if any) on the textures exhibited by quartz is not known. Thus, for the purposes of the following discussion, it is assumed the textures exhibited by quartz in jasperoid are primary.

Folk and Weaver (1952), in their textural study of cherts, considered nucleation (i.e., spacing of the centers of crystallization) as the dominant parameter in determining whether chalcedonic or microcrystalline quartz will form. Microcrystalline quartz develops when crystal growth begins at numerous, closely spaced centers of crystallization; the randomly oriented quartz microcrystals growing in all directions until they meet the advancing edge of another quartz microcrystal. The closeness of the spacing is assumed to be a function of rate of formation of quartz nuclei which, in turn, determines the grain-size distribution in microcrystalline quartz. Chalcedonic quartz, on the other hand, forms from only a few centers of crystallization, resulting in limited interference which allows for optically continuous fibrous structures. White, Brannock and Murata (1956) concluded that the degree of supersaturation (which determines rate of nucleation) with

respect to any form of silica is the dominant parameter in determining how the silica phase will be deposited (e.g., megacrystalline or microcrystalline).

Even though, the work of Oehler (1976) and Folk and Weaver (1952) has been directed towards the formation of cherts, their data and conclusions are also applicable to jasperoid formation. The following genetic interpretation, is largely an integration of the above works consistent with the observations recorded in Chapter IV.

Jigsaw-puzzle Texture

Jigsaw-puzzle texture (Figure 26) is thought to result from either: (1) recrystallization of Type II, spherulitic texture, (2) rapid conversion of silica gel to quartz, or (3) a combination of the above.

Oehler (1976, p. 1148) states:

> "In natural cherts, mild recrystallization may destroy the original fibrous textures of spherulites, converting them to anhedral quartz grains with the interlocking mosaic texture typical of most cherts. In some cases, when recrystallization has not been pervasive, regions with abundant quartz microspheres can be seen to grade into regions of interlocking quartz grains (for example, Figs. 9C, 9D), and many spherulites can be seen to have been partially converted to anhedral quartz (Figs. 9E through 9H). In most cases, recrystallization is more prevasive, but even so, when viewed in transmitted (unpolarized) light, ghosts of original microspheres frequently are evident, at least locally (Fig. 9E)."

Figures 38a, 38b, 29 and 39 illustrate this same process in Kelly district jasperoid.

A rapid rate of formation of quartz nuclei, resulting in many closely spaced centers of crystallization in a silica gel, is an alternative method for producing jigsaw-puzzle texture. As mentioned above, the relative spacing of these centers will determine whether Type II, spherulites or jigsaw-puzzle quartz will initially form. Preservation of fossil fragments (Figure 27) probably resulted from a relatively slower molecule-for-molecule replacement. Such preservation would require delicate equilibrium conditions which might account for its infrequent occurrence.

Water-filled cavities commonly present in jigsaw-puzzle texture, are most likely fluid inclusions; however, some may also be relict holes from Type II, spherulites (Oehler, 1976, Figure 8L). Rapid conversion of silica gel to quartz can account for desiccation-like fracturing by not permitting diffusion of water to keep up with crystallization of the gel. Keller (1941) hypothesized that undulose extinction exhibited by microcrystalline quartz in cherts resulted from strain developed as silica passed from a colloidal state to a crystalline state. This same process is thought to occur in jasperoid. Other methods of producing undulose extinction in jigsaw-puzzle quartz are: (1) externally imposed stress (e.g., tectonic movement), and (2) recrystallization of Type II, spherulites (Figures 38a and b).

Jigsaw-puzzle-Xenomorphic Texture

Jigsaw-puzzle-xenomorphic texture (Figure 30) is similar to jigsaw-puzzle, but contains patches of coarser-grained quartz. The larger grains of quartz and the features they display can originate in a number of ways:

(1) Locally reduced growth rate in a silica gel. Nucleation centers are more widely spaced than they are in jigsaw-puzzle texture. In this case, the relative cleanliness of the coarser grains (Figure 30b) results from a slower growth rate which allows the exclusion of impurities by pushing them aside. Undulose extinction can be interpreted as resulting from imperfect crystallization from a gel, and/or externally imposed stress.

(2) Local recrystallization of jigsaw-puzzle quartz. The relative cleanliness of the larger quartz grains is attributable to the recrystallizing grain pushing the impurities toward its edges. Undulose extinction can result from externally imposed stress, and/or imperfect recrystallization (coalescence). Spry (1969, p. 156) discusses this latter process:

> " ... whereby adjacent crystals with somewhat different orientations become joined together to give a single crystal. In the early stages of the process the large secondary grain has a mosaic (growth) substructure and consists of lattice regions of slightly different orientation (sub-grains) so that it has undulose and patchy extinction but this disappears to give a crystal with uniform orientation."

(3) Direct recrystallization of small closely spaced Type II, spherulites. The relative cleanliness and undulose extinction displayed by the coarser quartz grains can be described by the same processes discussed in (1) except in the case where chalcedonic fibers push the impurities away.

(4) Direct precipitation of quartz from solution locally within the gel. Oehler (1976) found that in experimental products containing greater than 60 percent quartz, small doubly terminated quartz crystals formed on the spherulites. He interpreted this as suggesting that spherulites grow as long as the concentration of silica in solution is high enough to maintain a colloid (i.e., supersaturation); when the concentration of silica falls below the super-saturation level, quartz can directly precipitate from relatively dilute solutions. The same process can be invoked to explain the coarser-grained quartz in jigsaw-puzzle-xenomorphic texture. The fine-grained quartz fraction of this texture results from the rapid conversion of silica gel to quartz but, locally within the gel, microenvironments are present where the level of silica saturation is below that needed for a colloid so that quartz precipitates directly from solution. The cleanliness of the quartz results to precipitation from solution and a relatively slow growth rate.

(5) by any combination of the above methods.

Xenomorphic-Granular Texture

The possible process(es) by which xenomorphic-granular texture developed are similar to those described for jigsaw-puzzle-xenomorphic quartz. They are:

(1) local fluctuations in the rate of formation of quartz nuclei during crystallization of a silica gel;

(2) recrystallization of jigsaw-puzzle-xenomorphic quartz;

(3) recrystallization of Type II, spherulites (Figure 40);

(4) direct precipitation of quartz from solution; and

(5) a combination of the above.

The reader is referred to the previous section for the details of these processes. There are, however, several features exhibited by xenomorphic-granular quartz which place constraints on its mode of formation. Features such as those described on p. 82 and the observations made on the jasperoid-limestone transition zone (p. 106) indicate that direct precipitation of quartz from solution is probably the dominant origin of this texture. Based on its mode of occurrence (p. 82), it is hypothesized that xenomorphic-granular texture is developed at a later point in the crystallization of a gel than jigsaw-puzzle-xenomorphic.

Xenomorphic Texture

Xenomorphic texture is thought to originate by (1) recrystallization of Type II, spherulites (Figure 48b),

and (2) recrystallization of finer-grained quartz by coalescence as described on p. 129(Bailey, 1974, p. 90-92).

Subidiomorphic Texture

Subidiomorphic texture results from direct precipitation of quartz from solution (Lovering, 1972). This texture forms (Bailey, 1974, p. 92):

> "Where space has been sufficient to prevent early grain boundary interference between grains during crystallization or recrystallization, some quartz have developed a subhedral to occasionally euhedral shape."

Bailey also suggests that when this texture is associated with other microtextures, recrystallization by simple grain growth may be more likely.

In Kelly district jasperoid subidiomorphic texture developed where sufficient space was available so grain boundary interference would not inhibit the formation of elongate, quartz grains. This requires widely spaced quartz nuclei with a slow growth rate. The texture is interpreted as a late-stage phenomena in jasperoid formation where the concentration of silica is below the level needed for colloidal silica deposition, allowing for quartz to precipitate directly from solution. No evidence was found to support the hypothesis that subidiomorphic texture may result from the recrystallization of other microtextures.

Minor Microcrystalline Textures

Vugs in Kelly district jasperoid are the result of at least two processes: (1) calcite dissolution as described

on p.114, and (2) volume reduction related to conversion of silica gel to quartz. No criteria was established to differentiate between these two types. Bailey (1974, p. 110) interpreted the occurrence of concentric fractures around vugs as developing from stresses present during the desiccation of a gel, however, no such structures are present in Kelly district jasperoid examined.

The origin of brecciated and spherulitic textures (Type I and II) has been already discussed (p.94 and 95, respectively). Two processes of recrystallization have been identified with respect to Type II, spherulites, coalescence (p.129) and direct recrystallization, Figure 55.

Genesis of Megascopic Features

The origin of most megascopic features described in Chapter IV, has either been provided with the descriptions or is obvious from them. Megascopic such as: fractures (p. 60), ribbon-rock, vugs and solution-type breccia originate from the crystallization of a silica gel. Crystallization of the gel results in a volume reduction producing solution breccia, desiccation-vugs and -fractures which are filled to varying degrees by coarse-grained quartz precipitated from solution. The genesis of ribbon-rock remains unclear. Any interpretation as to its origin must be consistent with the following observations:

1. no preferential mode of occurrence

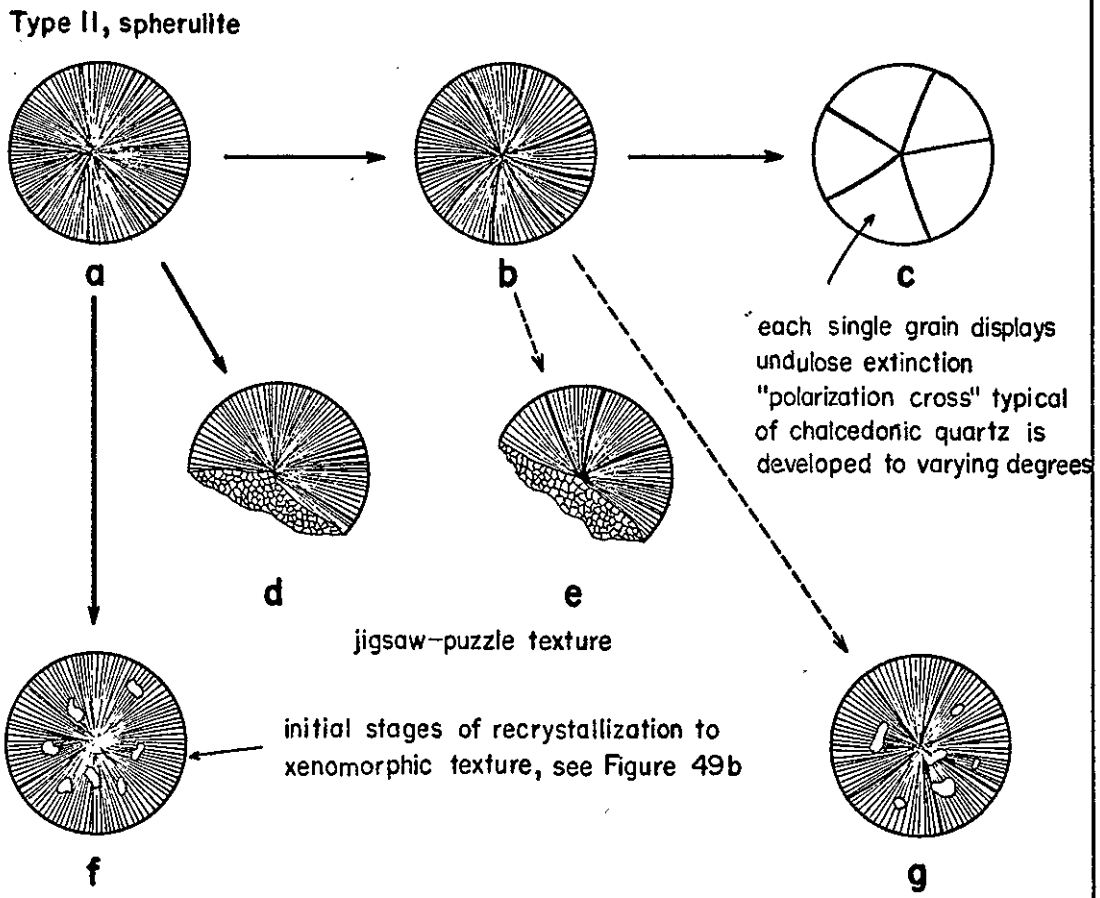

Figure 55. Idealized illustration of the two processes by which Type II, spherulites recrystallize. One process, Steps (a) through (c) is by coalescence as described on p.129. The other, Steps (a) to (d), (a) to (f), (b) to (c) and (b) to (g) is by direct recrystallization. Lines (b) to (e), and (b) to (g) are dashed because the processes have not been observed in Kelly district jasperoid.

of ribbon-rock is apparent to the writer in the study area;

2. the thickness of the individual microcrystalline and coarse-grained layers in ribbon-rock is fairly consistent throughout the area (Figures 20-24);
3. the layering in ribbon-rock is parallel (ideal ribbon-rock) to sub-parallel (irregular, and brecciated-vuggy ribbon-rock) to the jasperoid-limestone contact (Figure 23);
4. vugs in ribbon-rock are generally parallel to the layering in the structure;
5. the competence of the microcrystalline layers in irregular, and brecciated-vuggy varieties must have been such as to allow brittle fracture (Figures 21, 22, 24).

If ribbon-rock structure is directly related to desiccation of a gel, then it is clear that shrinkage must occur normal to the jasperoid-limestone contact. To what extent the thin-bedded, platy nature of the upper Kelly Limestone influenced the occurrence of ribbon-rock is uncertain. But it is probably not very significant for ribbon-rock is locally present in vertical fault zones within the upper Kelly Limestone, and in lower and middle portions of Kelly Limestone which do not contain thin-bedded, platy horizons. It is my contention that the formation of ribbon-rock is closely related to processes active during the crystallization of the gel, but the mechanism of formation is not yet clear.

Interpretation of Fluid Inclusion Data

Paragenetic and temperature data (Figures 53 and 54, respectively) may be combined, as in Figure 56, to define the change in temperature with time. The temporal relationships between vein barite and calcite are uncertain (see p.117). Microcrystalline quartz deposition may have occurred in the relatively narrow temperature interval of 235° to 285°C as evidenced by fluid inclusión temperatures from barite texturally contemporaneous with this phase of jasperoid deposition (the occurrence of intergrown barite and microcrystalline quartz is used as evidence for contemporanity). The fluorite, coarse-grained quartz, and calcite yield lower fluid inclusion temperatures, and may have been deposited after the desiccation of the silica gel. Because of the limited data from fluid inclusions in coarse-grained quartz (p.123), temperatures obtained from fluid inclusions in fluorite (145°-235°C) are interpreted as closely approximating the temperature range of coarse-grained quartz deposition. This is justifiable because even though the fluorite deposition is clearly later than the one measured quartz sample, its crystallization temperatures bracket that of the quartz. It is suspected that if more determinations are made on coarse-grained quartz in Kelly district jasperoid temperatures as high as 245° will be obtained. Bailey (1974, p. 173) reports a similar range (150°-200°C) for the deposition of the Drum Mountain jasperoid on the basis of oxygen-isotope

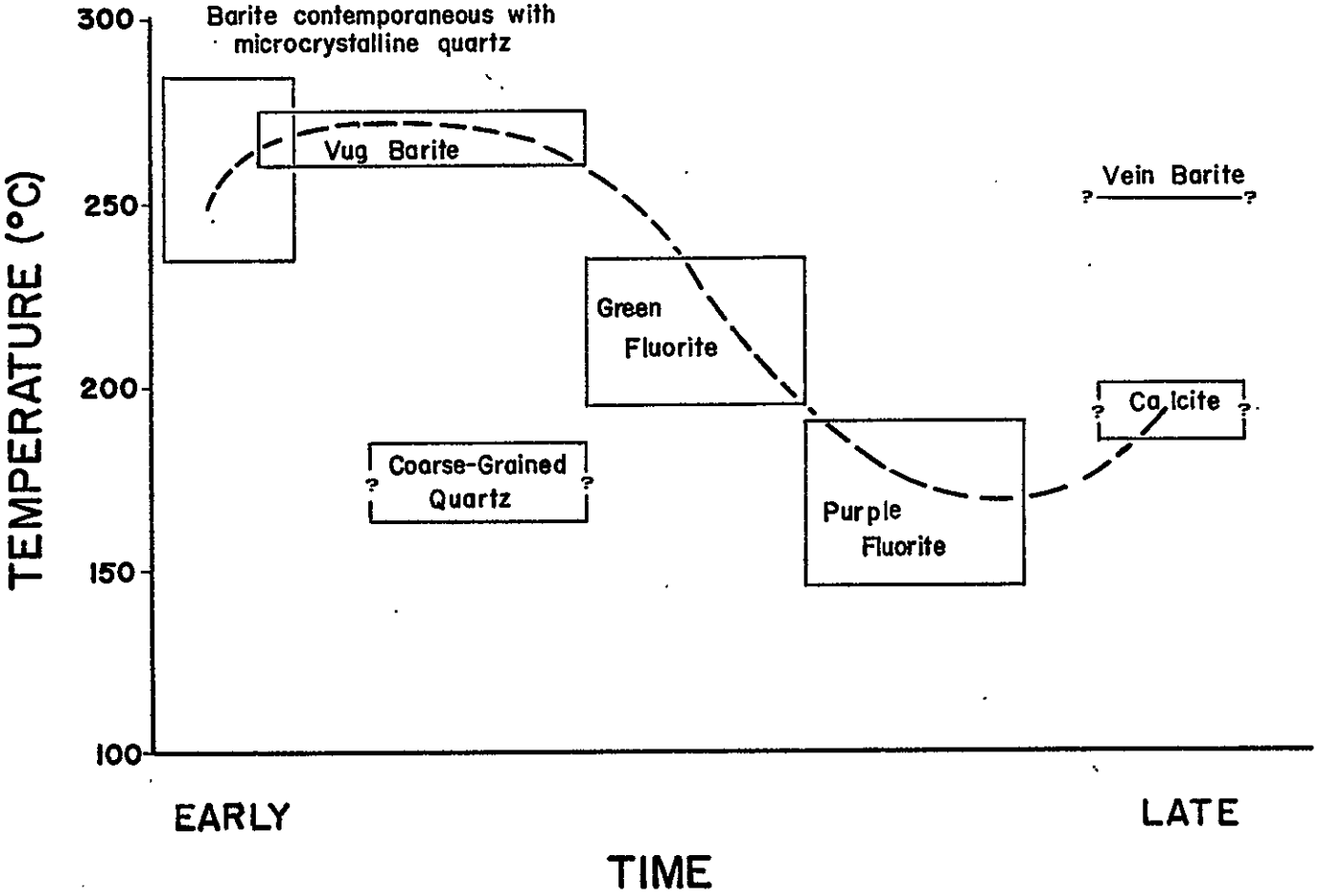

Figure 56. Temperature v. time diagram for minerals in the Kelly district jasperoid amenable to fluid inclusion analysis.

and fluid inclusion analyzes on microcrystalline quartz. Temperature data reported in this study concurs with that of Allmendinger (1975, p. 154) for barite (185° to about 250°C) and fluorite (165° to 185°C) in the Kelly mining district. Analysis of fluorite inclusions did not indicate areal temperature zonation. However it does suggest good hydrologic communication among the cavities and fissures of the fault zones during fluorite mineralization (Allmendinger, 1975, p. 91).

In summary, the data suggest that the Kelly district jasperoid was deposited between 145° and 285°C, but because of the small number of inclusions studied, the data presented here is not definitive. Rather, it represents a first approximation to the actual temperatures of deposition.

Proposed Origin of the Jasperoid

Source of the Silica. Lovering (1972) suggested that the silica in jasperoid bodies could have been derived from one or more of the following sources:

1. emanations from a cooling magma;
2. by reaction of a hypogene mineralizing solution with wall rock minerals en route to the site of silicification;
3. by solution of chert, siliceous organisms, siliceous shale beds, and argillaceous and siliceous fractions already present in the host rock; and

4. weathering of overlying adjacent rocks.

Bailey (1974) reports intensive sericitic alteration of K-feldspar in two intrusives of the Central Drum Mountains, Utah by hot, acidic solutions (Reaction 1)

$$3KAlSi_3O_8 + 2H^+ + 12H_2O = KAl_2(AlSi_3O_{10})(OH)_2 + 2K^+ + 6H_4SiO_4 \quad (1)$$

may result in the solution of significant quanties of SiO_2 to form the Drum Mountain jasperoid. An equivalent equation can also be written for the sericitization of Na-feldspar.

A similar source can be postulated for the silica in the Kelly district jasperoid. Intrusive rocks in the southern part of the district such as, the latite porphyry of Mistletoe Gulch, the quartz monzonite of the Linchburg mine and the white rhyolite dikes all exhibit varying degrees of sericitic (argillic and propylitic) alteration (see Chapter II). Estimates as to the amount of silica introduced into the Kelly Limestone range between 1.7×10^{13} and 1.1×10^{14} gms of SiO_2. The lower estimate is calculated relative to a 4 foot bed of jasperoid, 4 miles long and 1/2 mile wide; this is roughly equivalent to the area of silicification shown in Plate 1. The upper limit is based upon a cylindrical zone of alteration with a radius of 2 miles and 4 feet high. If all the silica is derived from the alteration of K-spar alone, then approximately 10^{11} to 10^{12} moles of it need to be altered. This requires a volume of sericitized K-spar of approximately

0.01 to 0.1 km^3. If a stock of ideal quartz monzonite composition (10% quartz, 45% K-spar and 45% plagioclase) occupying a volume of 5 km^3 is envisioned, only 6.25% (or 0.14 km^3) of its K-spar is required to be sericitized to produce the maximum amount of silica estimated (about 10^{14} gms). Unfortunately, no quantitative estimates on the amount of sericitization of K-spar in the intrusives of the Kelly district (mentioned above) are available. It does not seem unreasonable, however, as a first approximation, to assume that the sericitization of K-spar alone could provide significant quantities of SiO_2 to account for the silicic alteration present in the district. These estimates are conservative because the sericitization and argilization of plagioclase was not considered. In addition, other possible sources of silica are: (1) silica-rich fluids emanating from the cooling magma, (2) silica released by wall-rock alteration as the hypogene mineralizing fluids migrate toward the site of silica deposition, and (3) silica contained in normal groundwaters.

Nature of Solutions that Dissolve and Transport Silica. An extensive discussion of the nature of the solutions which transported and dissolved silica in the Kelly district is difficult as a result of the lack of:

1. geochemical analyzes of the jasperoid, and
2. minerals precipitated contemporaneously with the jasperoid which would place

definitive limits on the chemical environment.

Several characteristics of the solution can be implied on the basis of silica solubility studies and the geologic setting of the alteration. An acidic solution can be inferred because of the requirement imposed by the replacement of significant quantities of silicates with quartz and the removal of large quantities of aluminum (Helgeson and Garrels, 1968; e.g., silicified Precambrian argillite located just southeast of the Grand Ledge tunnel, Chapter III). Furthermore, from the vast amount of data being accumulated on hydrothermal systems, one can be reasonably confident that hot, acidic, saline solutions were responsible for the mineralization and alteration in the Kelly district.

Numerous studies conducted on the solubility of quartz and amorphous silica (Alexander et al., 1954; Kennedy, 1944, 1950; Holland, 1967; Krauskopf, 1959; Morey et al., 1964; Sharp, 1965; Shettel, 1974; Siever, 1962; etc.) have shown that the solubility of silica is essentially independent of pressure (for pressures less than 1 kb), ionic strength of the solution, pH (in the acidic pH range), or oxidation-reduction reactions below a temperature of approximately 300°C. Under these conditions, temperature is the only major control on silica solubility. From solubility studies (Fournier, 1967), it can be inferred that the solutions under discussion were supersaturated with respect to quartz. He states that in slightly acidic waters, below

350°C, it is difficult to avoid supersaturation of silica in contact with quartz. Fournier also points out that in the type of alteration discussed in the preceding section (Source of the Silica), the pore solutions are initially saturated with silica in respect to quartz. Silica released during this type of alteration (see above), if not precipitated directly (Blakestad, 1976 does not report any overgrowths on original quartz grains in the quartz monzonite of the Linchburg Mine) results in supersaturation of the solutions with respect to quartz. The resulting silica concentration gradients cause silica to migrate from the area of alteration.

Deposition of Silica. The preferential occurrence of jasperoid in the Kelly Limestone suggests a strong carbonate control on the deposition of silica. Precipitation of silica under the conditions described in the preceding section occurs as the result of one or more of the following processes:

1. decreasing the temperature of the solutions;
2. mixing of two solutions: (a) of different temperatures both saturated with respect to amorphous silica; or (b) a hot, undersaturated solution with respect to amorphous silica and a cool, saturated solution with respect to either quartz or amorphous silica (Banazak, 1974);
3. increasing the CO_2 content of the

solutions (Lindgren, 1901; Lovering and Patten, 1963; Shettel, 1974); and

4. sudden changes in pressure such as solution cavities and brecciated zones, on silica saturated solutions.

A process for the hydrothermal silicification of the Kelly Limestone is postulated utilizing methods (1) and (3). Since there is no available data on the character of the fluids which precipitated the jasperoid, method (2) is excluded from the discussion. The effects of process (4) are not considered because they are only of local significance. Any process hypothesized must account not only for the precipitation of microcrystalline quartz but also coarse-grained quartz. Temperature data (Figure 54) has been superimposed on the amorphous silica, quartz solubility curves of Fournier and Rowe (1966), Figure 57. Zones A and B in this figure respectively represent the inferred temperature ranges of microcrystalline quartz (silica gel) deposition (235°-285°C) and coarse-grained quartz deposition (145°-235°C). $\overline{CDEF}$ (Figure 57) represents one possible path solutions may follow in first precipitating microcrystalline quartz and then coarse-grained quartz. The following interpretation, although qualitative, appears reasonable and is consistent with available data.

Let us assume that solutions migrating from plutonic rocks are extensively supersaturated with respect to quartz at some high temperature, about 350°C (point C

Figure 57. Quartz and amorphous silica solubility curves after Fournier and Rowe (1966). Superimposed on these curves is the temperature data discussed in p. 122-123. Zones A and B respectively represent the probable temperature range microcyrstalline (silica gel) and coarse-grained quartz deposition. CDEF is a diagramatic representation of one possible path a solution which first precipitates microcrystalline quartz and then coarse-grained quartz may follow.

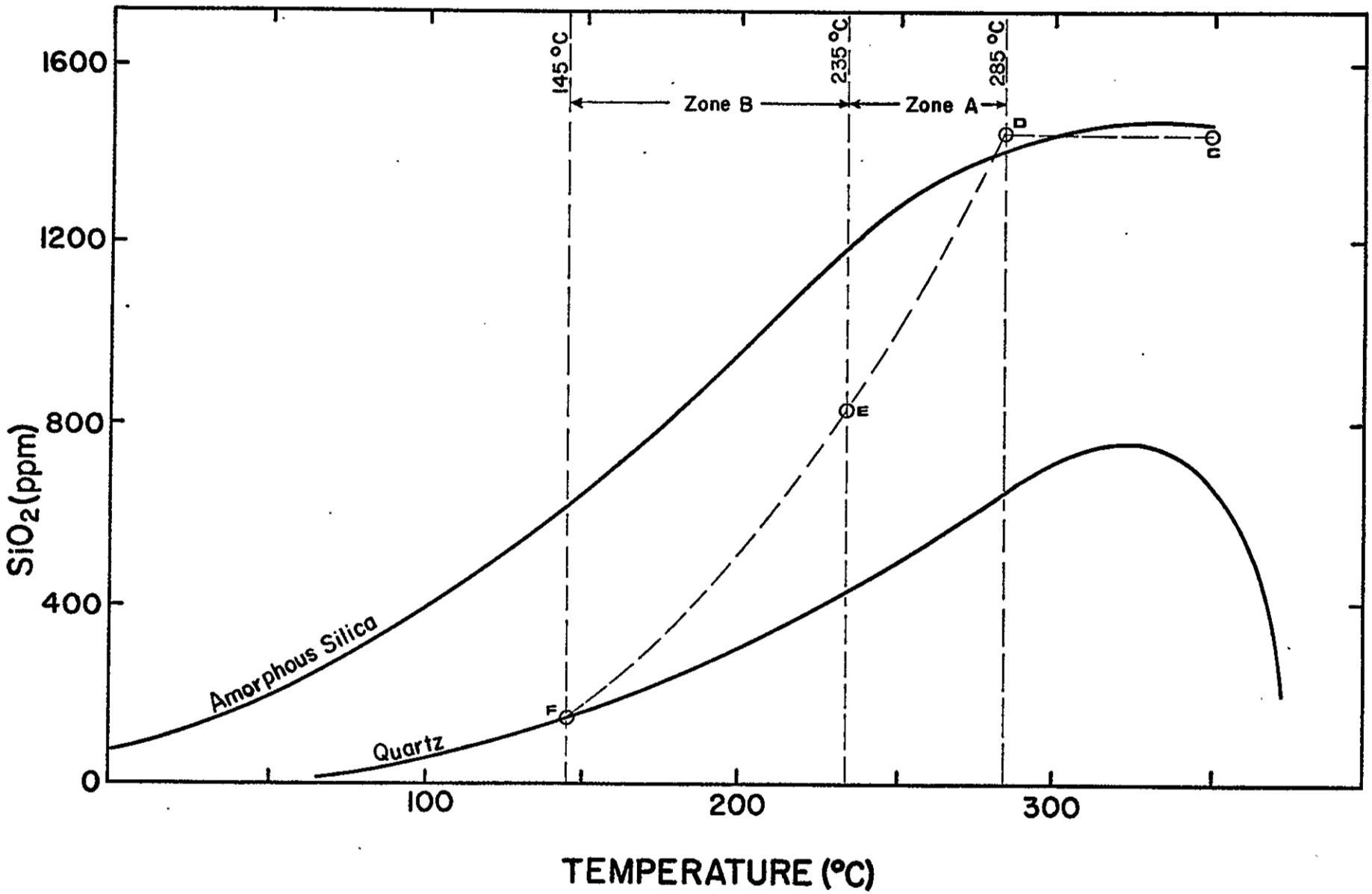
1600
1200
800
400
0
SiO2(ppm)
145 °C
235 °C
285 °C
Zone B
Zone A
D
D'
E
F
Amorphous Silica
Quartz
100
200
300
TEMPERATURE (°C)

Figure 57). As the solutions rise towards the surface along fault and fracture conduits, they cool along $\overline{CD}$ (Figure 57) and change from undersaturated to supersaturated relative to amorphous silica when the temperature falls below 300°C. Krauskopf (1956) showed that supersaturated solutions do not necessarily precipitate silica upon cooling but become colloidal with time. Even though Krauskopf's study was conducted at low temperatures, it is probably also valid at relatively high temperatures (such as 300°C), as evidenced by Fournier (1967) who reported that when solutions are cooled from 300°-350°C at a moderate rate, amorphous silica rather than quartz will precipitate.

Fluid flow up near vertical conduits became difficult when the relatively impermeable Sandia Formation was reached (Chapter III), thus allowing the solutions to migrate laterally into the Kelly Limestone along several receptive horizons (p. 45). As the temperature of the solutions decreases the solubility of silica decreases and the supersaturation of silica increases. This tendency is further reinforced by the generation of CO_2 as the limestone is replaced by silica (Reaction 2).

$$CaCO_3 + H_2O + CO_2 + H_4SiO_4 = SiO_2 + Ca^{2+} + 2HCO_3^- + 2H_2O$$

The ability of CO_2 to precipitate silica gel from supersaturated solutions has been demonstrated by Lovering and Patten (1963). Recent investigations by Shettel (1974) also indicate

that increasing CO_2 content of the fluid causes supersaturation of the fluid with respect to silica and the precipitation of this silica. The combination of decreasing temperature and increasing the CO_2 content of the solutions which favors the precipitation of amorphous silica (as silica gel) is thought to have begun at 285°C (Figure 56; point D Figure 57) in the Kelly district. This combination of factors decreases the solubility of amorphous silica in solution sufficiently as to allow the precipitation of amorphous silica to occur in the relatively wide temperature range of 285°-235°C (Zone A Figure 57). Silica gel continues to form as long as the level of supersaturation of the solution is high. When this level falls below the supersaturation threshold quartz precipitates directly from solution. A tentative temperature range for the deposition of coarse-grained quartz is 235°-145°C (respectively, points E and F in Figure 57, Zone B) based upon homogenization temperatures obtained from fluid inclusions in fluorite (p.122; Figure 56).

Desiccation of the silica gel probably occurs soon after deposition allowing coarse-grained quartz, barite, fluorite and calcite to precipitate in vugs and fractures produced by the volume reduction which incurs as the gel crystallizes. The rate at which silica gel converts to quartz and forms the various textures exhibited by microcrystalline quartz is not known.

Mechanism of Limestone Replacement. Several theories

on the mechanism of limestone replacement by silica have been proposed by various authors. Disagreement occurs as to the form of the precipitating silica and the exact mechanism of limestone replacement.

As suggested by megascopic and microscopic textural evidence (Chapter IV), replacement of limestone by silica gel (which precipitates as amorphous silica) is dominant in the early stages of jasperoid formation. As the gel crystallizes, it not only contracts in volume (generating vugs and fractures) but also yields silica solutions dilute with respect to amorphous silica but saturated (or super-saturated) with respect to quartz (Figure 57). Thus, in the later stages of jasperoidization precipitation of quartz directly from solution (into open spaces) is dominant. This process is probably repeated many times producing the complex megascopic and microscopic features present in the jasperoid.

Irving (1911) suggested two mechanisms of limestone replacement which could be differentiated by the type of host rock-jasperoid contact. One mechanism involves silica-bearing solutions penetrating the wall rocks along localizing structures and forming numerous centers of silicification. As silicification proceeds, these centers coalesce to form a solid jasperoid mass which grades outward through a zone of decreasing silicification to unaltered limestone (i.e., a gradational contact is developed). In the other mechanism, silicification

advances from a localizing structure in well-defined "wave-fronts", producing a sharp jasperoid-host rock contact. This latter mechanism has been postulated by Loughlin and Koschmann (1942) for the Kelly district jasperoid.

Lovering (1972) also presents two models for silicifying limestone and suggests criteria for their recognition. In one model original host rock textures are preserved. For this type pf replacement Lovering requires: (a) simultaneous dissolution of the host rock and precipitation of silica; (b) deposition of silica with sufficient competence to withstand the existing pressures, yet sufficiently permeable to allow passage of silica-bearing fluids to the replacement interface by diffusion; (c) conditions which allow for the precipitation of silica and removal of host rock; and (d) conditions allowing for replacement of large volumes of host rock. It should be noted that criteria (b) through (d) apply to replacement processes in general not just replacement with preservation of original host rock textures. To preserve original limestone textures during silicification molecule-for-molecule replacement must occur with a conservation of volume between the precipitating and dissolving phases. The second model for replacement accounts for destruction of original host rock textures. This mechanism does not involve the simultaneous dissolution of limestone and precipitation of silica. Lovering reports that silica deposited by this

mechanism commonly forms subidiomorphic texture (p. 85), however, it is this author's belief that any of the microscopic textures described in Chapter IV can develop. Preservation of original host rock textures is a function of the conservation of volume; if volume is not conserved between the precipitating and dissolving phases original textures cannot be preserved.

In Kelly district jasperoid, all four mechanisms described above are probably operative at different times varying with fluctuating physico-chemical conditions. Silicification can proceed outward from a localizing structure, initially forming many centers of silicification within a favorable limestone horizon. Coalescence of these centers produces a solid jasperoid mass. Since the contact between jasperoid and Kelly Limestone is sharply gradational over a distance of less than one inch, the permeability of the limestone must have been relatively low and diffusion of silica very slow. Isolated pods in essentially unaltered limestone (Figure 13) may represent the incipient stages of this process. Silicification advancing as a wave from a localizing structure can also account for the observed sharply gradational contact by the same argument presented above. Conservation of volume during the silicification process is a relatively rare occurrence as evidenced by the scarcity of preservation of original host rock textures as in Figure 27.

Regardless of the exact mechanism of limestone

replacement, the silica deposited was competent enough to withstand the existing pressures without deformation and sufficiently permeable to allow passage of silica-bearing fluids. The replacement of large volumes (p. 139) of limestone probably proceeded by diffusion of silica through the silica gel, and movement of solutions along zones of high permeability (Chapter III). Lindgren (1933) and Hosler (1947) have shown that large-scale replacement is predominantly dependent on transport by moving solutions and to a lesser degree by local diffusion over short distances.

Chapter VII: SUMMARY AND CONCLUSIONS

The primary purpose of this thesis has been to investigate the occurrence of jasperoid in the Kelly Limestone and to develop a genetic model consistent with the available data. An area approximately 2 miles square in the eastern portion of the Kelly mining district was mapped with attention directed towards the geologic setting and its influence on the distribution, controls and genesis of jasperoid.

Jasperoid occurs predominantly in the upper Kelly Limestone as a tabular mass, just below the Sandia Formation, and crops out along the crest of the Magdalena Range southward from Tip Top Mountain to North Baldy and westward on several dip slopes of Kelly Limestone. Its distribution has been modified relative to Loughlin and Koschmann's map (1942) to include dip slopes where jasperoid remnants standing topographically and stratigraphically above unsilicified Kelly Limestone and numerous pieces of silicified float provide evidence for the former existence of a jasperoid horizon.

Both stratigraphic and structural controls were found to influence the occurrence of jasperoid and these parameters were divided into two categories: primary controls and features of unknown importance. Primary structural controls consist of faults and fissures which acted as channel-ways for silica-rich solutions. Primary stratigraphic controls

are (1) the Kelly-Sandia contact which consists of the relatively impermeable Sandia Formation overlying the upper Kelly Limestone, and (2) favorable horizons (biosparrudites) within the Kelly Limestone that were susceptible to replacement by silica. It is assumed that the biosparrudite horizons were more receptive to silicic alteration than biomicrite and micrite horizons because of its greater permeability. The preferential occurrence of jasperoid in the upper Kelly Limestone, however, is thought to be primarily the result of the overlying, relatively, impermeable Sandia Formation which caused the solutions to migrate laterally into the upper Kelly. Stratigraphic and structural features of unknown importance are: pinches and swells in jasperoid horizons, arm-like extensions of jasperoid into limestone, silicified pods in essentially unaltered limestone, and some minor fractures.

Detailed petrographic examination of the Kelly district jasperoid suggests that it was deposited as a silica gel which converted to fine-grained quartz exhibiting a variety of quartz microtextures. Recrystallization paths have been proposed for several microtextures identified in the jasperoid. The generalized crystallization trend is silica gel (amorphous silica) crystallizing to chalcedonic quartz (Type II, spherulitic texture) and/or microcrystalline quartz exhibiting a jigsaw-puzzle texture. Type II, spherulites recrystallize to most of the major

microcrystalline quartz textures described in this study (jigsaw-puzzle, jigsaw-puzzle-xenomorphic, xenomorphic-granular, and xenomorphic). The coarser-grained quartz microtextures (jigsaw-puzzle-xenomorphic, xenomorphic-granular, xenomorphic, and subidiomorphic) form by: (1) recrystallization of existing quartz, (2) crystallization of quartz from solution, (3) variable rates of quartz nucleation, and (4) some combination of the above. Deposition of silica gel indicates that the solutions were supersaturated with respect to amorphous silica. Desiccation of the gel resulted in shrinkage and produced desiccation fractures, vugs, and solution breccia. Open spaces were filled to varying degrees by coarse-grained quartz which precipitated from relatively dilute solutions with respect to amorphous silica.

The major source of silica for the Kelly district jasperoid is thought to be from the argillization and sericitization of feldspars in several igneous rocks within the district. Transportation of silica was by hot, acidic solutions that were probably supersaturated with respect to quartz. Deposition occurred as a result of decreasing temperature and increasing P_{CO_2} in the solutions as they encountered favorable horizons in the Kelly Limestone. Jasperoid formation occurred both by replacement of limestone and silica deposition in open spaces with replacement by silica gel dominant in the early stages and precipitation of coarse-grained quartz (in voids) dominant in the later

stages. Fluid inclusion studies indicate that Kelly district jasperoid was deposited in the temperature range of 145° to 285°C with microcrystalline and coarse-grained quartz forming in the range of 235° to 285°C and 145° to 235°C, respectively. These temperatures are based on uncorrected homogenization temperatures (with respect to pressure) obtained from fluid inclusions in barite, fluorite and coarse-grained quartz in Kelly district jasperoid.

Part II: DIFFERENTIATION OF CHERT FROM JASPEROID BY X-RAY DIFFRACTION LINE RESOLUTION

Introduction

Statement of the Problem

Two types of microcrystalline quartz, chert and jasperoid (see p. 3 for definition of jasperoid) have been observed in the Kelly Limestone (Mississippian), Kelly mining district, New Mexico. The chert occurs as brown, red, white-to-light gray nodules and lenses predominantly in the upper Kelly Limestone; jasperoid crops out as a large gray, white, brown-to-red tabular mass preferentially in the uppermost Kelly Limestone just below the Sandia Formation (p. 50).

The combination of the following field observations lead to the hypothesis that some of the microcrystalline quartz, previously interpreted as chert may be jasperoid:

1. the amount of chert increases with stratigraphic height in the upper Kelly Limestone (Siemers, 1973, reports that at Tip Top Mountain, Plate 1, chert nodules increase in size until in the thinner upper beds they occur as lenticular masses attaining thicknesses of 6 inches and lengths of 4 feet);
2. locally, "chert" nodules occur immediately below a jasperoid horizon (Figure 58; Butler and Singewald (1940) report the existence of jasperoid nodules in the Horseshoe and Sacramento districts, Colorado);
3. the presence of a faulted section of

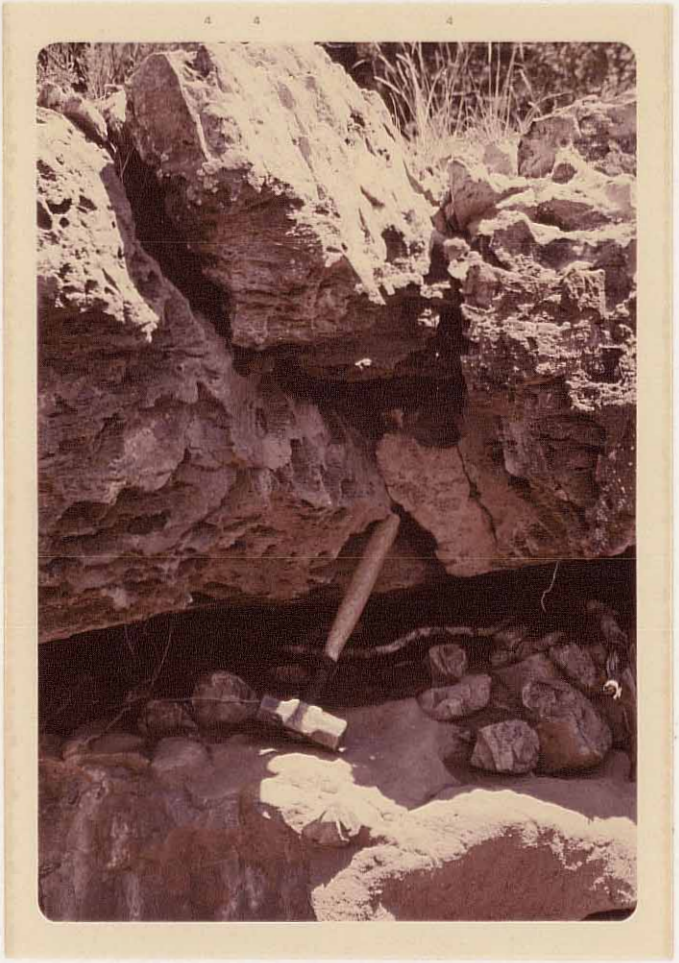

Figure 58. "Chert" nodules occurring immediately below a jasperoid horizon.

Kelly Limestone where the hanging wall contains jasperoid with no chert while the converse is true in the footwall (Figure 59); and

4. lenticular "chert" seems to grade into jasperoid (Figures 60 and 61).

Lovering (1962) states that the distinction between chert and jasperoid is difficult to make and in the absence of conclusive field evidence, no clear distinction can be made. However, the need for a reliable means of differentiating chert from jasperoid (especially if the presence of the latter is indicative of a mineralizing event) led this author to investigate the possibility of using X-ray diffraction line resolution.

Method of Investigation

A qualitative X-ray diffraction line resolution study was conducted to differentiate between chert and jasperoid upon the supposition that if both were initially deposited as amorphous silica, hydrothermal jasperoid should display a coarser crystallite size than chert which is diagenetic (Renault, personal commun., 1975). Klug and Alexander (1954) have shown that deterioration in the quality of the diffraction peaks of quartz at high angles of 2θ is characteristic of crystallites smaller than 1 to 5 microns in diameter. Thus, if the supposition (given above) is correct, hydrothermal jasperoid should yield a stronger diffraction pattern of quartz at high 2θ values than chert. Five peaks, the $212\alpha_1$, $212\alpha_2$, $203\alpha_1$, $203\alpha_2$ & $301\alpha_1$, and $301\alpha_2$ in the

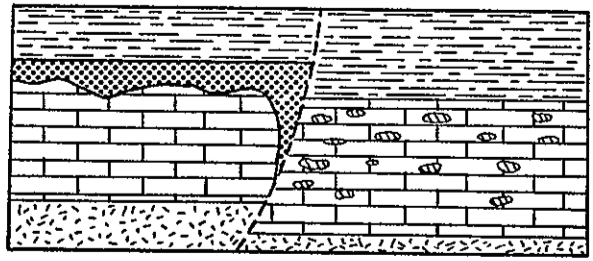

Figure 59. Faulted section of Kelly Limestone with development of jasperoid in the hanging wall and chert in the footwall. Some "chert" nodules in footwall may be jasperoid.

Figure 60. "Chert" lense (C) seems to grade into a jasperoid horizon.

Figure 61. Another example of what appears to be a "chert" lense (C) grading into a jasperoid zone (J). Note the presence of vugs in the vicinity of the jasperoid.


Jasperoid
C
Unaltered
Limestone


J
unaltered
Limestone

quartz X-ray diffraction spectra between 67° and 69° 2θ were studied; because of the close spacing of these peaks their relative resolution should primarily be a function of line breadth and consequently crystallite size. Lattice distortions produced by mechanical stress may also affect the resolution to a minor degree (Murata and Norman, 1976). This set of peaks will hereafter be referred to as the 68° quintuplet following the terminology of Murata and Norman.

Four types of microcrystalline quartz were analyzed: chert and jasperoid from the Kelly district, chert from an area of thermal and hydrothermal activity (North Fork Canyon chert, from North Fork Canyon southeast of the Kelly district), and normal chert (chert from areas remote from any known thermal and/or hydrothermal event). All cherts are of either Mississippian or Pennsylvanian age. Kelly district jasperoid is of late Oligocene - early Miocene age (Chapin, personal commun., 1975).

Previous Works

Hathaway (1972) showed that a wide range in 'crystallinity' (see below) exists in cherts from deep-sea sediments, as evidenced by the 68° quintuplet profile. Murata and Norman (1976) developed a 'crystallinity' index for quartz minerals based on the relative intensity of the $212\alpha_1$ peak. Their results are: (1) in cherts of similar age, those which have undergone a metamorphic event exhibit a higher

degree of 'crystallinity', (2) clear euhedral quartz (e.g., quartz from Herkimer County, New York — Herkimer Diamonds) displays the highest degree of 'crystallinity', and (3) some Precambrian cherts exhibit only moderate degrees of 'crystallinity' suggesting that time is not the only factor increasing 'crystallinity'. The work described in this thesis has been conducted independently of the studies done by Hathaway (1972) and Murata and Norman (1976).

Strictly speaking, the terms 'degree of crystallinity' or 'crystallinity' are not used correctly by the above authors in reference to the 68° quintuplet. As mentioned, this profile is primarily a function of crystallite size. Crystallinity deals with the regular arrangement of atoms in a space lattice; crystallite can be defined as the arrangement of atoms in a crystal into blocks, each block being an ideal crystal but adjacent blocks not being accurately fitted together so that each block is an independent, ideal crystal (Zachariasen, 1967). Silica minerals may all posses the same degree of crystallinity but vary in crystallite size (Bodine, personal commun., 1976).

Experimental Procedure

A detailed description of the sample preparation method is given in Appendix I. The prepared samples were mounted in a well, approximately 1.4 cm by 1.2 cm by 0.05 cm in size, etched into a glass slide with hydrofluoric acid. X-ray diffraction patterns were obtained using Cu K-alpha

radiation produced by a Norelco diffractometer equipped with a graphite monochrometer. Samples were analyzed under the following instrumental conditions: 40 KV/20 ma, divergence, scatter and receiving slit settings of 1/2° - 4° - 1/2°, time constant of 10 sec; scan rate of 1/8° per minute with a chart recorder speed of 1 inch/minute. In addition, instrumental conditions were adjusted at the beginning of each day's run with a silicon-pellet standard.

Six mixtures of Brazilian agate and quartz from the Ottawa Sandstone were prepared in the following proportions:

(1) 100% Quartz from the Ottawa Sandstone
(2) 75% " " " " " + 25% Brazilian Agate
(3) 50% " " " " " + 50% " "
(4) 25% " " " " " + 75% " "
(5) 12.5% " " " " " + 87.5% " "
(6) 100% Brazilian Agate

to determine the most sensitive peaks in the 68° quintuplet and the reproducibility of the samples. The 68° quintuplet profile for these mixtures varied from a broad hump for 100% Brazilian agate to well-defined peaks for the 100% quartz from the Ottawa Sandstone (Figure 62). Similar observations have been obtained by Hathaway (1972) for cherts and Murata and Norman (1976) for a variety of silica minerals.

As a qualitative measure of peak resolution, the relationship $R = 100 \times (P - V)/P$ was used (R is the percent resolution, P is the net intensity of a peak and V is the net intensity of the valley between the $212\alpha_1$ and $212\alpha_2$ peaks. The resolutions of the $212\alpha_1$ (R_1) and the $203\alpha_1$

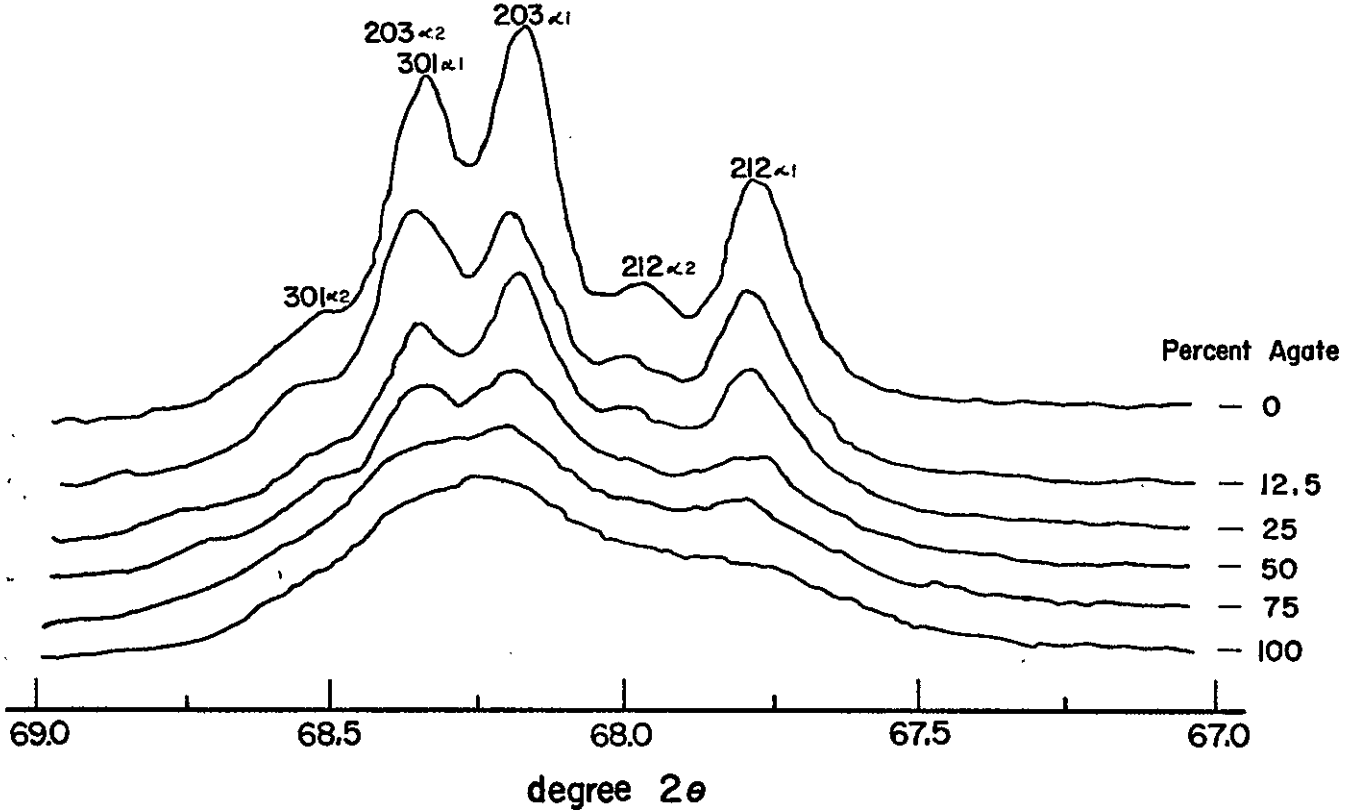

Figure 62. 68° quintuplet profiles for the six mixtures of quartz from the Ottawa Sandstone and Brazilian agate.

(R_2) were determined to be the most sensitive in the 68° quintuplet on the basis of five replications on each mixture analyzed. Both R_1 and R_2 were measured relative to the valley between $212\alpha_1$ and the $212\alpha_2$ peaks (Figure 63). The R_1 measurement was found to be much more sensitive than the R_2 measurement.

Figure 64 depicts R_1 and R_2 as functions of percent quartz from the Ottawa Sandstone along with the standard deviation for each mixture. The reproducibility of the resolution measurements is determined by (1) crystallite size distribution in the sample material, (2) amount of powder being irradiated, (3) mounting technique, (4) firmness of the packing and (5) flatness of the mounted sample surface. Factors (3) and (5) were kept constant while (2) and (4) were varied within limited ranges to test the effects of sample preparation variability. The relative error of the measurement was within 11% for R_1 and 14% for R_2.

Forty-one naturally occurring samples: 13 Kelly district cherts, 12 Kelly district jasperoids, 13 normal cherts and 3 North Fork Canyon cherts were analyzed. Table 1 provides the location, host formation (where known), and age for the normal chert and North Fork Canyon chert samples. Quartz was the only SiO_2-polymorph present in the samples analyzed.

Results

R_1 and R_2 for the various samples analyzed are given

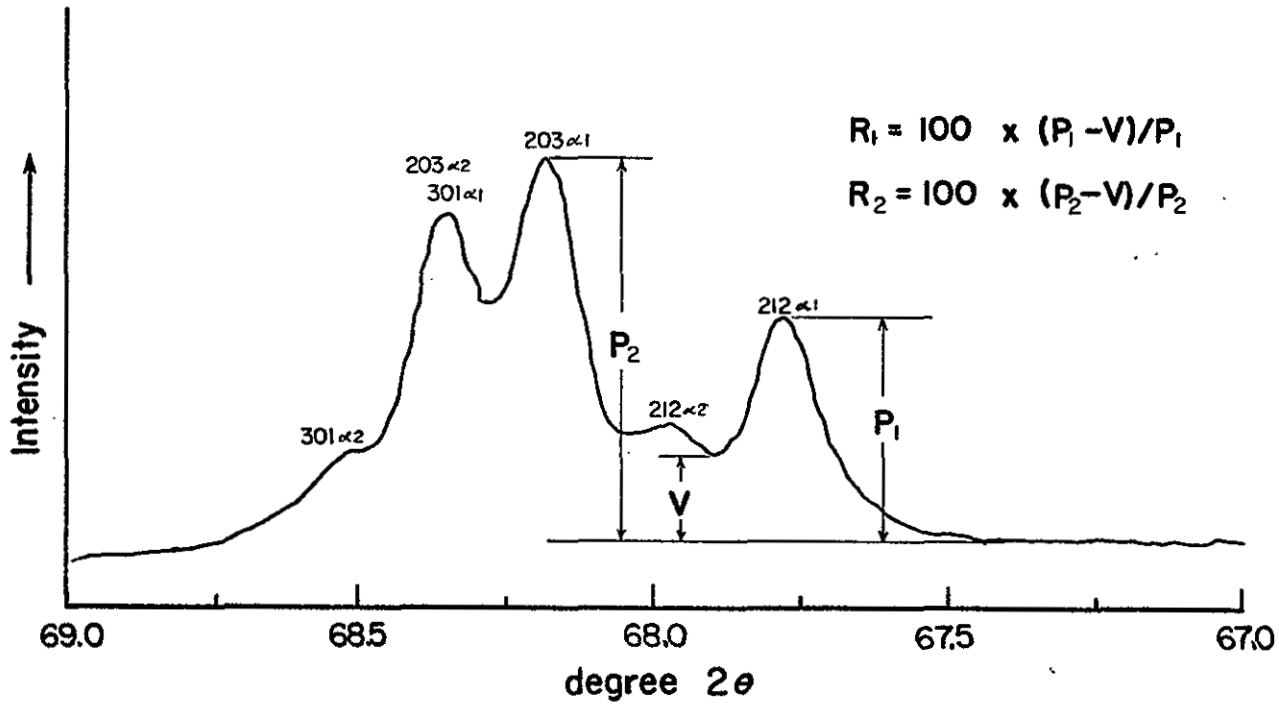

Figure 63. Typical 68° quintuplet for 100% quartz from the Ottawa Sandstone. Method for computing R_1 and R_2 is illustrated.

Figure 64. Plot of R_1, R_2 and their standard deviations as a function of percent quartz from Ottawa Sandstone. The R_2 value for 100% quartz from Ottawa Sandstone has been slightly offset for the sake of clarity.

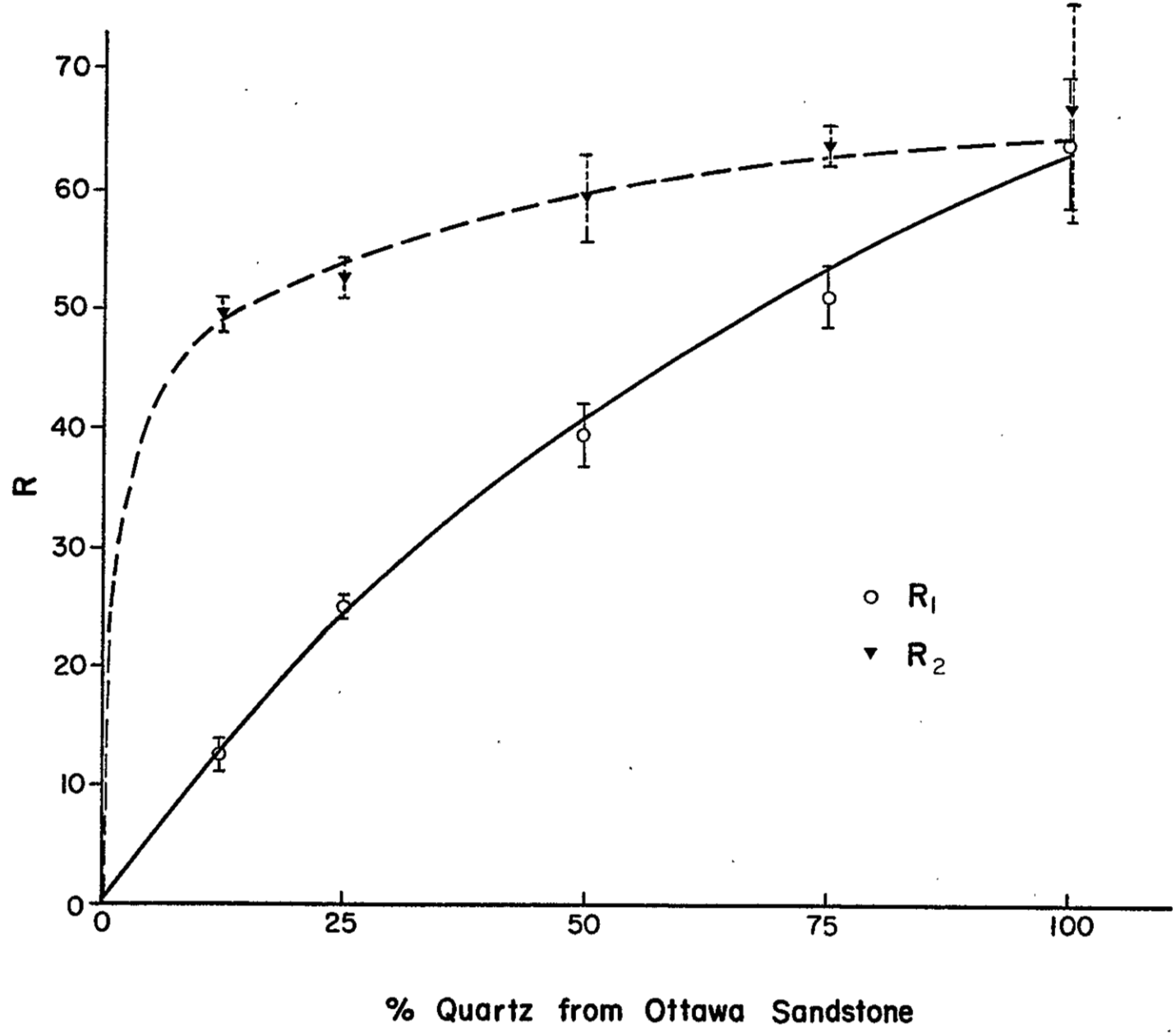
70
60
50
40
30
20
10
0
R
0
25
50
75
100
% Quartz from Ottawa Sandstone
R1
R2

Table 1. Location of normal chert (C) and North Fork Canyon chert (NFC). All samples are Pennsylvanian in age and from the Madera Formation except for C -2, C -3, C -4, C -5 and C -6 (host formation not known) and NFC-2 which comes from the Sandia Formation (see Figure 2).

Sample	Location, State
C -1	c., NE¼, SE¼, NW¼, Sec. 2, T. 2 S., R. 2 W., New Mexico
C -2	SW¼, SW¼, Sec. 12, T. 2 S., R. 1 W., New Mexico
C -3	T. 48 N., R. 13 W., Missouri
C -4	T. 48 N., R. 15 W., Missouri
C -5	T. 49 N., R. 30 W., Missouri
C -6	Kansas
C -10	Sec. 30, T. 2 N., R. 2 W., New Mexico
C -11	Sec. 26, T. 2 N., R. 3 W., New Mexico
C -12	Sec. 23, T. 1 N., R. 1 E., New Mexico
C -13	Sec. 31, T. 3 N., R. 5 E., New Mexico
C -14	c., NE¼, SE¼, NW¼, Sec. 2, T. 2 S., R. 2 W., New Mexico
C -15	c., NE¼, SE¼, NW¼, Sec. 2, T. 2 S., R. 2 W., New Mexico
C -16	c., NE¼, SE¼, NW¼, Sec. 2, T. 2 S., R. 2 W., New Mexico
NFC-1	NE¼, Sec. 28, T. 3 S., R. 3 W., New Mexico
NFC-2	NE¼, Sec. 28, T. 3 S., R. 3 W., New Mexico
NFC-3	NE¼, Sec. 28, T. 3 S., R. 3 W., New Mexico

in Figures 65 and 66, respectively. Figures 65a and 65c illustrate that R_1 for most normal chert is less than 21 which is much lower than the range in R_1 exhibited by Kelly district jasperoid, 30-48. There are, however, three normal cherts which have R_1 values in the range 30-36. These are samples C -1, C -4, C -5 (Table 1). Field data for C -1 (given below) suggest that it may have witnessed a hydrothermal episode. R_1 for Kelly district chert is given in Figure 65b; these values overlap both the Kelly district jasperoid and normal chert fields, with almost 40% of the samples exhibiting R_1 values greater than R_1 (Kelly district jasperoid). North Fork Canyon chert exhibit a range in R_1 of 42-51 (Figure 65a). This range is slightly greater than that displayed by Kelly district jasperoid but lies within the upper range of Kelly district chert (Figure 65b).

The results portrayed in Figure 66 are less obvious than in Figure 65 due to the lower sensitivity of R_2, nevertheless, the data (Figure 66) is analogous to that of R_1. Figure 67 is a covariance diagram for R_1 vs. R_2 for the samples analyzed. A significant separation occurs between normal chert and Kelly district jasperoid; the overlap is attributable to the three anamalous normal chert samples mentioned above.

Interpretation of the Results

Figures 65, 66, and 67 indicate that a significant

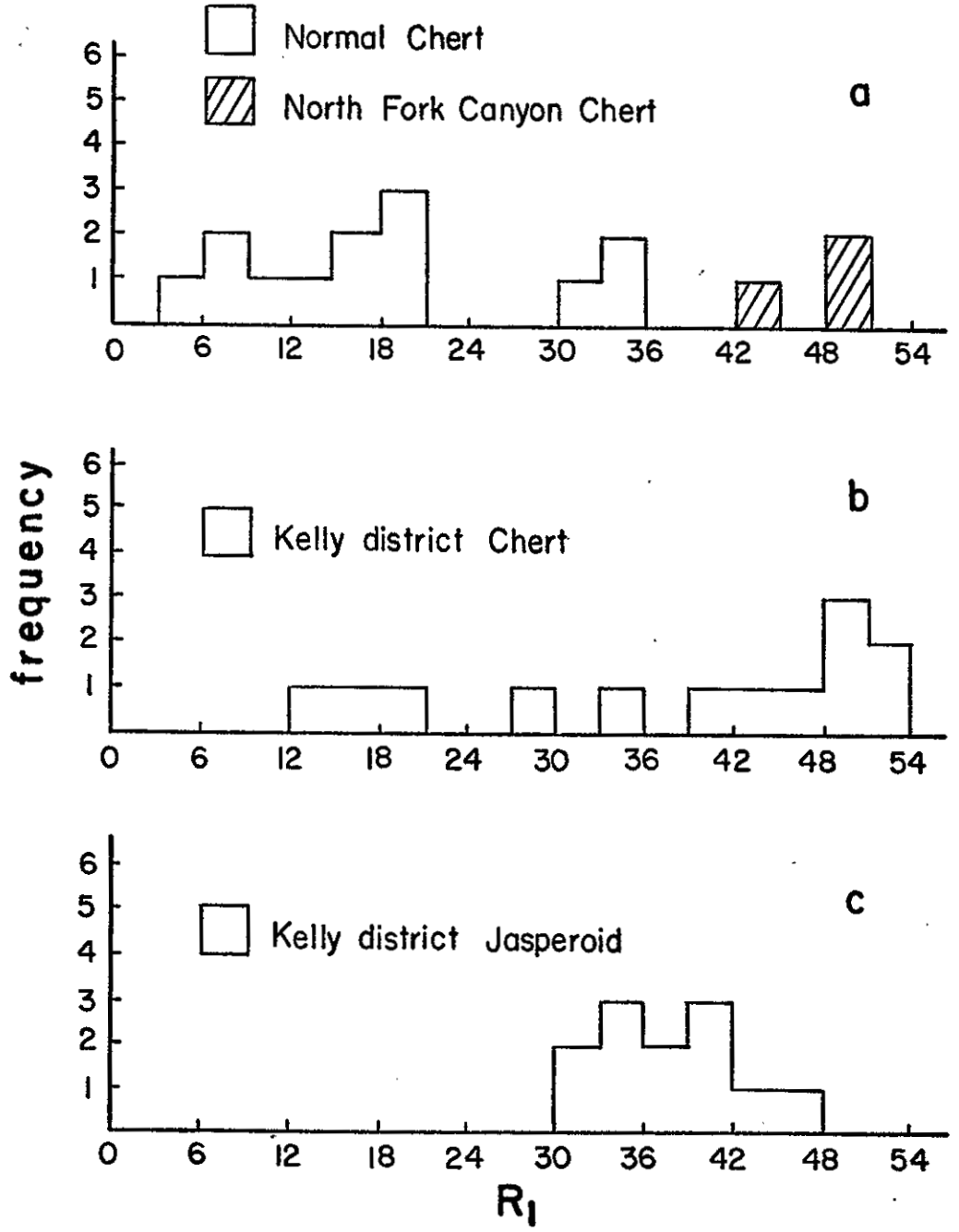

Figure 65. Frequency distribution diagram of R_1 values for (a) normal chert and North Fork Canyon chert, (b) Kelly district chert, and (c) Kelly district jasperoid.

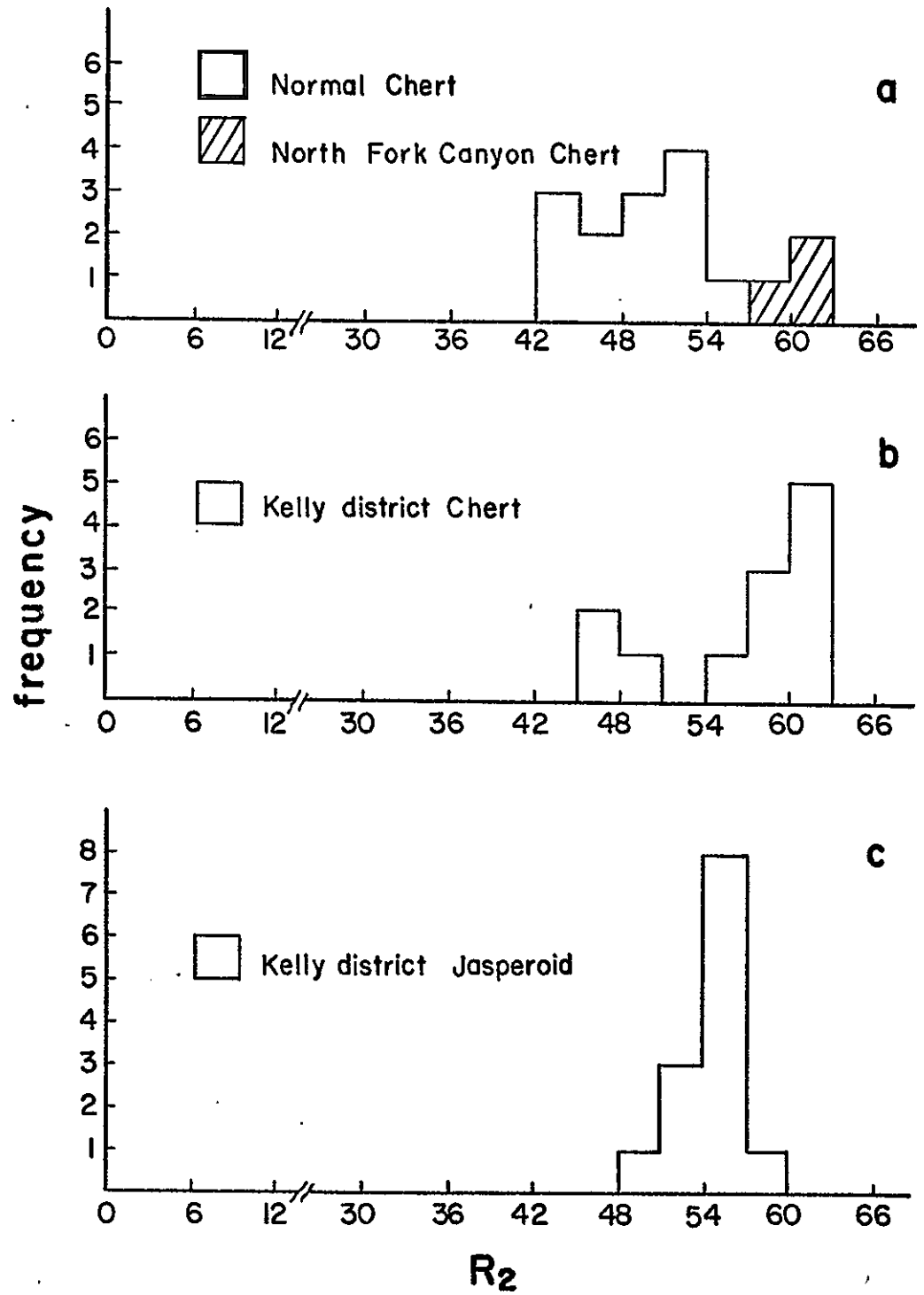

Figure 66. Frequency distribution diagram of R_2 values for (a) normal chert and North Fork Canyon chert, (b) Kelly district chert, (c) Kelly district jasperoid.

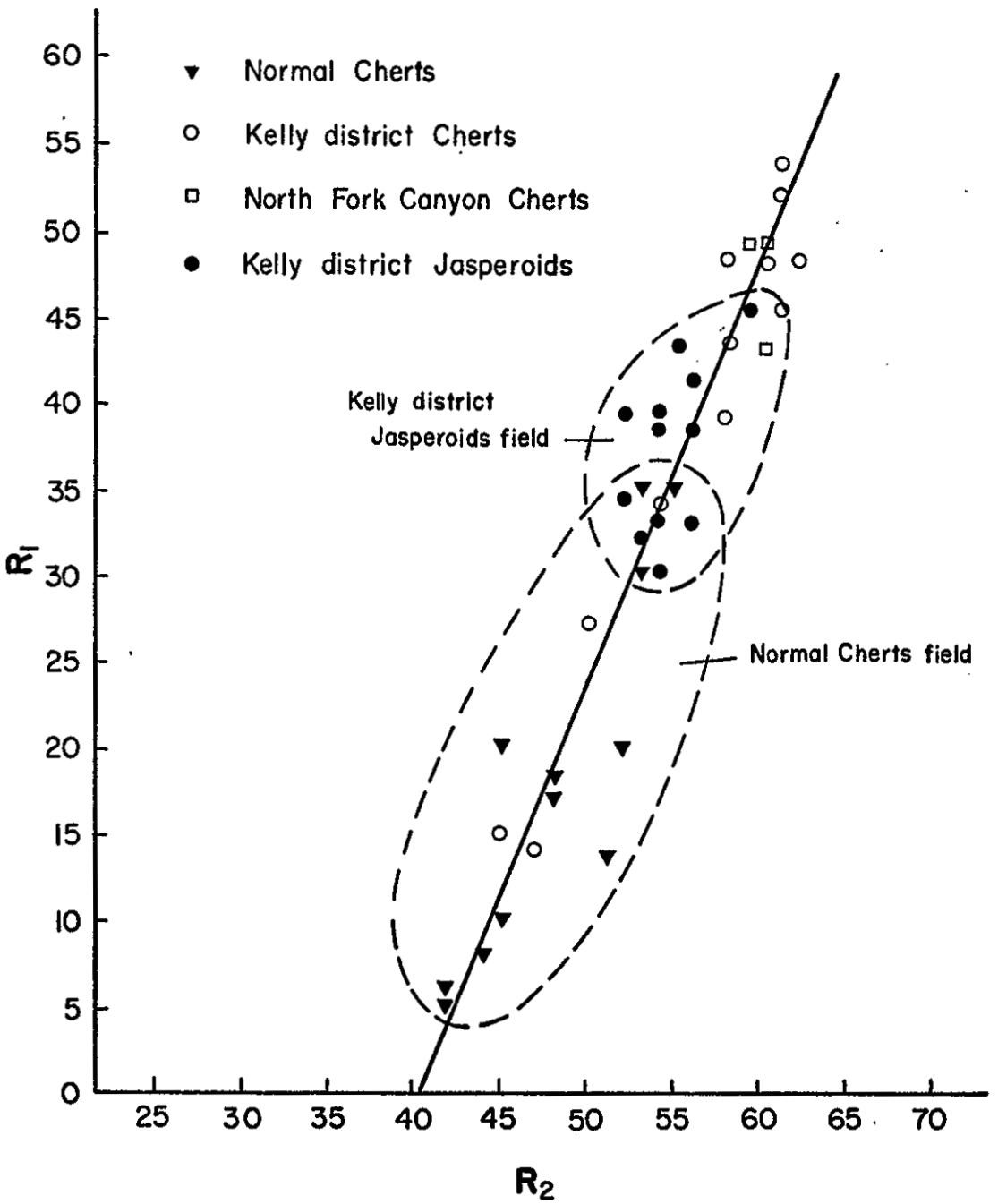

Figure 67. Covariance diagram of R_1 vs. R_2 for Kelly district chert and jasperoid, normal chert, and North Fork Canyon chert.

difference exists between normal chert and Kelly district jasperoid; Kelly district chert overlaps both these fields. As mentioned, three normal cherts lie in the lower portion of the Kelly district jasperoid region. Field data (Figure 68) suggest that one of these samples (C -1) may have been affected by a hydrothermal event. Four chert samples (C -1, C -14, C -15 and C -16) were taken at intervals away from a silicified fracture zone (Chamberlin, personal commun., 1976). C -1, the closest sample to the silicified zone, displays the highest R_1 value. The other three samples have R_1 values of less than 21 and are in the range observed for normal chert. These data imply that the R_1 value for C -1 is a result of its proximity to the silicified zone (i.e., C -1 has been modified by a hydrothermal event). If these observations are valid, the other two normal chert samples (C -4 and C -5, p.171) displaying R_1 values greater than 30 may have also experienced a similar event. These interpretations are tentative, however, because of the limited sample base.

A straight line has been plotted through the data points in Figure 67 to illustrate a continuum in percent resolution with normal chert at the low end, Kelly district jasperoid and North Fork Canyon chert at the high end. Kelly district chert falls along this line with the largest concentration being at the high end.

The implication of the results is that when normal chert is subjected to a hydrothermal event it may display

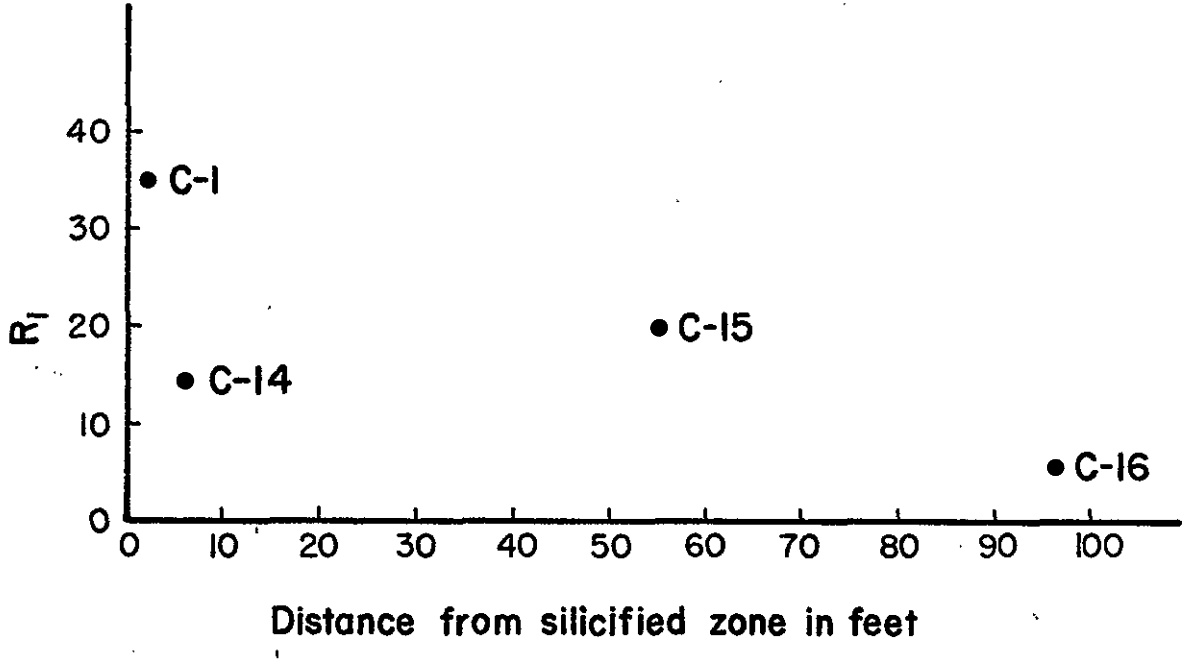

Figure 68. Plot of R_1 vs distance from a silicified zone for four normal chert samples taken from c., NE¼, SE¼, NW¼, Sec. 2, T.2S., R.2W., New Mexico.

R values equal to, or greater than jasperoid being deposited by the same event. Normal chert increases its R value by increasing the size of its crystallites. The range in R exhibited by Kelly district chert may be related to varying degrees of modification on the crystallite size distribution by the hydrothermal fluids.

Thus, Kelly district chert can be interpreted as being a mixture of either (1) normal chert and chert which has been subjected to varying degrees of modification by hydrothermal activity, or (2) normal chert, hydrothermally modified chert, and jasperoid. The X-ray diffraction line resolution study has not permitted an exact determination of the nature of Kelly district chert.

The observations and interpretations presented above are best summarized in Figure 69 which is a normality plot (cumulative % vs. R_1) for all the samples studied except North Fork Canyon chert. An examination of this figure shows that:

1. Kelly district jasperoid and normal chert plot as two lines indicating that they represent two distinct populations with mean R_1 values of 38.6 and 19.3 and standard deviations of 8.11 and 10.72, respectively;
2. a single line cannot be drawn through Kelly district chert indicating that these samples represent more than one population; and
3. Kelly district chert appears to fall

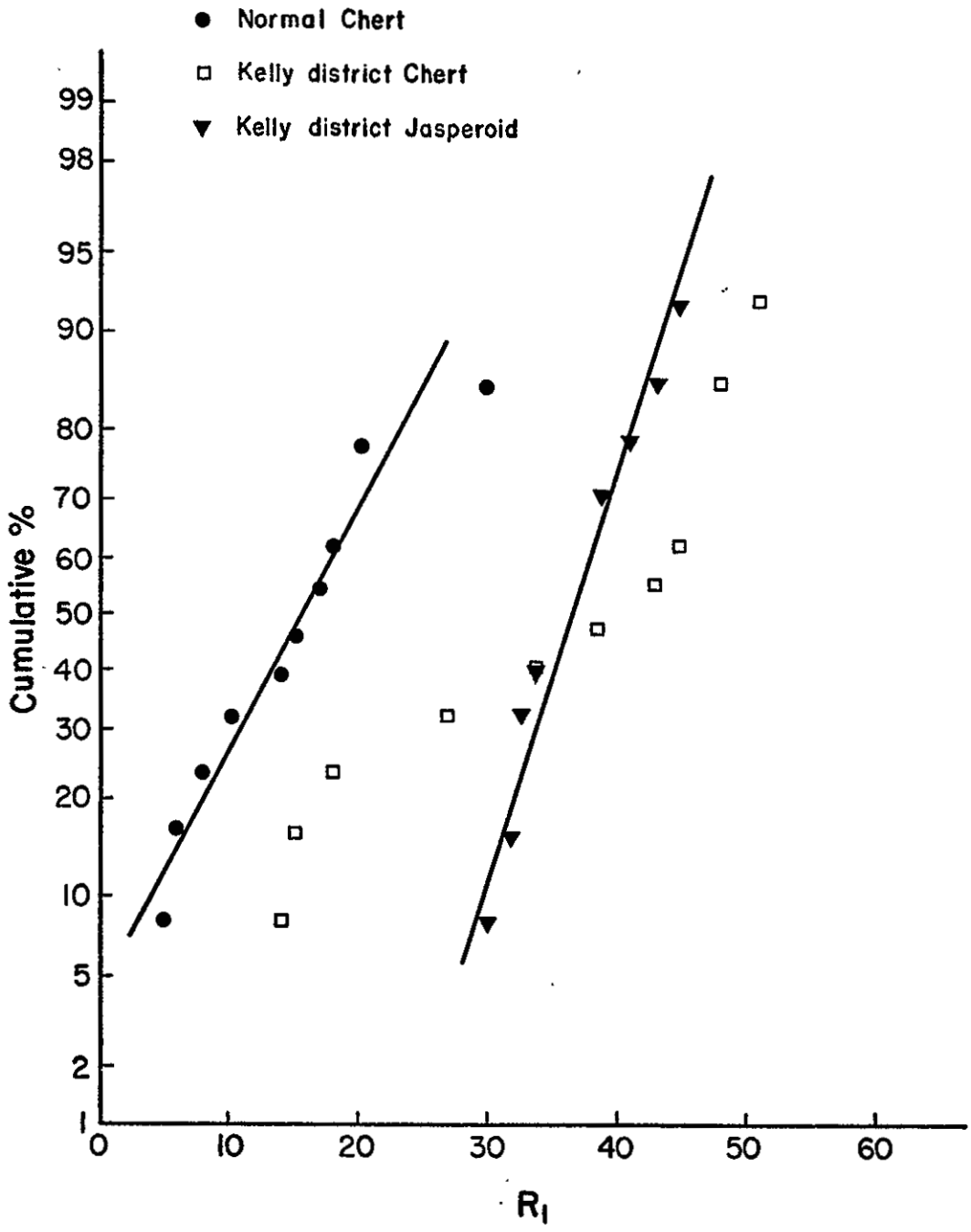

Figure 69. Normality plot for Kelly district chert, Kelly district jasperoid, and normal chert.

into three separate populations (a) normal chert, (b) cherts which have undergone varying degrees of modification by hydrothermal fluids, and (c) jasperoid.

Correlation of Petrographic Textures with X-Ray Results

Three thin sections of Kelly district chert, three of normal chert, one of North Fork Canyon chert and six of Kelly district jasperoid were analyzed for petrographic textures and optical grain size to see if a correlation could be demonstrated with R values. Table 2 presents the petrographic textures for these samples along with their respective R_1 values (R_2 is not considered because of its lower sensitivity). The reader is referred to p. 73-85 for detailed descriptions of the petrographic textures. Figures 70-76 are photomicrographs illustrating the predominant petrographic texture in several samples listed in Table 2; the R_1 value for each respective sample is also given. No correlation was found between petrographic textures or optical grain size and R_1 values. This lack of correlation suggests that crystallite size distribution (which determines R_1) is independent of optical grain size and texture.

Summary and Conclusions

A significant difference has been demonstrated between normal chert and Kelly district jasperoid; R_1

Table 2. R_1 values and petrographic texture(s) (major, minor) for three Kelly district cherts (KDC), three normal cherts (C), one North Fork Canyon chert (NFC), and six Kelly district jasperoid (KDJ). Samples are listed in order of increasing R_1 within each group.

Sample	R_1	Petrographic Texture(s) (major, minor)
KDC 187-3	18	jigsaw-puzzle, jigsaw-puzzle-xenomorphic & Type II, spherulitic
KDC 123-1	39	jigsaw-puzzle-xenomorphic, jigsaw-puzzle & Type II, spherulitic
KDC 11-1	52	jigsaw-puzzle, xenomorphic-granular
C -16	5	jigsaw-puzzle, xenomorphic-granular
C -11	17	jigsaw-puzzle, jigsaw-puzzle-xenomorphic & xenomorphic-granular
C -4	35	jigsaw-puzzle, xenomorphic-granular & Type II, spherulitic
NFC-2	49	jigsaw-puzzle-xenomorphic
KDJ 71-1	32	jigsaw-puzzle, xenomorphic-granular & Type II, spherulitic
KDJ 116-2	33	jigsaw-puzzle, xenomorphic
KDJ 216-1	34	jigsaw-puzzle, jigsaw-puzzle-xenomorphic & xenomorphic-granular
KDJ 193-1	38	subidiomorphic, jigsaw-puzzle-xenomorphic
KDJ 31-1	39	jigsaw-puzzle-xenomorphic & subidiomorphic Type II, spherulitic & xenomorphic-granular
KDJ 225-4	45	jigsaw-puzzle

Figure 70. Photomicrograph of normal chert (C) sample 16. Predominant texture is jigsaw-puzzle, however, minute calcite grains produce the fuzzy image shown, R_1 = 5 (crossed-nicols, 160x magnification).

Figure 71. Photomicrograph of Kelly district jasperoid (KDJ) sample 216-1. Predominant texture is jigsaw-puzzle, opaque areas are Fe-oxides, R_1 = 34 (crossed-nicols, 160x magnification).

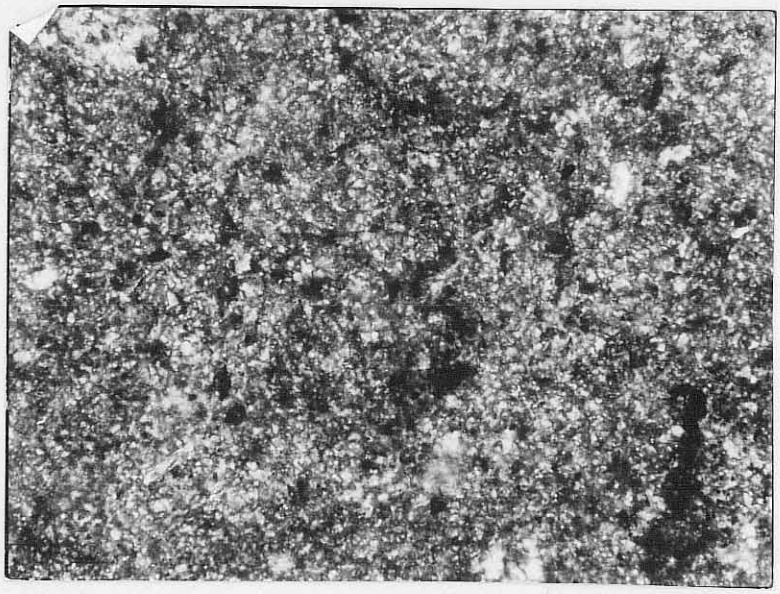

0.1 mm

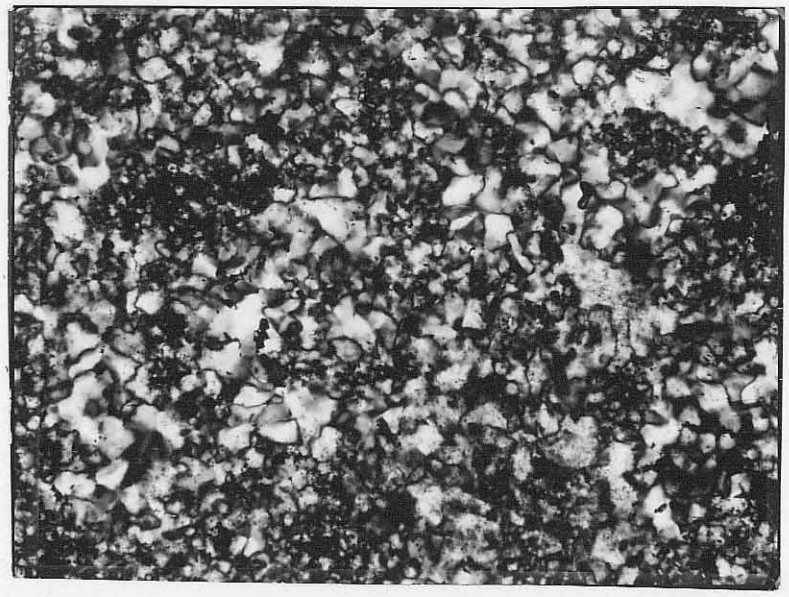

0.1 mm

Figure 72. Photomicrograph of Kelly district jasperoid (KDJ) sample 193-1. Predominant texture is subidiomorphic, R_1 = 38 (crossed-nicols, 25x magnification).

Figure 73. Photomicrograph of Kelly district chert (KDC) sample 123-1. Predominant texture is jigsaw-puzzle-xenomorphic, R_1 = 39 (crossed-nicols, 160x magnification).

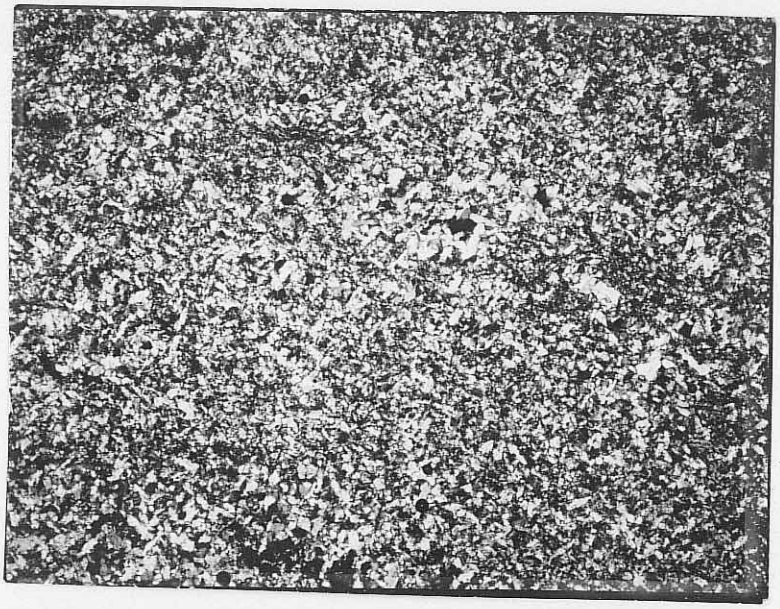

1 mm

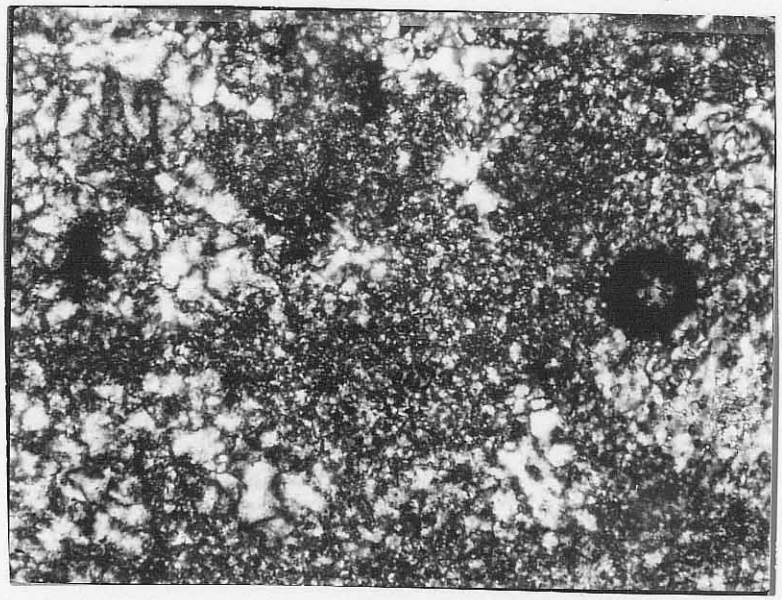

0.1 mm

Figure 74. Photomicrograph of Kelly district jasperoid (KDJ) sample 225-4. Predominant texture is jigsaw-puzzle, R_1 = 45 (crossed-nicols, 100x magnification)

Figure 75. Photomicrograph of North Fork Canyon chert (NFC) sample 2. Predominant texture is jigsaw-puzzle-xenomorphic, calcite grains (C) are also present, R_1 = 49 (crossed-nicols, 100x magnification).

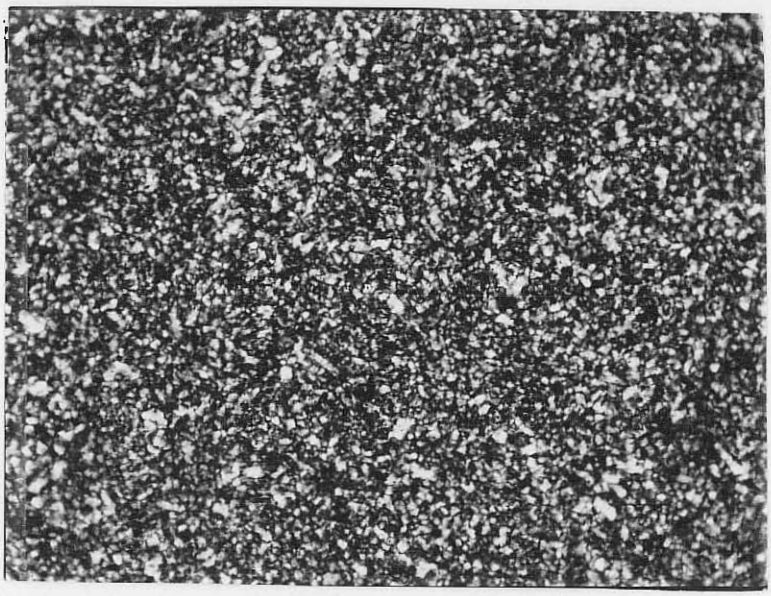

0.25 mm

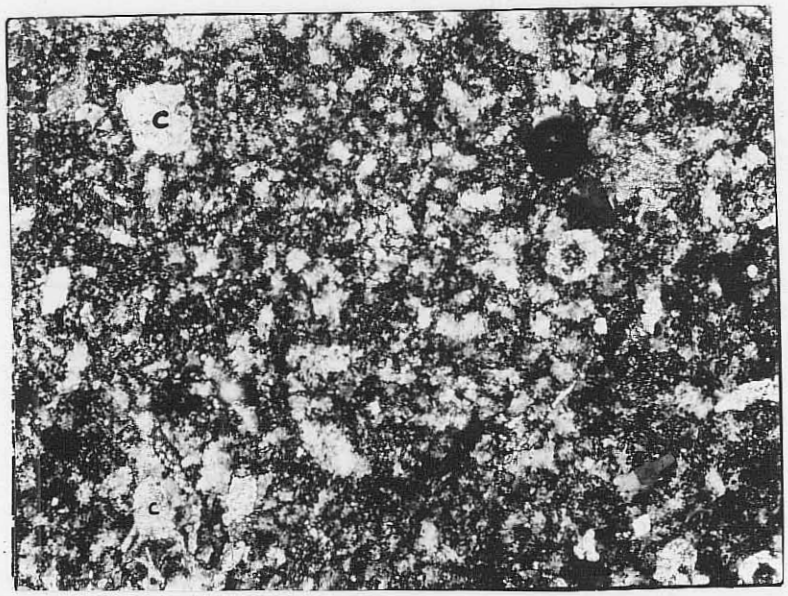

0.25 mm

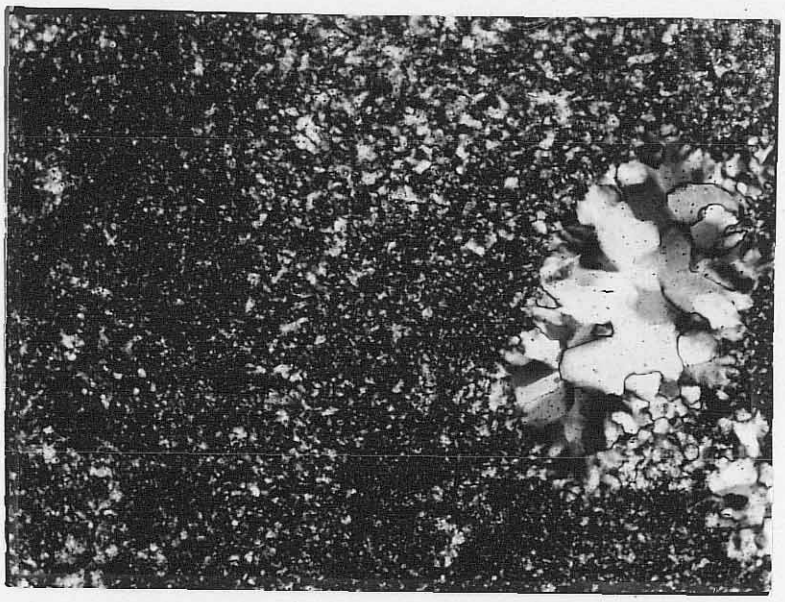

Figure 76. Photomicrograph of Kelly district chert (KDC) sample 11-1. Predominant texture is jigsaw-puzzle, xenomorphic-granular is also shown, R_1 = 52 (crossed-nicols, 128x magnification).

(Kelly district jasperoid) is greater than R_1 (normal chert). Although three normal cherts lie in the Kelly district jasperoid field, preliminary data suggest that these cherts may have witnessed a hydrothermal event. Kelly district chert cannot be uniquely categorized as being either normal chert or jasperoid by X-ray diffraction line profile analysis. Kelly district chert has been interpreted as being a mixture of normal chert, jasperoid, and chert which has been subjected to a hydrothermal event. A continuum in R_1 values exist with normal chert at the low end and Kelly district jasperoid and North Fork Canyon chert at the high end. Kelly district chert form a continuum of R_1 values between these two end members.

Petrographic analysis of several samples analyzed by X-ray diffraction line profile analysis revealed that R is not a function of textures or grain size observed in thin section. This suggests that no correlation exists between crystallite size distribution and optical grain size or petrographic textures. The effects of hydrothermal events superimposed upon normal chert cannot be seen optically but can be determined by X-ray diffraction line profile analysis.

In cherts of similar age, those which have undergone a hydrothermal event exhibit significantly higher R values. These results are in agreement with those of Murata and Norman (1976) on metamorphic and nonmetamorphic

cherts, see page 176. The data presented in this preliminary report suggest that qualitative X-ray diffraction analysis can be used in differentiating chert in mineralized areas from chert in non-mineralized areas.

APPENDIX I

Sample Preparation Method for X-ray Diffraction Line Resolution

Preparation of microcrystalline silica samples for X-ray diffraction line resolution was accomplished by the following procedure:

1. Hand specimens were reduced to pieces approximately 3 mm in size.
2. Crushed samples were placed in a highly concentrated HCl (about 75% HCl solution) bath overnight to remove any carbonate material.
3. Samples were washed with distilled water and air dried.
4. Pure microcrystalline silica was hand picked with the aid of a binocular microscope.
5. Samples were crushed in a diamet mortar until they passed a 45-mesh screen.
6. Crushed material was ground in a Fisher Model 155 mortar grinder until a particle size of 44 microns or less was achieved.
7. Ground samples were filtered 3 times with acetone to remove any fine material less than 8 microns.
8. Final mechanical grain size was between 8 and 44 microns.

LIST OF REFERENCES

Adams, S. F., 1920, A microscopic study of vein quartz: Econ. Geol., v. 15, p. 623-664.

Alexander, G. B., Heston, W. M., and Iler, R. K., 1954, The solubility of amorphous silica in water: Jour. Phys. Chem., v. 58, p. 453-455.

Allmendinger, R. J., 1975, A model for ore-genesis in the Hansonburg mining district, New Mexico: Unpub. Ph.D. dissertation, New Mexico Institute of Mining and Technology, 190 pp.

Armstrong, A. K., 1955, Preliminary observations on the Mississippian System northern New Mexico: New Mexico Bureau of Mines and Mineral Resources Circular 39, 42 pp.

_____, 1958, The Mississippian of west-central New Mexico: New Mexico Bureau of Mines and Mineral Resources Memoir 5, 32 pp.

Austin, C. F., 1960, Some schelite occurrences in the Magdalena mining district of New Mexico: New Mexico Bureau of Mines and Mineral Resources Circular 55, 17 pp.

Bailey, G. B., 1974, The occurrence, origin and economic significance of gold-bearing jasperoids in the central Drum Mountains, Utah: Unpub. Ph.D. dissertation, Stanford University, 300 pp.

Banazak, K. J., 1975, Genesis of the Mississippi Valley-type lead-zinc ores: Unpub. Ph.D. dissertation, Northwestern University, 132 pp.

Banks, N. G., 1970, Nature and origin of early and late cherts in the Leadville Limestone, Colorado: GSA Bull., v. 81, p. 3033-3048.

Barton, S. F., 1967, Crystallite-size determination from X-ray line broadening and spotty patterns, in: Handbook of X-rays, Kaelble, E. M., (ed.), McGraw-Hill Book Company, p. 17-1 - 17-8.

Bassett, H., 1954, Silicification of rocks by surface waters: Am. Jour. Sci., v. 252, p. 733-735.

Bastin, E. S., 1950, Interpretation of ore textures: GSA Memoir 45, 101 pp.

Blakestad, R. B., 1976, Geology of the Kelly mining district, Socorro County, New Mexico: Unpub. M.S. thesis, University of Colorado, 139 pp.

Blatt, G. B., Middleton, G., and Murray, R., 1972, Origin of Sedimentary Rocks, Prentice-Hall, Inc., 634 pp.

Brown, D. M., 1972, Geology of the southern Bear Mountains, Socorro County, New Mexico: Unpub. M.S. thesis, New Mexico Institute of Mining and Technology, 110 pp.

Bush, J. B., Cook, D. R., Lovering, T. S., and Morris, H. T., 1960a, The Chief Oxide-Burgin area discoveries, East Tintic district, Utah, A case history — Part 1, USGS studies and exploration, by T. S. Lovering and H. T. Morris: Econ. Geol., v. 55, p. 1116-1147.

_____, 1960b, The Chief Oxide-Burgin area discoveries, East Tintic district, Utah, A case history — Part 2, Bear Creek Mining Company studies and exploration, by J. B. Bush and D. R. Cook: Econ. Geol., v. 55, p. 1507-1548.

Butler, R., and Singewald, Q., 1940, Zonal mineralization and silicification in the Horseshoe and Sacromento districts, Colorado: Econ. Geol., v. 35, p. 793-838.

Campbell, A. A., and Fyfe, W. S., 1960, Hydroxyl ion catalysis of the hydrothermal crystallization of amorphous silica, A possible high temperature pH indicator: Am. Mineralogist, v. 45, p. 464-468.

Carr, R. M., and Fyfe, W. S., 1958, Some observations on the crystallization of amorphous silica: Am. Mineralogist, v. 43, p. 908-916.

Carter, N. L., Christie, J. M., and Griggs, D. T., 1964, Experimental deformation and recrystallization of quartz: Jour. Geol., v. 72, p. 687-733.

Chamberlin, R. M., 1976, Rotated early-rift faults and fault blocks, Lemitar Mountains, Socorro County, New Mexico (abs.), in: GSA Abstracts with programs, v. 8, #6, p. 807.

Chapin, C. E., 1974, Composite stratigraphic column of the Magdalena area: New Mexico Bureau of Mines and Mineral Resources, Open File Report 46.

Chapin, C. E., Blakestad, R. B., and Siemers, W. T., 1975, Geology of the Magdalena area, Socorro County, New Mexico, in: Field trips to New Mexico, Rocky Mountain Sect. of the Am. Assoc. Petroleum Geologists, p. 43-49.

Chapin, C. E. and Chamberlin, R. M., 1976, Geologic road log of the Socorro-Magdalena area, New Mexico: New Mexico Bureau of Mines and Mineral Resources, Unpublished road log for Field Trip 4, Annual Rocky Mountain Section Geol. Soc. America, Albuquerque, N.M.

Corwin, J. F., Herzog, A. H., Owen, G. E. Yalman, R. G., and Swinnerton, A. C., 1953, Mechanism of hydrothermal transformation of silica glass to quartz under isothermal conditions: Am. Chem. Soc., v. 75, p. 3933-3934.

Cox, G. H., Dean, R. S., and Gottschalk, V. H., 1916, Studies in the origin of Missouri cherts and zinc ores: Missouri Univ. School Mines Bull., Tech. Ser. 3, 34 pp.

Drewes, H., 1962, Stratigraphic and structural controls of mineralization in the Taylor mining district near Ely, Nevada, in: Short papers in geology, hydrology, and topography: USGS PP. 450-B, p. B1-B3.

Duke, D. A., 1959, Jasperoid and ore deposits in the East Tintic mining district: Unpub. M.S. thesis, University of Utah, 54 pp.

Engel, A. E. J., Clayton, R. N., and Epstein, S., 1958, Variation in isotopic composition of Oxygen and Carbon in Leadville (Mississippian, Colorado) and its hydrothermal and metamorphic phases: Jour. of Geol., v. 66, p. 374-393.

Ernst, W. G., and Blatt, H., 1964, Experimental study of quartz overgrowths and synthetic quartzites: Jour. of Geol., v. 72, p. 461-470.

Ernst, W. G., and Calvert, S. E., 1969, An experimental study of the recrystallization of procellanite and its bearing on the origin of some bedded cherts: Am. Jour. Sci., v. 267-A, p. 114-133.

Eslinger, E. V., Mayer, L. M., Durst, T. L., Hower, J., and Savin, S. M., 1973, An X-ray technique for distinguishing between detrital and secondary quartz in the fine-grained fraction of sedimentary rocks: Jour. Sed. Pet., v. 43, p. 540-543.

Folk, R. L., and Weaver, C. E., 1952, A study of the texture and composition of chert: Am. Jour. Sci., v. 250, p. 498-510.

Fournier, R. O., 1967, The porphyry copper deposit exposed in the Liberty open-pit mine near Ely, Nevada. Part II. The formation of hydrothermal alteration zones: Econ. Geol., v. 62, p. 207-227.

Fournier, R. O., and Rowe, J. J., 1966, Estimation of underground temperatures from the silica content of water from hot-springs and wet- stroms wells: Am. Jour. Sci., v. 264, p. 685-695.

Glossary of Geology, 1972, Gary, M., McAfee, R., Jr., and Wolf, C. L., (eds.), American Geological Institute, Washington, D. C., 805 pp.

Gilluly, J., 1932, Geology and ore deposits of the Stockton and Fairfield Quadrangles, Utah: USGS PP. 173, p. 97-101.

Gordon, C. H., 1907a, Mississippian formations in the Rio Grande valley, New Mexico: Am. Jour. Sci., 4th series, v. 24, p. 58-64.

_____, 1907b, Notes on the Pennsylvanian formation in the Rio Grande valley, New Mexico: Jour. of Geol., v. 15, p. 805-816.

Haas, J. L., Jr., 1971, The effect of salinity on the maximum thermal gradient of a hydrothermal system at hydrostatic pressure: Econ. Geol., v. 66, p. 940-946.

Hagni, R. D., and Grawe, O. R., 1964, Mineral paragenesis in the Tri-State district Missouri, Kansas, Oklahoma: Econ. Geol., v. 59, p. 449-457.

Haranczyk, C., 1969, Noncolloidial origin of colloform textures: Econ. Geol., v. 64, p. 466-468.

Hathaway, J. C., 1972, X-ray mineralogy studies — Leg II, pt. 2, in: Hollister, C. D., Ewing, J. I., and others, 1972, Initial Reports Deep Sea Drilling Project, v. 11: Washington, U.S. Govt. Printing Office, p. 772-789.

Hatschek, E., and Simon, A. L., 1912, Gels in relation to ore-deposition: Inst. of Mining and Met., Trans., v. 21, p. 451-480.

Helgeson, C. C., and Garrels, R. M., 1968, Hydrothermal transport and deposition of gold: Econ. Geol., v. 63, p. 622-635.

Herrick, C. L., 1904, Laws of formation of New Mexico mountain ranges: Am. Geologist, v. 33, p. 301-312.

Holland, H. D., 1967, Gangue minerals in hydrothermal ore deposits, in: Geochemistry of hydrothermal ore deposits, Barnes, H. L., (ed.), Holt, Rinehart, and Winston, Inc., 670 pp.

Hosler, W. T., 1947, Metasomatic processes: Econ. Geol., v. 42, p. 384-395.

Howd, F. H., 1957, Hydrothermal alteration in the East Tintic mining district, in: Utah Geol. Soc. Guidebook to the geology of Utah, v. 12, Geology of the East Tintic Mountains and ore deposits of the Tintic mining district: Utah Geol. and Mineralog. Survey, p. 124-134.

Howd, F. H., and Barnes, H. L., 1975, Ore solution geochemistry IV. Replacement of marble by sulfides: Econ. Geol., v. 5, p. 968-981.

Irving, J. D., 1911, Replacement ore-bodies and the criteria for their recognition: Econ. Geol., v. 6, p. 527-561.

Jacka, A. D., 1974, Replacement of fossils by length-slow chalcedony and associated dolomitization: Jour. Sed. Pet., v. 44, p. 421-427.

Keith, H. D., and Padden, F. J., Jr., 1964, Spherulitic crystallization from the melt. I. Fractionation and impurity segregation and their influence on crystalline morphology: Jour. Applied Phys., v. 35, p. 1270-1285.

Keller, W. D., 1941, Petrography and origin of the Rex chert: GSA Bull., v. 52, p. 1279-1298.

Kennedy, G. C., 1944, The hydrothermal solubility of silica: Econ. Geol., v. 39, p. 25-36.

_____, 1950, A portion of the system silica-water: Econ. Geol., v. 45, p. 629-653.

Klug, H. P., and Alexander, L. E., 1954, X-ray Diffraction Procedures: New York, John Wiley & Sons, 716 p.

Knopf, A., 1918, Geology and ore deposits of the Yerington district, Nevada: USGS PP. 114, 68 pp.

Kottlowski, F. E., and Stewart, W. T., 1970, Part I: The Wolfcampian Joyita uplift in central New Mexico: New Mexico Institute of Mining and Technology, State Bureau of Mines and Mineral Resources, Memoir 23, p. 7.

Krauskopf, K. B., 1956, Dissolution and precipitation of silica at low temperatures: Geochim et Cosmochim Acta, v. 10, p. 1-26.

_____, 1959, The geochemistry of silica in sedimentary environments, in: Silica in Sediments, Ireland, H. A., (ed.), Soc. Econ. Paleont. and Min. Spec. Pub., p. 4-19.

_____, 1967, Introduction to Geochemistry, McGraw-Hill Company, New York, 721 pp.

Krewedl, D. A., 1974, Geology of the central Magdalena Mountains, Socorro County, New Mexico: Unpub. Ph.D. dissertation, University of Arizona, 128 pp.

Lasky, S. G., 1932, The ore deposits of Socorro County, New Mexico: New Mexico Bureau of Mines Bull., 8, 139 pp.

Lebedev, L. M., 1967, Metacolloids in Endogenic Deposits: Plenum Press, New York, 298 pp.

Lindgren, W., 1901, Metasomatic processes in fissure veins: Am. Inst. Mining Engineers Trans., v. 30, p. 578-692.

_____, 1933, Mineral Deposits, (4th ed.): New York, McGraw-Hill Book Co., 930 pp.

_____, 1925, Metasomatism: GSA Bull., v. 36, p. 247-261.

Lindgren, W., and Loughlin, G. F., 1919, Geology and ore deposits of Tintic mining district, Utah: USGS PP. 107, p. 154-158.

Lindgren, W., Graton, L. C., and Gordon, C. H., 1910, The ore deposits of New Mexico: USGS PP. 68, p. 241-258.

Loughlin, G. F., and Koschmann, A. H., 1942, Geology and ore deposits of the Magdalena mining district, New Mexico: USGS PP. 200, 168 pp.

Lovering, T. G., 1962, The origin of jasperoid in limestone: Econ. Geol., v. 57, p. 861-889.

_____, 1972, Jasperoid in the U.S. — Its characteristics, origin, and economic significance: USGS PP. 710, 164 pp.

Lovering, T. G., and Patten, L. E., 1962, The effect of CO_2 at low temperature and pressure on solutions super-saturated with silica in the presence of limestone and dolomite: Geochim. et Cosmochim. Acta, v. 26, p. 789-796.

Lovering, T. G., and Heyl, A. V., 1974, Jasperoid as a guide to mineralization in the Taylor mining district and vicinity near Ely, Nevada: Econ. Geol., v. 69, p. 46-58.

McKinstry, H. E., 1955, Structure of hydrothermal ore deposits: Econ. Geol. 50th Anniv., p. 195-198.

McKnight, E. T., 1935, Zinc and lead deposits of northern Arkansas, USGS Bull. 853, p. 132-138.

Mitsyuk, B. M., 1974, Mechanism of hydrothermal synthesis of quartz: Geochemistry International, v. 2, p. 1151-1156.

Morey, G. W., Fournier, R. O., and Rowe, J. J., 1964, The solubility of amorphous silica at 25°C: Jour. Geophys. Research, v. 69, p. 1995-2002.

Murata, K. J., and Norman, M. B., II, 1976, An index of crystallinity for quartz: Am. Jour. Sci., v. 276, p. 1120-1130.

Oehler, J. H., 1976, Hydrothermal crystallization of silica gel: GSA Bull., v. 87, p. 1143-1152.

Park, C. E., Jr., and MacDiarmid, R. A., 1964, Ore Deposits: W. H. Freeman and Company, San Francisco, 522 pp.

Park, C. F., Jr., and Cannon, R. S., 1943, Geology and ore deposits of the Metaline Quadrangle, Washington: USGS PP. 202, 81 pp.

Park, D. E., 1971, Petrology of the Tertiary Anchor Canyon stock, Magdalena Mountains, central New Mexico: Unpub. M.S. thesis, New Mexico Institute of Mining and Technology, 92 pp.

Pettijohn, F. J., 1957, Sedimentary Rocks, (2nd ed.): Harper and Row, Inc., 718 pp.

Proctor, P. D., 1964, Fringe zone alteration in carbonate rocks, north Tintic district, Utah: Econ. Geol., v. 59, p. 1564-1587.

Roedder, E., 1967, Fluid inclusions as samples of ore fluids, in: Geochemistry of hydrothermal ore deposits, Barnes, H. L., (ed.), Holt, Rinehart, and Winston, Inc., 670 pp.

_____, 1968, The noncolloidal origin of "colloform" textures in sphalerite ores: Econ. Geol., v. 63, p. 451-471.

_____, 1972, Composition of fluid inclusions, in: Data of Geochemistry, Chapter JJ: USGS Prof. Paper 440-JJ, U.S. Govern. Printing Off., Washington, 164 pp.

Roedder, E., Heyl, A. V., and Creel, J. P., 1968, Environment of ore deposition at the Mex-Tex deposits, Hansonburg district, New Mexico, from fluid inclusions: Econ. Geol., v. 63, p. 336-348.

Rove, O. N., 1947, Some physical characteristics of certain favorable and unfavorable horizons: Econ. Geol., v. 42, p. 161-193.

Sharp, W. E., 1965, The deposition of hydrothermal quartz and calcite: Econ. Geol., v. 60, p. 1635-1644.

Shettel, D. L., Jr., 1974, Solubility of quartz in supercritical H_2O-CO_2 fluids: Unpub. M.S. thesis, Pennsylvania State University, 60 pp.

Siever, R., 1962, Silica solubility, 0° - 200°C, and the diagenesis of siliceous sediments: Jour. of Geol., v. 70, p. 127-150.

Siemers, W. T., 1973, Stratigraphy and petrology of Mississippain, Pennsylvanian and Permian rocks in the Magdalena area, Socorro County, New Mexico: Unpub. M.S. thesis, New Mexico Institute of Mining and Technology, 133 pp.

_____, in preparation, Pennsylvanian System of Socorro County, New Mexico: Unpub. Ph.D. dissertation, New Mexico Institute of Mining and Technology.

Siemers, W. T., and Blakèstad, R. B., 1976, Revision of upper Paleozoic stratigraphy in the Magdalena area, New Mexico (abs.), in: GSA Abstracts with programs, v. 8, p. 629.

Spry, A., 1969, Metamorphic Textures: Pergamon Press, Oxford, England, 350 pp.

Spurr, J. E., 1898, Geology of the Aspen mining district, Colorado, USGS Monograph XXXI, p. 216-221.

Taliafero, N. L., 1934, Contraction phenomena in cherts: GSA Bull., v. 45, p. 189-232.

Tatlock, D. B., 1966, Rapid modal analysis of some felsic rocks from calibrated X-ray diffraction patterns, USGS Bull. 1209, 41 pp.

Titley, S. R., 1958, Silication as an ore control, Linchburg Mine, Socorro County, New Mexico: Unpub. Ph.D. dissertation, Univ. of Arizona, 153 pp.

_____, 1959, Geological summary of the Magdalena mining district, Socorro County, New Mexico, in: 10th Annual Field Conference, N.M.G.S., p. 144-148.

_____, 1961, Genesis and control of the Linchburg orebody, Socorro County, New Mexico: Econ. Geol., v. 56, p. 695-722.

_____, 1963, Lateral zoning as a result of monoascendent hydrothermal process in the Linchburg mine, New Mexico, in: Kutina, J. (ed.), Symposium on Problems of Postmagmatic Ore Deposits: I.A.G.O.D., Prague, v. 1, p. 312-316.

Weiner, W. F., and Koster Van Gross, A. F., 1976, Petrographic and geochemical study of the formation of chert around the Thonton reef complex: GSA Bull., v. 87, p. 310-318.

White, D. E., Brannock, W. W., and Murata, N. J., 1956, Silica in hot-spring waters: Geochim et Cosmochim Acta, v. 10, p. 27-59.

White, J. F., and Corwin, J. F., 1961, Synthesis and origin of chalcedony: Am. Mineralogist, v. 46, p. 112-119.

Williams, H., Turner, F. I., and Gilbert, C. M., 1954, Petrography — An Introduction to the Study of Rocks in Thin Section: W. H. Freeman and Company, San Francisco, 406 pp.

Yalman, R. G., and Corwin, J. F., 1957, Hydrothermal reactions under supercritical conditions, III. The effect of pH on the crystallization of silicon-dioxide: Jour. Phys. Chem., v. 61, p. 1432-1437.

Young, E. J., and Lovering, T. G., 1966, Jasperoids of the Lake Valley mining district, New Mexico: USGS Bull., 1222-D, 27 pp.

Zachariasen, W. H., 1967, Theory of X-ray Diffraction in Crystals: Dover Publication, Inc., p. 156-176.

This thesis is accepted on behalf of the faculty of the Institute by the following committee:

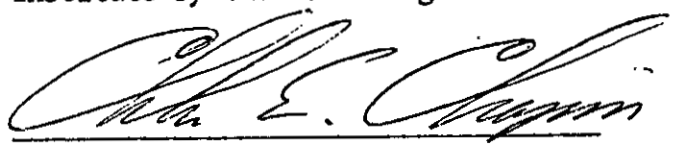

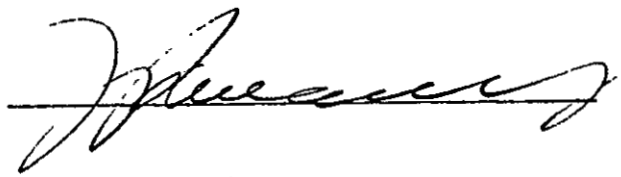

R E Beane

Date 9/7/77

PLATE I

GEOLOGIC MAP OF THE EASTERN PORTION OF THE KELLY MINING DISTRICT SOCORRO COUNTY NEW MEXICO

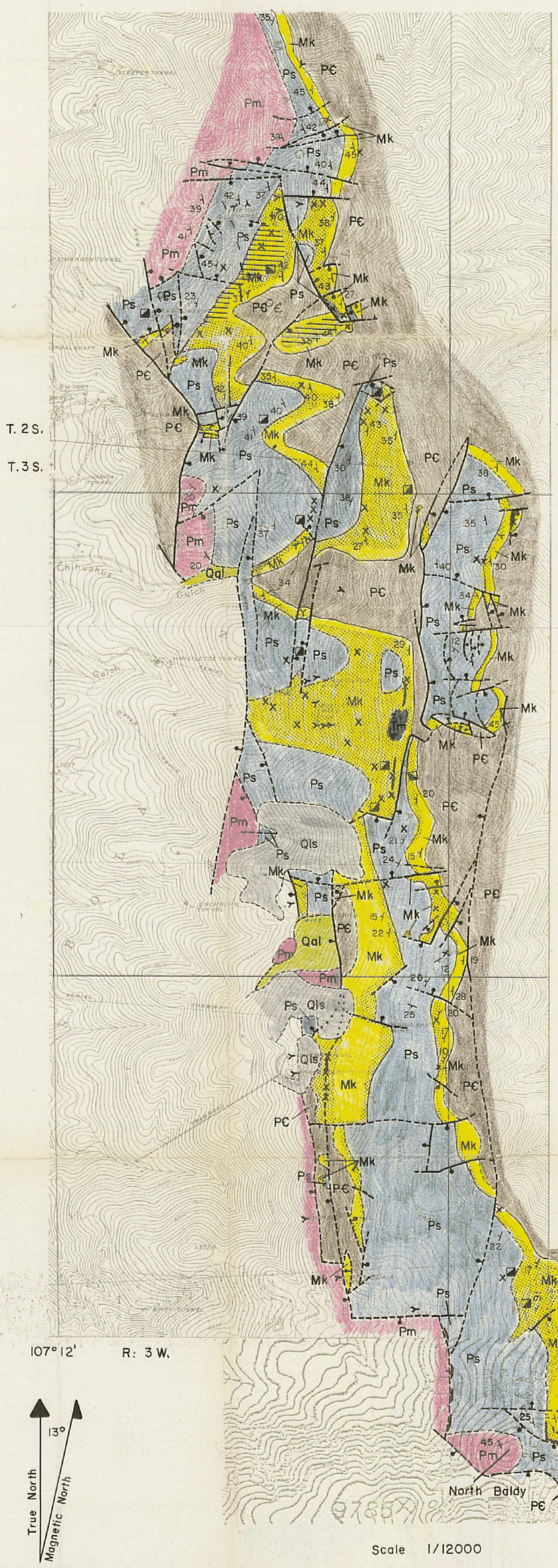

EXPLANATION

QUATERNARY

- Qal — Alluvium
- Qls — Land Slide

TERTIARY

- Twr — White Rhyolite dikes and sills
- Tm — Mafic dikes and sills

PALEOZOIC

- Pm — Madera Limestone
- Ps — Sandia Formation
- Mk — Kelly Limestone (stippling indicates silicification)

UNCONFORMITY

PRECAMBRIAN

- PC — (undivided argillite, schist, gabbro, felsite, granite and diabase)

Contact, dashed where approximate

Fault, ball on downthrown side, dashed where approximate

12 — Strike and dip of bedding

× — Mineral prospect

Adit

Shaft

Silicified Kelly Limestone (jasperoid)

Jasperoid inferred on basis of silicified float and/or remnants of jasperoid standing topographically and stratigraphically above the surrounding limestone

U. S. G. S. Magdalena District New Mexico (1922), Contour Interval 25 Feet.

U. S. G. S. Magdalena 15 - minute quadrangle (1959). Contour Interval 40 Feet.

DATUM IS MEAN SEA LEVEL

13° — True North, Magnetic North

Approximate Mean Declination, 1964

Scale 1/12000

0 1/8 1/4 1/2 3/4 1 miles

200 100 0 500 1000 meters

Geology mapped by Iovenitti, 1977 (modified after Loughlin and Koschmann, 1942; Blakestad, 1977).

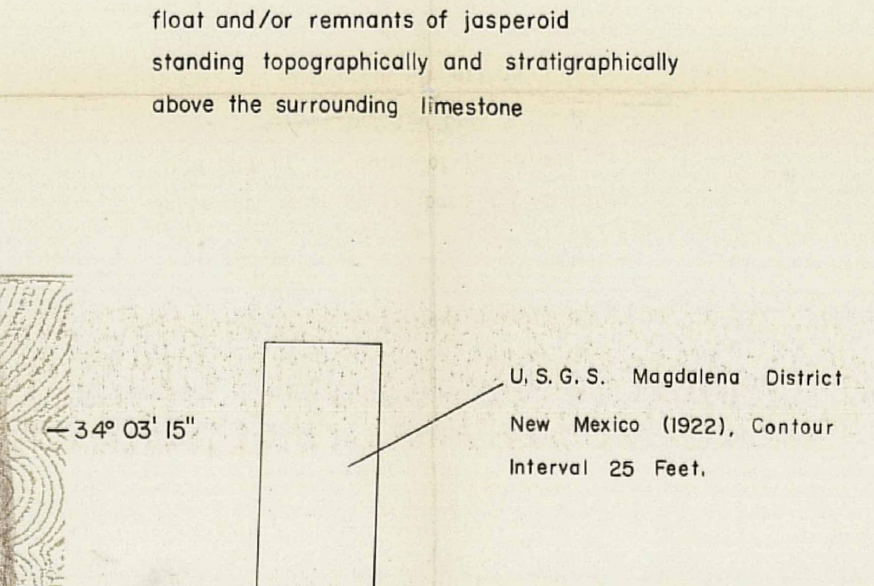

Index map of New Mexico and Socorro County